

Wave-Particle uncertainty principle in neurons. From oscillatory synapses to action potential

By Alexandra Pinto

WAVE-PARTICLE UNCERTAINTY PRINCIPLE IN NEURONS. FROM OSCILLATORY SYNAPSES TO ACTION POTENTIAL

ALEXANDRA PINTO CASTELLANOS

⁷¹
SUBMITTED TO THE FACULTY OF MATHEMATICS AND NATURAL SCIENCES UZH
AND THE DEPARTMENT OF INFORMATION TECHNOLOGY AND ELECTRICAL
ENGINEERING ETH

JOINT DEGREE MSc IN NEURAL SYSTEMS
AND COMPUTATION

DEPARTMENT OF MNF UZH AND D-ITET ETH
UZH ETH
ADVISER: RUEDI STOOP
COLLABORATOR: YOKO UWATE

ZURICH 2017

© Copyright by Alexandra Pinto Castellanos, 2017.
All rights reserved.

Abstract

The main interest of this thesis, is to answer the wave to pulse generation problem in the chemical synapses of our nervous system. The current state of the art in this respect is pretty scarce and unclear, regarding conservation of information and frequency at the interior of the synaptic cleft. The curiosity to solve this p₇blem was mainly raised by the fact that the trains of action potentials certainly encode and transmit information along the nervous system but most of the time neurons are not transmitting action potentials, 99 percent of their time are in the sub threshold domain were only small signals without the energy to emanate an action potential are the ones that carry the majority of information, the one that let us perceive the world in one way, the same synchronised way that let us have a language, memory and in general, activities that don't require the fast response inter neuron communication as in electric synapses.

The model that is proposed in this thesis for a synapse, is an oscillatory constructive and destructive interference pattern of wave activity, that smooths the train of action potential and keeps its frequency. Synapses are presented here as a system composed of an input wave that is transformed through interferometry as slits in analogy to Young's experiment but with the real synaptic distribution or ionic structural distribution depending on the level of analysis that wants to be achieved.

The creation of the synapse network in order to have the real biological distribution of the "slits", required the acquisition of the position and volume of a real neuron topology and the detection of each synapse was done using an algorithm that is able to fill in the empty space inside the neuron to quantify it and extract the contact points with surrounding neurons. Each synapse in the real neuron image, is replaced by an oscillation that depends on the wavelength of the input signal. The collective synaptic interference pattern of waves will reflect the points of maximum amplitude for the density wave synaptic function were the location of the "particle" in our case action potential, has its highest probability.

Acknowledgements

Thanks God for the knowledge you give me and you give to the people around me. Thank you for life, health and the happy feeling of having you in my heart, thanks to you I can be forgiven and I am able to forgive.

⁸"En verdad, Dios esta muy cerca, para salvar a los que le honran; su gloria vivir en nuestra tierra. El amor y la verdad se darán cita, la paz y la justicia miraran desde el cielo. El Señor mismo traer la lluvia y nuestra tierra dar su fruto. La justicia irá delante de él, y le preparará el camino"

¹⁰"Love and faithfulness meet together; righteousness and peace kiss each other. Faithfulness springs forth from the earth, and righteousness looks down from heaven. The Lord will indeed give what is good, and our land will yield its harvest. Righteousness goes before him and prepares the way for his steps." Psalm 85

Jan, I have always thought that successful people are the ones who are able to help and it is providing this help that success happens. Thanks

5

"Sure I am this day we are masters of our fate, that the task which has been set before us is not above our strength: that its pangs and toils are not beyond our endurance. As long as we have faith in our own cause and an unconquerable will to win, victory will not be denied us." C. Winston

5

"You ask, what is our aim? I can answer in one word: Victory. Victory at all costs -Victory in spite of all terror- Victory, however long and hard the road may be, for without victory there is no survival." C. Winston

Contents

Abstract	iii
Acknowledgements	iv
List of Figures	viii
1 Introduction	1
1.1 Motivation and applications	1
1.2 Overview and Contributions	2
1.3 Consequences and Impact	3
1.4 Organization of document	4
2 Overview and Survey	5
2.1 Objectives and purpose	5
2.1.1 Proposed work Master Thesis December 2016	5
2.1.2 Theory Background	7
2.1.3 Experimental Biological facts on subthreshold activity	10
3 Methodological Proposal	15
3.1 Synapses collective behavioras synchronous oscillators model.	15
3.1.1 Particle wave duality in neurons. Why waves at synapses?	16
3.2 First stage results	17
3.2.1 Structure of a Neuron from a Stack of SEM Images	17
3.2.2 Data processing and organisation	18
4 Results	23
4.1 Hopf systems and synapse relation	23
4.1.1 Van Der Pol Oscillators coupled with Inductance-Resistance	23
4.1.2 Van Der Pol Oscillators coupled with Resistance	34
4.1.3 Van Der Pol Oscillators coupled with Inductance	43

4.2	Experimental Results	52
4.2.1	Setup Electronic Circuit	52
4.2.2	Results experimental setup	53
4.3	Sub-threshold dynamical analysis	56
4.3.1	Signal-Coupled Sub-threshold Hopf-Type Systems Show a Sharpened Collective Response	56
4.3.2	Four Subcritical coupled systems in a Network	64
4.4	Analysis of a Biophysical synaptic model	69
4.4.1	General aspects	69
4.4.2	⁶ Ca ²⁺ Dynamics	71
4.4.3	⁶ Glutamate release dynamics in bouton	73
4.4.4	Glutamate dynamics in synaptic cleft	74
4.4.5	Astrocyte Ca ²⁺ dynamics	74
4.4.6	⁶ Glio-transmitter release dynamics in astrocyte	76
4.4.7	Glutamate dynamics in extra-synaptic cleft	78
4.4.8	Dendrite Spine-head dynamics	78
4.4.9	Oscillatory behaviorin the Model	80
5	Results: Theoretical Proposal	85
5.1	The synapse as a system	86
5.1.1	Vesicles and Diffusion at the synaptic cleft	87
5.1.2	A train of action potentials crossing the synapse	91
³¹ 6	Conclusion and Future directions	93
6.1	Summary of contributions	93
6.2	Vision for the future	94
6.2.1	Medium term goals	95
6.2.2	Long term goals	95
	Bibliography	96

List of Figures

3.1	Workflow of proposal made in December 2016	16
3.2	The data in the reconstruction of the following neurons was acquired from Seung's Laboratory at MIT	18
3.3	19
3.4	Output from the data files provided by Seung's Lab	19
3.5	Result of the neuron analysis after applying the ball's algorithm . .	20
3.6	Visualisation obtained from Rhinos software	21
3.7	Visualisation of three neurons as obtained in the data files provided by Seung's Lab	21
4.1	Left: Limit cycle appearance in relation Y against X for one oscillator. Right: Anti-phase synchronisation in relation X_2 and X_1 of two oscillators.	31
4.2	Limit cycle appearance in relation X_1 and X_2 against Y_1 and Y_2 for two oscillators.	32
4.3	Relation X_2 against X_1 . Left: Same initial conditions. Right: Different initial conditions	33
4.4	Oscillatory responses against dimensionless time. Left: X_1 and X_2 . Right: Y_1 and Y_2	33
4.5	Left: Limit cycle appearance in relation Y against X for one oscillator. Right: In-phase synchronisation in relation X_2 and X_1 of two oscillators.	39
4.6	Limit cycle appearance in relation X_1 and X_2 against Y_1 and Y_2 for two oscillators.	40
4.7	Relation X_2 against X_1 . Left: Same initial conditions. Right: Different initial conditions	41

4.8	Oscillatory responses against dimensionless time. Left: X_1 and X_2 . Right: Y_1 and Y_2	42
4.9	Left: Limit cycle appearance in relation Y against X for one oscillator. Right: In-phase synchronisation in relation X_2 and X_1 of two oscillators with the same initial conditions.	48
4.10	Limit cycle appearance in relation X_1 and X_2 against Y_1 and Y_2 for two oscillators.	49
4.11	Relation X_2 against X_1 . In-phase synchronisation for same initial conditions and anti-phase synchronisation for different initial conditions	50
4.12	Oscillatory responses against dimensionless time under same initial conditions. Left: X_1 and X_2 . Right: Y_1 and Y_2	51
4.13	Oscillatory responses against dimensionless time under different initial conditions. Left: X_1 and X_2 . Right: Y_1 and Y_2	51
4.17	behaviorof the Hopf system considering it as a coupled system of two real differential equations.	57
4.18	Oscillatory decay to fixed point of two Hopf systems with close frequencies	57
4.19	Influence of the coupling term.	59
4.20	g_c as function of μ and the ratio of characteristic frequencies of the oscillators.	61
4.21	10 oscillators with different characteristic frequency, for $\mu = -0.2$ and $\mu = -0.3$	62
4.22	behaviorof the subcritical system	63
4.23	Two coupled subcritical systems with the same small value for μ but different frequencies.	64
4.24	Network topology to couple the 4 systems.	65
4.25	Response of the real part of each system compared with the others. This is the long term response of the systems, once transient effects have dissipated.	66
4.26	Another network topology to couple the 4 systems.	67
4.27	Response of the real part of each system compared with the others. This is the long term response of the systems, once transient effects have dissipated.	68

4.28	HH model variable for study. v: V_{pre} , pre-synaptic potential. Plotted using the model provided by [Tewari & Majumdar 2012]	70
4.29	HH model variables for study. m: Gating variable for Na channel (activation), h: Gating variable for Na channel (inactivation), n: Gating variable for K channel (activation). Plotted using the model provided by [Tewari & Majumdar 2012]	70
4.30	Bouton Ca Dynamics. The corresponding 2 variables of the model are p: intracellular IP_3 concentration, q: fraction of activated IP_3R , gating variable. Plotted using the model provided by [Tewari & Majumdar 2012]	72
4.31	Bouton Ca Dynamics. The corresponding 4 graphs are as follows: m_c : Gating variable for Ca channel, c_{fast} : Ca due to AP, c_{er} : ER Calcium concentration also c_{slow} scaled, c: c_i total Ca concentration, Plotted using the model provided by [Tewari & Majumdar 2012]	73
4.32	Astrocyte Ca dynamics. ca: Calcium concentration and IP_3 concentration. Plotted using the model provided by [Tewari & Majumdar 2012]	75
4.33	Astrocyte Ca dynamics. Top Site 1,2,3 of Synaptic- Like Microvesicle (SLMV) release machinery with calcium bound. Bottom: Fraction of releasable SLMVs, Fraction of effective SLMVs, Fraction of inactivated SLMVs. Plotted using the model provided by [Tewari & Majumdar 2012]	77
4.34	Dendrite Spine-head dynamics. m_{ampa} : AMPAR gating variable, V_{post} : Post-Synaptic Membrane potential. Plotted using the model provided by [Tewari & Majumdar 2012]	79
4.35	Calcium concentration in the Endoplasmatic Reticulum inside the presynaptic neuron. Plotted using the model provided by [Tewari & Majumdar 2012]	80
4.36	Calcium channel opening probability. Plotted using the model provided by [Tewari & Majumdar 2012]	81
4.37	m_{IP_3} is the gating variable responsible of initiating astrocytic Ca^{2+} oscillations. Plotted using the model provided by [Tewari & Majumdar 2012]	82
4.38	Two variables involves in synaptic vesicle release. Plotted using the model provided by [Tewari & Majumdar 2012]	83

4.39	13 Glutamate release dynamics in bouton. Top: Releasable fraction of vesicles, Effective fraction of vesicles in synaptic cleft, Inactivated fraction of vesicles, Fraction of Vesicles to be released. Bottom: Glutamate concentration in cleft. Plotted using the model provided by [Tewari & Majumdar 2012]	84
5.1	7 A train of action potentials in the pre-synaptic neuron, is smoothed out by being converted into an oscillation of neurotransmitters concentrations in the synaptic cleft. This neurotransmitters concentration is then turned into low amplitude electrical signal in the post-synaptic neuron. The original frequency of the train of action potentials is preserved.	85
5.2	Vesicles, neurotransmitters and synaptic cleft as a system that transforms the train of spikes into a smoothed out version with the same primary frequency.	86
5.3	A neurotransmitter concentration leaves the pre-synaptic neuron with a certain velocity, as it travels through the synaptic cleft, it spreads by diffusion of its concentration.	87
5.4	The synapse as a system.	90
5.5	A train of action potentials written as Dirac's delta. The time interval between one action potentials is T	91

Chapter 1

Introduction

1.1 Motivation and applications

Reality, perception and waves are my motivation. From my perspective they are synonyms since it is the way in which nature phenomena is presented to me. Networks of neurons have the task of conveying an n dimensional input space, that is each signal detected by each neuron, into a finite four dimensional space, that is our output space. This transformation from input to output must be created in a continuous manner such that our perception of time and space could be smooth and efficient with limited number of errors. The main interest and curiosity around this thesis proposal is the fact that the vast majority of neurons never get to make an action potential, the electrical signal that scientist detect as the main attribute for encoding of the input signals (perceived reality). It is the desire of this thesis proposal to present and explain the wave oscillatory state of the synaptic connectivity as the main encoding for the continuous high dimensional input state. This is also in agreement with the fact that given the sparse number of action potentials and its discrete nature, it is not a good candidate to encode the complete information that is incoming constantly.

An action potential is presented in this thesis as the consequence of constructive interference produced by the wave of synaptic input. Its amplitude and saturation point are presented as dependent on the wavelength in the synaptic input where depending on the location and zones of constructive interference, we can have the highest points of detection of the wave density function as analogous to the Excitatory Postsynaptic Potentials (EPSP), using the simple rules of interference where we only need as

parameters the size and distribution of synapses or ion channels, depending on the level that is of interest, and the wavelength of the input wave as analogous to the laser.

The main purpose of this thesis is to explain that even in the absence of action potential detection, there are other points of constructive interference that contain valuable information about the input and that are independent events from the highest amplitude, they only depend on the wave pattern. On the other hand, the highest points of destructive interference are analogous to the inhibitory postsynaptic potentials (IPSP).

1.2 Overview and Contributions

Modelling of synapses has been a slow process that is constrained to advances in the interdisciplinary fusion of physics, both for measuring and data analysis, and advances in molecular biology or biophysics. Nonetheless, nowadays the constraints are also computational given that some models have detailed set of coupled equations with experimental parameters that are pretty accurate but solving them for each one of the 5×10^{13} synapses is an impossible computational task at this moment. The main consequence of this computational limit is that there are different forms of synapse modelling, from detailed biophysical models that sacrifice the possibility of analyzing the behavior of several synapses, to reductionist models that consider the phenomenon in a probabilistic way.

For the purpose of giving an idea of the different synaptic models and to better understand what is the common characteristic among them, this thesis explains three existing models in the following chapters. Let me clarify that the biological and molecular details of the synapsis are absolutely impressive and the fact that this thesis does not take into account the biophysical details of the neuron and its synapses is only due to the vision for being able to analyse the exact flow of information flow from the moment it enters through each neuron until it is projected into our senses and for this reason I wish to contemplate the nature of the input in its purest form, as interference patterns of interacting waves.

The contribution that this thesis wants to achieve starts by proposing the plausibility of modelling the synapse as a system that generates interference patterns taking as input a wave function and transforming it in such a way that the highest amplitude of constructive interference is where the action potential takes place, the other highest points are considered as Excitatory Postsynaptic Potentials (EPSP). Lastly, this thesis wants to propose a biological methodology to proof the hypothesis of the synaptic transformation using real neurons architectures and the detection of synapses in the real neuron structure. This real biological synaptic network will serve as templates for using real neural network architectures that have the biological efficacy for the ideal slits configuration to create an infinite possibility of computations.

The analysis of this connectomic topology in the sense of structural generation of wave interference could also be interpreted as a three dimensional Young's experiment whose slit's distribution, size and distance are given by the data acquired from the reconstruction of real neurons topology, also in analogy to the screen in Young's experiment, the screen in our case would be the projection of every single synaptic wave interference pattern in the postsynaptic neuron.

1.3 Consequences and Impact

Analysing synapses with the wave-particle viewpoint is computational efficient for studies of memory and learning where it is crucial to detect the appearance and disappearance of synaptic contacts and plasticity. With this framework, synapses are amplitudes of wave activity that vanish or emanate depending on the collective oscillatory behavior. This is a novel way for modelling interneuron communication that does not reside on the complexity of detailed biophysical neuronal models or its synapses, where as is presented in this document, it is necessary to compute around 25 coupled differential equations.

Another desirable characteristic of this proposal is the fact that the required noise generation, proper of real synaptic recordings, is implicit in the wave pattern generation as a consequence of the distribution and structural complexity that can be reduced as the location of the slit, again as analogous to Young's experiment, this

is a valuable feature given that it is not necessary to add extra noise terms that in the case of biophysical models or integrate and fire models, make the system harder to solve computationally.

This study is a potential tool for the analysis data where it is required a transformation from the Postsynaptic signal to the presynaptic or viceversa. This approach can also be useful in computational tasks both in software and hardware that can make use of real biological network architectures as templates of interference generators that are able to solve different computations.

1.4 Organization of document

This document have six chapters: Chapter 1 is the introduction with the aim for motivating the reader. Chapter 2 is the overview and theoretical concepts required to understand the main concept that the thesis wants to propose together with the explanation different synaptic models. Chapter 3 is the methodological proposal for the applicability and confirmation of this hypothesis. Chapter 4 is the analysis of Hopf systems through simulation, experiment and mathematical modelling in order to better understand the best mathematical tools in the nonlinear analysis of oscillations applied to biological synchronization and lastly is presented a tripartite biophysical model of a synapse and its oscillatory components are detected.

Chapter 5 is the theoretical development of the synaptic transformation from wave input to discrete particle output. Chapter 6 are the conclusions of this thesis and more importantly the medium and long term goals for future directions. It is my desire to motivate future collaborative work given that the task is immense and requires the expertise in many fields. In this chapter is also presented the intention of making this approach applicable to quantum machine learning.

Chapter 2

Overview and Survey

2.1 Objectives and purpose

2.1.1 Proposed work Master Thesis December 2016

The purpose of this thesis is the explanation and modelling of synapses as generators of interference wave patterns that transform the information from an input wave to a discrete density probability function. Synchronisation of synapses are a necessary component in the generation of a train of pulses along the axon. Additionally, this synchronisation is achieved when the spectrum of all the signal from the synapses, matches the frequency spectrum of the action potential.

Objectives

Proposal and modelling of synapses as non linear oscillators capable of generating interference pattern of activity and synchronisation.

- Research on the possibility and constraints for oscillation in the synapse.
- Oscillator model of a synapse
- Propose coupling between synapse
- Synchronisation constraints along synapses
- Relation between spectrum of the total synaptic signal and the frequency spectrum of the action potential.

- Use of real neural topologies for architectures of interference pattern generation

The structure of a neuron can be divided in three parts, receptor (dendritic tree), effector (axon) and nucleus where the receptor and effector converge. The dendritic membrane forms synapses with the axon's tips of other neurons, without any physical connection between them. The question at this point is: how information is conserved in this discontinuity? It is widely known that dendrites receive input from hundreds of axon tips of other neurons, combine the input, which is delivered to the axon [Pur 2008]. However, how dendrites combine and deliver this information is not known with certainty, then is function of the axon to transmit the output of the dendrites to other parts of the nervous system.

The nature of information at the synaptic cleft and along the axons is very different in amplitude and time scale, however it is finely tuned in order to keep the flow and coherence of information. Dendrites from the postsynaptic neuron, receive an almost continuous oscillatory wave of ionic current input from the connecting synaptic cleft that joins it with the presynaptic terminal and convert it to a discrete voltage pulse that travels along the axon to be converted again in an oscillatory wave [Bullock 1993]. It is described in this thesis that the wave to pulse basis transform takes place at the interior of each synapse, the mechanism is as follows: a pulse arrives on the axon terminal, this energy allows the entrance of positive calcium ions, which are going to move vesicles that carry neurotransmitters. This vesicles release their content outside the neuron where the oscillatory periodic wave takes the form of a field of ionic current. The mathematical details of this transformation are presented in chapter 5. The output of the dendrites is the sum of waves resulting from all synaptic cleft activity, which are then delivered to the initial segment of the axon [Hodgkin & Huxley 1990], in chapter 5 is presented a mathematical approach to this waves convergence.

There are two types of activity encoded at synapses, excitatory and inhibitory, depending on the type of neurotransmitter that is released in the synaptic cleft, this chemical wave if excite can let to synchronous behavior and generate a positive voltage or in case of inhibit can let to asynchronous behavior and generate a negative voltage in the postsynaptic neuron. It is proposed that at the synaptic cleft the signals are smoothed and convolved in order to create the oscillatory wave, that has

the same frequency as the originating train but have the important property that can be generate patterns of constructive (excitatory synapse) or destructive (inhibitory synapse) interference for amplification of information keeping the frequency content.
This information is then transmitted in space and delayed at the initial segment of the axon [Pur 2008]. Once the wave has acquired enough amount of amplification, the axon responds to this wave input by generating a pulse train, where each pulse has the same amplitude. But as a train of pulses, they keep the information flow frequency.

2.1.2 Theory Background

Information Flow

The effect of all synapses working together, can excite or inhibit the production of a pulse in the receiver neuron. As mentioned before, this two effects are called excitatory synapses and inhibitory synapses, depending on the averaging effect of all the activity, the general output can be excitatory or inhibitory but not both. For the purposes of this thesis, this general inhibitory or excitatory state, is the result of destructive or constructive wave pattern synchronisation.

Until now, it is considered that if two or more small inputs are given simultaneously, the responses are simply added, and the system is said to be linear. If two otherwise identical inputs are separated in time, and if the responses are identical except for time of onset, the system is time invariant [Eccles 1964]. Nonetheless, the mechanisms of synchronisation, its variables, and limiting factors are unknown. On the other hand, it must be taken into account that the coupling medium is going to be crucial in the synchronisation process, given that depending on the nonlinear nature of the synapse, it is possible to have in phase summation between presynaptic and postsynaptic neurons even when they are in anti phase, or it is possible to have anti phase behavior between the two cells even when they are in phase, examples of this behavior will be given for the case of the Van Der Pol oscillator when comparisons between coupling elements are taken into account.

Another important effect that must be taken into account, is the secondary effect that the neurotransmitter release of a presynaptic terminal can have in neigh-

bouring postsynaptic dendrites. There is a high possibility of having this cascade amplification given the analogous dispersive nature of the synapse signal and more importantly, given the required amplification of the signal.

The wave to pulse conversion process, depends on the steady state level of the total dendritic synchronisation, and its coincidence with the refractory period of the pulse (about 1 msec), during which no amount of stimuli can induce another pulse. Subsequently, there is a period lasting several milliseconds, in which an additional stimuli can induce a second pulse, only if the second stimuli is larger than the first. Given all this constraints, the wave to pulse transformation is nonlinear and variable in time, if a steady above-threshold current is passed across the membrane, the train pulse has a high frequency, but this frequency depend on many other parameters that make it variable in time.

Synchronisation in the nervous System

Biological oscillators like neurons and heart cells are usually modelled as nonlinear systems in a dimension 2 space. It is possible for this models to present limit cycles and synchronisation. Nonlinear electronics as the Van Der Pol Oscillator and the Josephson Junction are good models for neuronal oscillators. A neuron has cycles of activity that oscillate between states of above threshold and sub threshold activity. Once the cell has the required energy, at a point in its cycle it releases an electrochemical signal that enables the communication channel to connected with other neurons in a synchronous fashion. Using the phase space of the neuron, let the description of how close the neuron is to reach the above threshold firing state. This cycle has a characteristic period and an amplitude. This means that the oscillations will remain near a constant frequency, even when the neuron is perturbed [Matthews *et al.* 1991].

Synchronisation of synapses

Connectivity among neurons is required, and is present in massive amounts in order to generate synchronous coupling and amplification, with enough amplitude to transmit the analog oscillatory information of chemical synapses[Hebb 1949]. This activity should be nonlinear and self-sustaining, as was observed in biological oscillators.

This nonlinear synchronisation behavior was first studied in a bigger scale than in this thesis, and only taking into account the diffusion coupling by Katchalsky [KATCHALSKY 1976]. He pointed out that a large number of nonlinear elements diffusely coupled, will give their properties of energy flow to the whole system. In this way, the system stabilises in a zero equilibrium state for $E=0$. Subsequently, the 1 system is driven progressively away from equilibrium, until a critical level is reached where a phase transition occurs for $E \neq 0$.

Cable Equation and chemical synapses

The cable equation is a one-dimensional diffusion equation, and it has been widely used to model the dynamics of diffusion at chemical synapses. When a pulse discharges at the axon terminal, some of the vesicles in the pre-synaptic neuron discharge their contents into the synaptic cleft, this discharge has been understand as homogeneous. In chapter 5 of this thesis, I explain the oscillatory nature of this discharge, and in Chapter 4 the characteristics that can be observed in the coupling between oscillators.

The chemicals, ions and neurotransmitters directly in the synaptic cleft have not been measured. However, the concentration of this elements have been measured at the post-synaptic terminal, the concentration rises rapidly to a maximum value and then decays slowly[Pur 2008], components of the chemical information can be detected many milliseconds after a maximum of activity.

First theoretical study of Synchronisation.

Balthazar van Der Pol studied Synchronisation theoretically for the first time. He worked synchronising triode generators from vacuum tubes. This research gave rise to the field of nonlinear dynamics given that he observed that all initial conditions of the triode generator converged to the same final periodic orbit.[Strogatz 2001] In trying to model this behaviour, they found equations of the phenomenon that couldn't be solved as we are used to solve linear equations, nonlinear Van Der Pol system of equations, that we derive and analyse in this research for the case in which there are two Van Der Pol oscillators connected by one resistance, a separate case where they are connected by an inductance and connected by both Resistance and Inductance.

⁶⁸
A qualitative analysis of the system of equations is:

$$\ddot{X} + \mu \dot{X}(X^2 - 1) + X = 0 \quad (2.1)$$

From the first and last term we can have an idea of the system that we are analyzing, and how we are going to model it because these two terms reflect the nature of an harmonic oscillator that is modelled by inductance and capacitance. However, the term in the middle reflects a different oscillatory behaviour, this is a damping nonlinear term that is originated by the functioning of vacuum tubes. We can see that the damping in the system ²¹ can be positive or negative depending on the value of X . If $X > 1$, it is a normal damping that tends to make the amplitude of the oscillations decay. But, if $X < 1$ it is a negative damping which means pumping, this tends to amplify the amplitude of the oscillation [Strogatz 2001].

Another important effect that must be taken into account, is the secondary effect that the neurotransmitter release of a presynaptic terminal can have in neighbouring postsynaptic dendrites. There is a high possibility of having this cascade amplification given the analogous dispersive nature of the synapse signal and more importantly, given the required amplification of the signal.

¹
The wave to pulse conversion process, depends on the steady state level of the total dendritic synchronisation, and its coincidence with the refractory period of the pulse (about 1 msec), during which no amount of stimuli can induce another pulse. Subsequently, there is a period lasting several milliseconds, in which an additional stimuli can induce a second pulse, only if the second stimuli is larger than the first. Given all this constraints, the wave to pulse transformation is nonlinear and variable in time, if a steady above-threshold current is passed across the membrane, the train pulse has a high frequency, but this frequency depend on many other parameters that make it variable in time.

2.1.3 Experimental Biological facts on subthreshold activity

Two interesting neural models are mitral cells and pyramidal cells given the experimental detection of subthreshold oscillations among them, however this does not mean that oscillations cannot be found in other neurons or that it is not a general

property of neurons but that we have to look at the conditions of the networks or the synaptic distribution that is allowing this property in this neurons in comparison to the ones that do not have this.

The following section is an analysis of the paper [Desmaisons *et al.* 1999]. There are many complications in the modelling of sub-threshold oscillations, one of them is the slow versus fast time scale integration and the main question is why nonlinearity allows neurons to integrate synaptic events in a very precise temporal fashion. In this paper membrane potentials are filtered, stored and analyzed. The current injected to produce oscillations is of the form of the cosine function and the current injected to mimic the excitatory postsynaptic potentials (EPSP) is a poisson like function. they used as membrane potential the average potential during a period without spikes but including sub-threshold oscillations. The fast fourier transform is used to calculate the predominant sub-threshold frequency, the average cross correlation is going to give us the timing subthreshold oscillations.

It is interesting to recapitulate on how is it experimentally plausible to block EPSPs, they use three types of receptor antagonists, one for the iospecific ionotropic glutamate receptor, another for the NMDA receptor and one for the AMPA receptor. For the case in which it is desirable to block inhibitory postsynaptic potentials (IPSPs) that requires the activation of GABA receptors, then they use GABA receptor antagonist and Chloride channel blockade. For details regarding receptors and ionic conductances please refer to [Koch 1999]

The measurement of spontaneous subthreshold oscillations had an amplitudes of 2-5 mV. When the membrane potential is at -67 mV there was the first appearance of subthreshold oscillations, as found in [Desmaisons *et al.* 1999]. There is a high correlation in the frequency of oscillations and instantaneous spike frequency and the main finding that is the most interesting point for this thesis is that the action potentials were synchronized with the peak of the subthreshold oscillations. Another interesting finding is that oscillations were abolished after applying tetrodotoxin not calcium or ⁷⁶tassium affected their frequency but not their amplitude which suggest their importance in the modulation of the information content more than in the performance or efficacy, this is consistent with the periodicity of calcium oscillations

and it is a possible relation between the internal clock representations and their required synchronization with the external oscillation.

Spontaneous IPSP could reset the phase of spontaneous oscillations without affecting their amplitude frequency. Excitatory synaptic responses evoked by extracellular stimuli and the relationship between EPSP alone and the stimulation phase after subtraction of the sine wave response. Voltage dependent conductances do not participate in the phasing of spikes. Subthreshold oscillations of the membrane potential act as a timing device for the integration of EPSP into spikes. Whenever an EPSP impinges onto a mitral cell, the time corresponding to the highest probability for spike initiation will correspond to the peak of the next oscillation, when EPSPs occur in neighboring mitral cells with synchronized subthreshold oscillations, their triggered spikes will all occur within a narrow time window.

Granule cell activity may be synchronized, this permitting synchronization of GABA release onto clusters of mitral cells. If this interval is of the order of the mean interspike interval or longer, neurons act effectively as temporal integrators and transmit temporal patterns with only low reliability. If by contrast the integration interval is short compared to the interspike interval, neurons act essentially as coincidence detectors, relay preferentially synchronized input. Neurons that act as intrinsic pacemakers or cells that have selective membrane resonance in either sub or suprathreshold domains. Synaptic networks of intrinsically rhythmic neurons in layer 5 may generate or promote certain synchronised oscillations of the neocortex [Strogatz 2001].

Let me now consider the analysis of the paper [Zouweling *et al.* 2001], given its importance in our main for analysing the topology of real neurons and synapses distribution in the tuning of action potential generation. Models of how cellular properties affect reliability require subthreshold oscillations, resonance, reliable spike timing and intrinsic noise amplitude that will determine the number of reliable frequency bands. A nice biological example are prefrontal cortical pyramidal cell that have intrinsic preferences for restricted input frequency ranges, they also have sub-threshold oscillations and reliable spike trains when some input frequency bands are feed in.

When synaptic transmission is blocked it is possible to analyse the sub and suprathreshold responses of cells versus frequencies and amplitudes of sinusoidal current injections and it's found that the largest amplitude in the membrane potential correspond to the current input frequency ²⁷ similar to dominant frequencies of spontaneous subthreshold oscillations. It is also found resonance for subthreshold current injections and dendritic action potentials ⁴² are initiated more effectively by ²⁷ synchronous spatially clustered inputs than equivalent disperse inputs and the incorporation of noise in the pyramidal ⁷³ cell caused action potentials to occur outside this frequency range. The most important finding for the interest of this thesis is that influence of frequency content of the noise does not appear important for the study of reliability[⁷³ ouweling " et al. 2001].

A mathematical model for synaptic transmission

The following is an analysis of the model proposed by professor Llinas, please refer to [Llinás 1999]. The model considers a fifth order Michaelis-Menten kinetics consistent to the molecular changes that the ion channel suffer before opening, notice the cyclic behavior of the channel. This is the simpler model I could find that is computationally optimum for various synapses and at the same time is agrees with experimental voltage clamp data. The model is based in the following equations:

$$I_{Ca} = [G] \cdot j \quad (2.2)$$

$$[G] = [G]_0 \left[\frac{\kappa_1}{\kappa_1 + \kappa_2} [1 - \exp(-(\kappa_1 + \kappa_2)t)] \right]^n \quad (2.3)$$

$$j = \beta_1 \frac{Kc_0 \exp(-80V)}{1 + Kc_0 \exp(-80V)} \quad (2.4)$$

²³ Where j is the calcium current, V is the membrane voltage relative to absolute zero, K is the equilibrium constant in the transfer of ions from outside to inside. $[G]_0$ are the total of calcium channels open and close, $[G]$ are the open channels. κ is the Boltzmann constant and T is the absolute temperature. The forward and backward rate constants with z as the number of charges that moves across the membrane are:

$$\kappa_1 = \kappa_1^0 \exp(ez_1 V / \kappa T) \quad (2.5)$$

$$\kappa_2 = \kappa_2^0 \exp(ez_2 V / \kappa T) \quad (2.6)$$

if we compare this model with the one presented later in this document, we can appreciate the reduction in complexity while keeping the general observations. Even though this model is reduced, it also requires modelling the action potential with the HH equations in the presynaptic neuron and this is computationally hard. In the wave framework we are interested in the spontaneous latent activity of a neuron where the action potential stimulation is not required and where perturbations are generated by the interference pattern of activity. The notion of noise and background activity are relevant in this respect.

Noise and background activity

The following is an analysis of the noise input section in [Gerstner *et al.* 2014]. Here is well explained how must be modelled the noisiness of the input current, considering a deterministic and a stochastic component, this is with the aim of having models congruent with the noise results captured in the membrane voltage and synapses. If we do not add this term, the HH equations can not provide subthreshold fluctuations consistent with real data. For the case of the integrate and fire model of a neuron, the noise ⁵³ is added in the right-hand side of the differential equation of the voltage. The problem with this approach is that we result with stochastic differential equations that are hard to solve and computationally expensive. On the other hand, the explanation for this noise term is not consistent with biological measurements where the noise sources that come from ion channels and errors in transmission of neurotransmitter release are not enough with the amount of noise that this equations require to account and match with real data observations. That is why the wave interference proposal is self sustained in terms of noise given that it is produced by the different fluctuations given by the structure of the "slits".

Chapter 3

Methodological Proposal

3.1 Synapses collective behavioras synchronous oscillators model.

- Van der Pol oscillator as Synapse. Energy source through nonlinear resistor and pumping effect.
- Connection with inductance for magnetic field connectivity constraint.
- Generation of action potential at locations of maximum amplitude at interference pattern.
- Analog with Young's double slit problem for wave interference representation and wave-particle duality. Spatial locations of synapses are crucial in the interference pattern formation, connectomics is relevant.
- Synapses as wave generators that interfere to create a probability density of pulse generation in the form of constructive interference.
- This means that synapses cannot be added as discrete particles but they need to be added by the alternative additive and subtractive interference of waves. Pattern as a source of noise and possible tunneling effects analogy remembering that we are interested in the subthreshold regime where the ⁵⁷ amplitude of the signal is very small in comparison to the size of the barrier potential.

- Both, inhibitory and excitatory synapses (consequently excitatory and inhibitory neurons) can be modelled with the same equation but inhibition is expressed as the destructive interference.

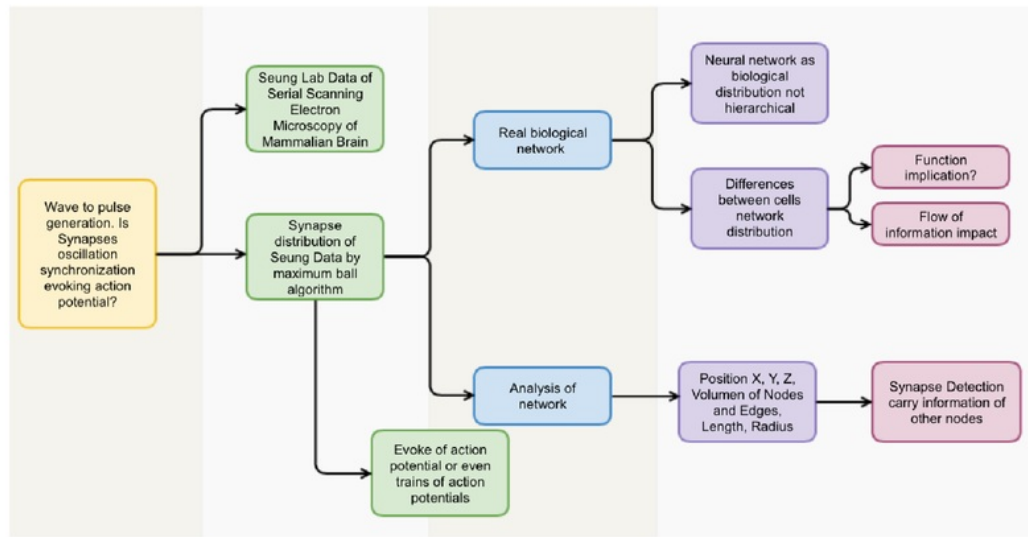


Figure 3.1: Workflow of proposal made in December 2016

3.1.1 Particle wave duality in neurons. Why waves at synapses?

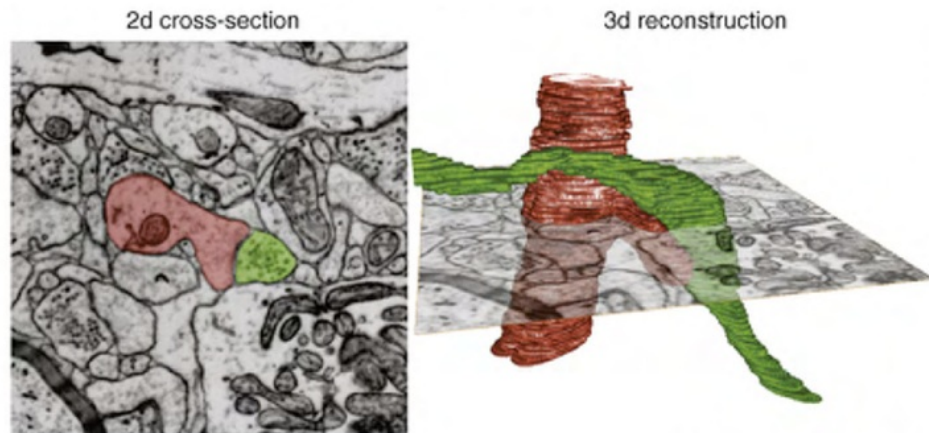
- Continuous flow of information, oscillations in nature are ubiquitous (mechanical (movement of fluids), electromagnetic (movement of ions))
- Explain the sparse activity of neurons (particle state or spike), most of the time neurons are not in the particle state (evoking action potentials) but they are not in the zero equilibrium point either, rest state requires the continuous flow of information (wave state).
- Transformation from the wave state to the particle state requires the addition and subtraction of waves in the interference pattern formation that depends on the other synapses and on the wave probability density.

- Model of the synapse is the same for all of them (biologically plausible oscillator) but location is special in the influence of the pattern formation (not always constructively).
- Learning in synapse (wave state) updates depending of the action potential (particle state). As the uncertainty principle where the certainty on position is constrained by the certainty in momentum and vice-versa
- Constant oscillation at the interior of the membrane, the potential is never zero, there is a non-stopping flow of information that happen without accounting for action potential initiation but assuming that it's interference is also responsible for background noise generation, then is a cyclic process that is sensible to small perturbations.
- Evoking an action potential can be observed as the fact that the wave synaptic state functions overlap and cause the locking of their phases creating a stronger state.
-

3.2 First stage results

3.2.1 Structure of a Neuron from a Stack of SEM Images

The following neurons were reconstructed thanks to the data acquired from Seung's Laboratory. It is of interest to work with this real data Biological Synapses network distributions. The connections and spatial distribution of synapses is going to be crucial in the interference pattern formation, it is desirable to work with real neurons topology. The process for the analysis of this data consists on the identification and segmentation of single neurons.



Source: Sebastian Seung (MIT)

Figure 3.2: The data in the reconstruction of the following neurons was acquired from Seung's Laboratory at MIT

3.2.2 Data processing and organisation

Using data from 3D neurons provided by Seung

- The 3D dataset provided by Seung consists of 776 single neurons, occupying a total of 36.18 GB (Around 6GB compressed).
- A neuron comes in one single file. The file comes in a binary format.
- The 3D geometry of the neuron is discretised in a 3D cartesian grid, that is around 1000x1000x1000.
- The file gives the (Z,Y,X) position of each voxel(one cubic element of the grid) that contains neuron in the grid.
- Once the data is organised, the result is a 3D representation of a neuron built by very small cubes.
- To export the file for the network extraction code the file size becomes immense, because cubes that did not have a neuron have to be exported to. The percentage of neuron in the 3D mesh is about 2 to 5 percent.

Visualization of a single neuron from the files.

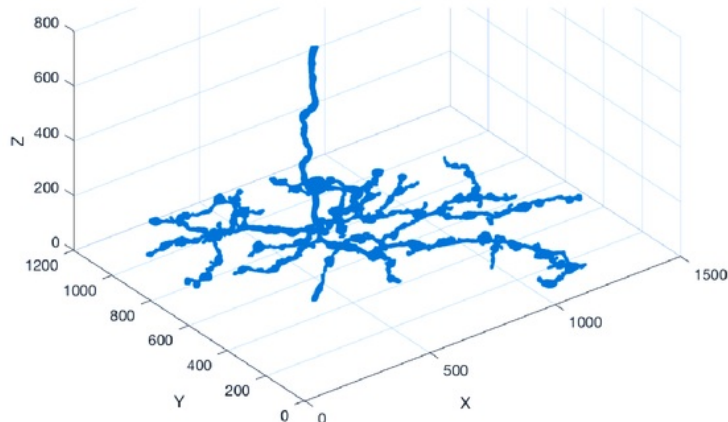


Figure 3.3

behavior

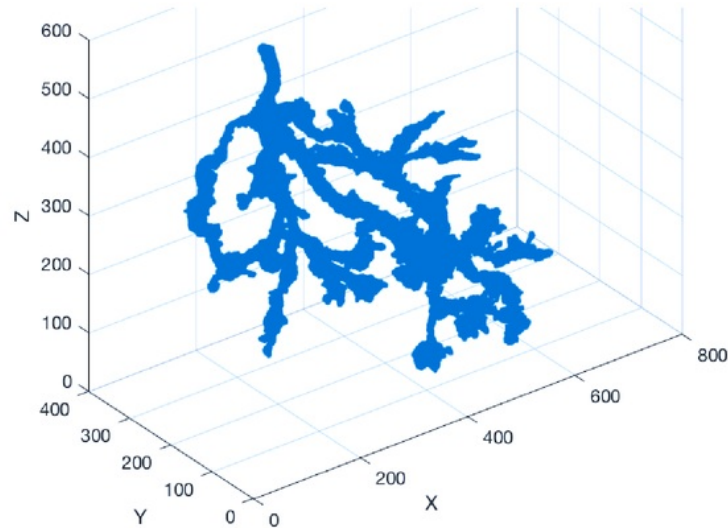


Figure 3.4: Output from the data files provided by Seung's Lab

Using the maximum ball algorithm to identify the synapses

- It provides a structural network of the neuron. Synapses can now be identified.

- The algorithm gives the location (X,Y,Z) of nodes and how they are connected in four files. An additional program provided by the author aids on the structural visualisation of the network.
- Implementation in a silicon-based neural architecture is highly convenient given that each node (synapse) are contact points that compare the input stimulus wave like signal acquired in the presynaptic neuron with the output wave probability density acquired in the postsynaptic neuron.
- Each synapse (slit as analog to the particle-wave duality) is the same (in terms of weight) but change depending on input output (in this sense is dynamic)
- Emphasis in location rather than in weight. Assuming Biological architecture and position are optimal and efficient.

Visualisation of a network.

For this visualisation of the obtained result from the ball's algorithm, a private software called Rhynos was used.

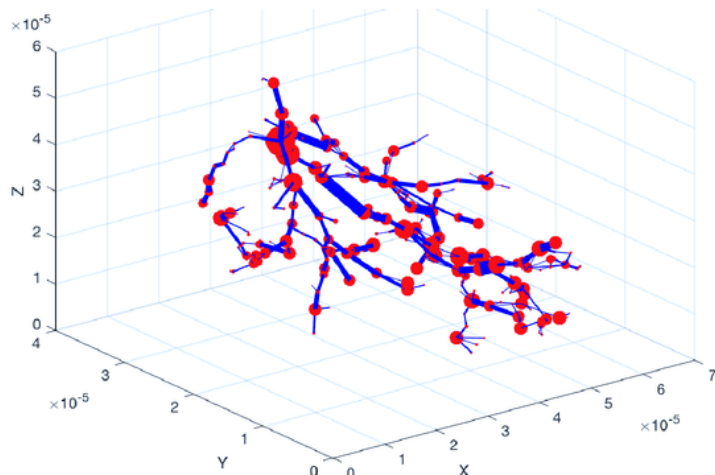


Figure 3.5: Result of the neuron analysis after applying the ball's algorithm

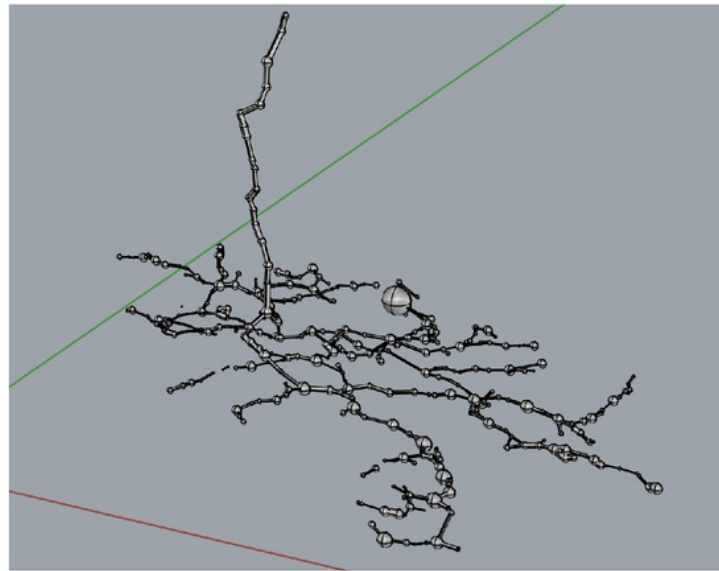


Figure 3.6: Visualisation obtained from Rhynos software

If the network architecture requires a bigger input, the connectome of a higher number of neurons can be build as presented in figure 3.7.

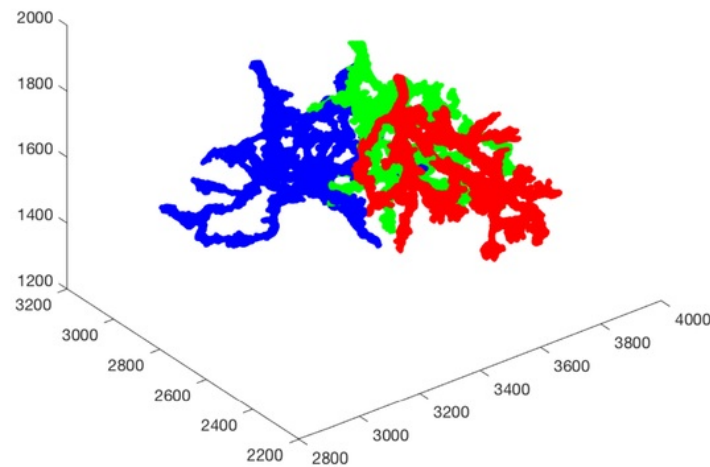


Figure 3.7: Visualisation of three neurons as obtained in the data files provided by Seung's Lab

The consequences of the proposed implementation is that it relies in dynamic variables and not constant. More accurate with real neurons and with nonlinear dynamics. More accurate with the fact that neuron activity is not gaussian but extremely sparse, like our analogy for the duality wave to particle. The wave is the input stimulus from sensory neurons (presynapse) and the pulse is the probability density in the postsynapse. The whole process is updated in the synaptic cleft.

Each synapse has wave like information from the stimulus and has an interaction is the form of wave interference with the other synapses in the network represented in the form of constructive and destructive interference patterns after information of the wave probability density is updated. The uncertainty principle of Heisenberg tell us that is not an increase in the number of synapses what makes the certainty in the pulse (spike) higher but the location and amplitude in the wave patter formation. Is the wave interaction what let us represent the probability density of the pulse and not the representation of the contact per se.

Each point contact is the representation of the synapse but is the meaning of the presence of another neuron. Information from this synapse is a value of uncertainty in the wave to pulse tranformation as the beautiful duality in wave to particle phenomenon in physics.

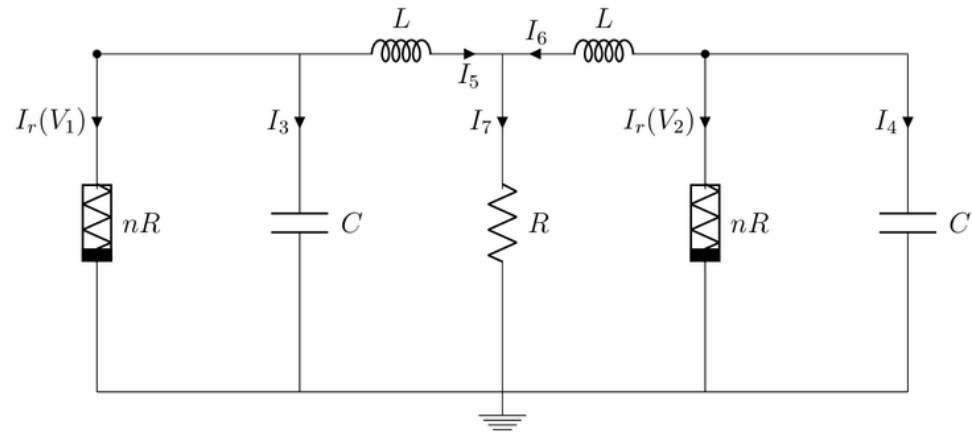
Chapter 4

Results

4.1 Hopf systems and synapse relation

4.1.1 Van Der Pol Oscillators coupled with Inductance-Resistance

Diagram of the electronic circuit model



Why is this circuit a good model for the study of synchronisation developed by Van der Pol? Because, the connection in series between the Inductance and Capacitor create an oscillation of the current and voltage to a resonance frequency. If the resistance weren't non linear, the amplitude of this oscillation will decrease to zero,

given the loss of energy caused by the resistance and the wires. However, this is not the case for this semiconductor resistance that we are going to analyse.

Equations for the electronic circuit model

Given the charges $+Q$ and $-Q$ inside the plates of the two capacitors and V_1 , V_2 being the voltage between the plates, then the capacitance C is given by:

$$V_1 = \frac{Q_3}{C}$$

$$V_2 = \frac{Q_4}{C}$$

Using Kirchhoff laws, we obtain the following equations that describe the system:

$$\begin{aligned} V_1 - L \frac{dI_5}{dt} - I_7 R &= 0 \\ V_2 + L \frac{dI_6}{dt} - I_7 R &= 0 \\ I_r(V_1) + I_3 + I_7 &= 0 \end{aligned} \tag{4.1}$$

$$\begin{aligned} I_7 &= I_5 + I_6 \\ I_r(V_2) + I_4 + I_7 &= 0 \\ -I_r(V) &= -g_1 V + g_3 V^3 \end{aligned} \tag{4.2}$$

- **Vacuum tubes, transconductance and Nonlinear resistance equivalence:** In our analysis of the system, there is a nonlinear resistance I_r in equation 4.1 and 4.2, that reflects the nonlinear resistance. This nonlinear resistance is a semiconductor and when a semiconductor is working in the triode region, its current ΔI_{out} is given by the transconductance g_m :

$$g_m = \frac{\Delta I_{out}}{\Delta V_{in}} \tag{4.3}$$

This is the relation between the Transconductance, that refers to the amount of conductance transferred. For our purpose, the semiconductor of interest is a vacuum tube, which transconductance is the change in the cathode voltage

with respect to a constant anode/cathode voltage and is given by:

$$g_m = \frac{\mu}{r_p} \quad (4.4)$$

In this relation for the vacuum tubes, we are relating the gain μ and the rate resistance r_p . Combining equations 4.3 and 4.4

$$\Delta I_{out} = g_m \Delta V_{in} \quad (4.5)$$

$$\Delta I_{out} = \frac{\mu}{r_p} \Delta V_{in} \quad (4.6)$$

$$\Delta I_{out} = \mu I_r \quad (4.7)$$

For solving this equations, it is necessary to create dimensionless variables for practicality. Remembering from our system of equations that:

- V_1 = Voltage in nonlinear resistance nR_1
- V_2 = Voltage in nonlinear resistance nR_2
- I_5 =Current in inductance L_1
- I_6 =Current in inductance L_2 .

Writing the set of equations in vector form, we have that:

$$\dot{X} = \begin{bmatrix} \dot{V}_1 \\ \dot{V}_2 \\ \dot{I}_5 \\ \dot{I}_6 \end{bmatrix} = \begin{bmatrix} -\frac{I_5}{C} - \frac{I_r(V_1)}{C} \\ -\frac{I_5}{C} - \frac{I_r(V_1)}{C} \\ (I_6 + I_5) \frac{R}{L} - \frac{V_1}{L} \\ (I_5 + I_6) \frac{R}{L} - \frac{V_2}{L} \end{bmatrix} = \vec{f}(x) \quad (4.8)$$

From the first component of our system of equations:

$$\dot{V}_1 = -\frac{I_5}{C} - \frac{I_r(V_1)}{C}$$

Using the equation for the nonlinear resistor, we have equation 4.2

$$C \frac{dV_1}{dt} = -I_5 + \mu(g_1 V_1 - g_3 V_1^3)$$

$$\begin{aligned}-I_3 &= \frac{dQ_3}{dt} = \frac{d}{dt}(CV_1) = C \frac{dV_1}{dt} \\ -I_4 &= \frac{dQ_4}{dt} = \frac{d}{dt}(CV_2) = C \frac{dV_2}{dt}\end{aligned}$$

Dimensionless set of equations

The results of equation 4.8 are the ones that we are going to make dimensionless. For this, we can declare the next variables:

$$V_1 = x_c X_1$$

$$t = t_c \tau$$

$$I = i_c \ell_1$$

Where $\ell = y$. We have to find x_c , t_c and i_c such that X_1 , τ and ℓ_1 don't have units. Replacing the dimensional variables in our system of equations:

$$\begin{aligned}\frac{Cx_c}{t_c} \frac{dX_1}{d\tau} &= -i_c \ell_1 + \mu(g_1 x_c X_1 - g_3 x_c^3 X_1^3) \\ \frac{dX_1}{d\tau} &= -\frac{i_c t_c}{C x_c} \ell_1 + \mu \left(\frac{g_1 x_c t_c X_1}{C x_c} - \frac{g_3 x_c^3 t_c X_1^3}{C x_c} \right) \\ \frac{dX_1}{d\tau} &= -\frac{i_c t_c}{C x_c} \ell_1 + \mu \left(\frac{g_1 t_c X_1}{C} - \frac{g_3 x_c^2 t_c X_1^3}{C} \right)\end{aligned}\quad (4.9)$$

To make the equations dimensionless, the terms that accompany the variables X_1 and X_1^3 must be set to 1, then:

$$\begin{aligned}\frac{g_1 t_c}{C} &= 1 \\ \frac{t_c}{C} &= \frac{1}{g_1}\end{aligned}\quad (4.10)$$

$$\frac{g_3 x_c^2 t_c}{C} = 1 \quad (4.11)$$

Replacing equation 4.10 in 4.11

$$\begin{aligned}\frac{g_3 x_c^2}{g_1} &= 1 \\ x_c &= \sqrt{\frac{g_1}{g_3}}\end{aligned}\quad (4.12)$$

LC characteristic equation

Now, we have to find the value of t_c , the result of this variable is very interesting because its value is where sine waves and oscillations are born, in order to do that we have to find the natural response of the system inductance-capacitance, so let's derive the famous characteristic equation of the LC system.

Using the relation of current voltage in a capacitor:

$$\begin{aligned} i &= -c \frac{dv}{dt} \\ v &= -\frac{1}{c} \int idt \end{aligned} \tag{4.13}$$

Now, from the relation of current voltage in an inductance:

$$v = L \frac{di}{dt} \tag{4.14}$$

Given that the voltage is the same, we can make equations 4.13 and 4.14 equal, obtaining:

$$\begin{aligned} L \frac{di}{dt} &= -\frac{1}{c} \int idt \\ L \frac{di}{dt} + \frac{1}{c} \int idt &= 0 \end{aligned}$$

Taking the derivative of the last expression:

$$\frac{d}{dt} \left[L \frac{di}{dt} + \frac{1}{c} \int idt = 0 \right]$$

Then, we get the second order homogeneous ordinary differential equation:

$$\begin{aligned} L \frac{d^2i}{dt^2} + \frac{i}{c} &= 0 \\ \frac{d^2i}{dt^2} + \frac{i}{Lc} &= 0 \end{aligned} \tag{4.15}$$

Solving for the current in the differential equation 4.15 with the next oscillatory initial guess:

$$\boxed{i(t) = Ke^{st}} \quad 66$$

Where K is the amplitude of the wave and s should have units of $1/t$ given that the exponential shouldn't have units. Then s has units of frequency. Replacing the proposed solution in equation 4.15.

$$\begin{aligned} \frac{d^2i}{dt^2} &= s^2Ke^{st} \\ s^2Ke^{st} + \frac{1}{LC}Ke^{st} &= 0 \\ s^2 + \frac{1}{LC} &= 0 \end{aligned}$$

²³ The last equation is the characteristic equation of the LC system.

$$s = \sqrt{-\frac{1}{LC}}$$

Given that s has units of 1 over time, we can conclude that:

$$\boxed{t_c = \sqrt{LC}} \quad (4.16)$$

Now, from equations 4.12 and 4.16, we can rewrite equation 4.9

$$\dot{X}_1 = -\frac{i_c t_c}{cx_c} \ell_1 + X_1 - X_1^3$$

Again setting the terms that accompany ℓ_1 to 1 and replacing the value of t_c and x_c :

$$\frac{i_c \sqrt{LC}}{C \sqrt{\frac{g_1}{g_3}}} = 1 \quad (4.17)$$

$$\boxed{i_c = \sqrt{\frac{C}{L}} \sqrt{\frac{g_1}{g_3}}} \quad (4.18)$$

After the last change of variable, we obtain:

$$\dot{X}_1 = -\ell_1 + X_1 - X_1^3 \quad (4.19)$$

Given our vector of equations in 4.8, we have that the third component for the current in the Inductance \dot{I}_5 is:

$$\begin{aligned}\dot{I}_5 &= (I_5 + I_6) \frac{R}{L} - \frac{V_1}{L} \\ L \frac{dI_5}{dt} &= (I_5 + I_6)R - V_1 \\ L \frac{di_c d\ell_1}{dt_c d\tau} &= i_c R(\ell_1 + \ell_2) - x_c X_1 \\ \frac{d\ell_1}{d\tau} &= \frac{i_c R t_c}{L i_c} (\ell_1 + \ell_2) - \frac{x_c t_c}{L i_c} X_1\end{aligned}\tag{4.20}$$

Replacing the values already found of x_c , t_c and i_c of equations 4.12, 4.10 and 4.17:

$$\begin{aligned}\frac{d\ell_1}{d\tau} &= \frac{R\sqrt{LC}}{L} (\ell_1 + \ell_2) - \sqrt{\frac{g_1}{g_3}} \frac{\sqrt{LC}}{L} \sqrt{\frac{L}{C}} \sqrt{\frac{g_3}{g_1}} X_1 \\ \frac{d\ell_1}{d\tau} &= R \sqrt{\frac{C}{L}} (\ell_1 + \ell_2) - X_1\end{aligned}$$

Setting a new variable $\boxed{\gamma = R \sqrt{\frac{C}{L}}}$, we obtain:

$$\dot{\ell}_1 = \gamma(\ell_1 + \ell_2) - X_1\tag{4.21}$$

Where variable ℓ can be named as variable $\ell = y$, then, our system of equations is:

$$\dot{X} = \begin{bmatrix} \dot{X}_1 \\ \dot{X}_2 \\ \dot{y}_1 \\ \dot{y}_2 \end{bmatrix} = \begin{bmatrix} y_1 + \mu(X_1 - X_1^3) \\ y_2 + \mu(X_2 - X_2^3) \\ \gamma(y_1 + y_2) - X_1 \\ \gamma(y_1 + y_2) - X_2 \end{bmatrix} = \vec{f}(x)\tag{4.22}$$

This is the case for just two Van Der Pol Oscillators, but it is easily extended to any number of oscillators.

Solving the system of equations with Matlab. Coupling with Inductance-Resistance

Listing 4.1: System of Linear Equations to be solved for Resistance-Inductance Coupling

```

function [X_dot] = RLcoupling(gamma, mu, t, X)
    11
    x1=X(1);
    x2=X(2);
    y1=X(3);
    y2=X(4);
    x1_dot=mu*(x1 -x1^3)-y1;
    x2_dot=mu*(x2 -x2^3)-y2;
    y1_dot=x1-gamma*(y1+y2);
    y2_dot=x2-gamma*(y1+y2);
    X_dot=[x1_dot; x2_dot; y1_dot; y2_dot];
end

```

12
Listing 4.2: Solver used to solve the System of Linear Equations of the Resistance-Inductance Coupling

```

% Two RL coupled oscillators solver
% Current parameter gamma = R sqrt(C/L)
gamma=0.1;
tSolution=[0,5000];
tStable=4000;
% Voltage parameter mu=g1 sqrt(L/C)
mu=0.1;
% STABLE SOLUTION
Xo=[1.4;1.4;1.4;1.4];
[t,X] = ode23t(@(t,X)RLcoupling(gamma,mu,t,X), tSolution, Xo);

% DIFFERENT INITIAL CONDITIONS
Xo=[1.4;-1.4;1.4;1.4];
[t2,X2] = ode23t(@(t,X)RLcoupling(gamma,mu,t,X), tSolution, Xo);

```

The values that were chosen for the coupling variable of the currents across each oscillator $\gamma = R\sqrt{\frac{C}{L}} = 0.1$ and for the magnitude of the non linearity variable μ were 0.1 for both. This value for μ , means that they were weakly coupled, the coupling was relative to the attractiveness of the limit cycle. The dominant effect of the coupling is to influence the motion of each oscillator around its limit cycle, without affecting its amplitude [Matthews *et al.* 1991]. Given that $0 < \mu < 1$, the vector field is not changing too much and as a consequence the expected orbits would be nearly circular. In the code, the variable tStable is used just for plotting purposes, because we are

interested in making the graph of the system when is already in a stable convergence point at the end of the solution.

Results of Simulation coupling Inductance-Resistance

Current-voltage relation for one oscillator and voltage-voltage relation for two oscillators

The appearance of the limit cycle is shown in fig: 4.1 when we take the relation between current Y_1 against voltage X_1 for one oscillator. This limit cycle is showing the periodicity nature of this relation given that their trajectories are converging to this circular trajectory in phase space, indicative of the nonlinear, self-sustained oscillator [Kawato *et al.* 1982].

On the other hand, the relation between voltages X_2 against X_1 for two oscillators is showing the anti-phase characteristic of their coupling. Their states have the same absolute values but opposite signs when the coupled oscillators achieve anti-synchronisation. Huygens was the first who observed the anti-synchronisation phenomenon also known as the anti-phase synchronisation [Jiang *et al.* 2016].

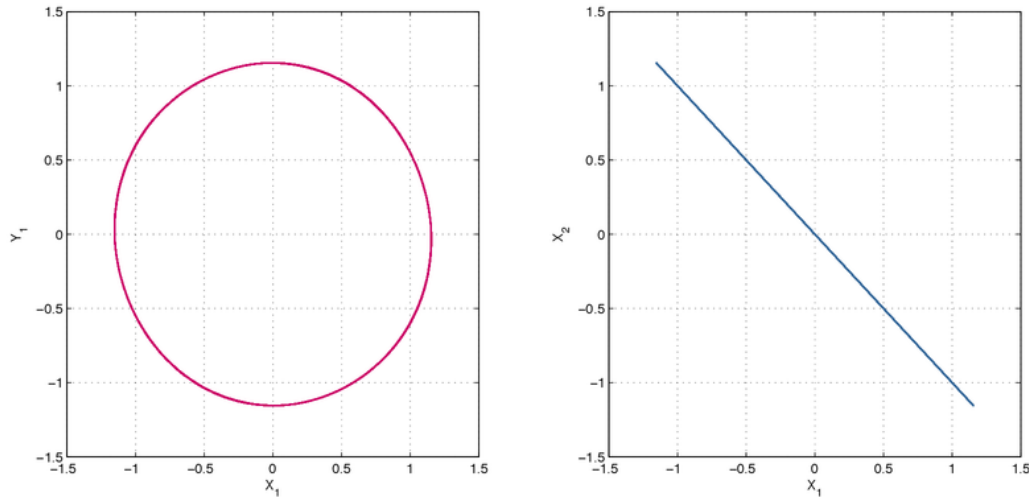


Figure 4.1: Left: Limit cycle appearance in relation Y against X for one oscillator. Right: Anti-phase synchronisation in relation X_2 and X_1 of two oscillators.

Current-voltage relation for two oscillators

Remembering that the current properties of the system reside in the variable Y and the voltage in X , then the current voltage behaviours of the two coupled oscillators are shown in fig: 4.2, here we see that the two oscillators are exactly attracted to the same limit cycle. This means that the coupling is not affecting their amplitude.

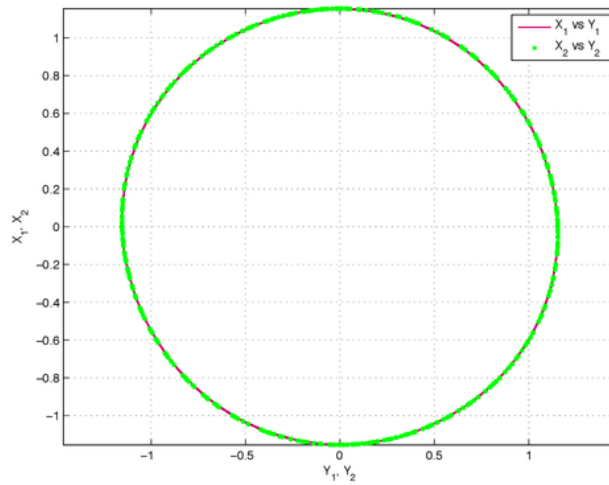


Figure 4.2: Limit cycle appearance in relation X_1 and X_2 against Y_1 and Y_2 for two oscillators.

Current-voltage relation for two oscillators with different initial conditions

Now, we are interested in analysing the case in which each oscillator has different initial conditions, they have the same absolute value but different sign in the voltage variable X_2 . As fig:4.3 shown, the change to anti-phase in the second oscillator doesn't have an effect in the coupling behaviour. The intuitive explanation to the observance of just anti-phase coupling for the RL connection between two oscillators is that the oscillations in the voltage of each oscillator will never be in phase given the nature of the inductance because it has a dynamic ⁶⁵ **second derivative term of the charge with respect to time** and the sign will always be in anti-phase with respect to the other given that this term is changing this sign repetitively and given that there are two inductance, the in-phase coupling is hard given this constant change in the sign.

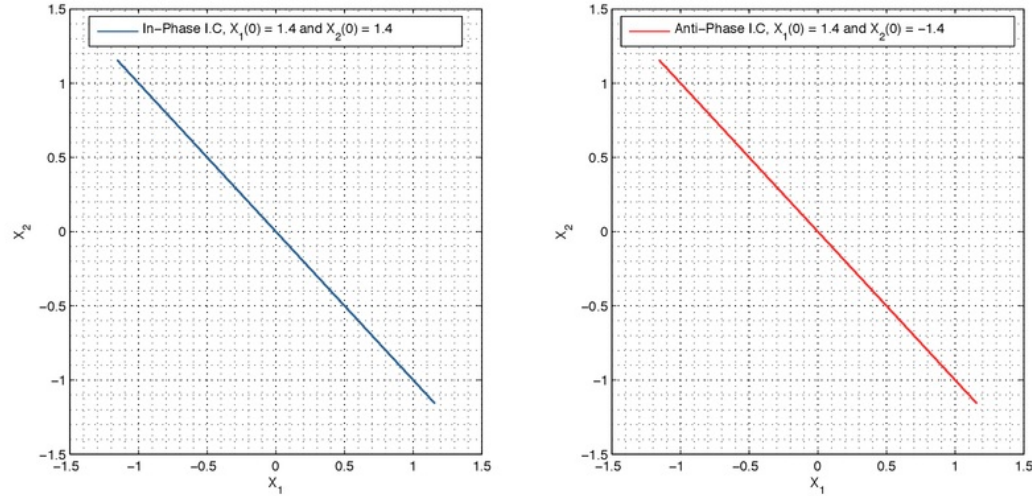


Figure 4.3: Relation X_2 against X_1 . Left: Same initial conditions. Right: Different initial conditions

Oscillatory responses of current and voltage

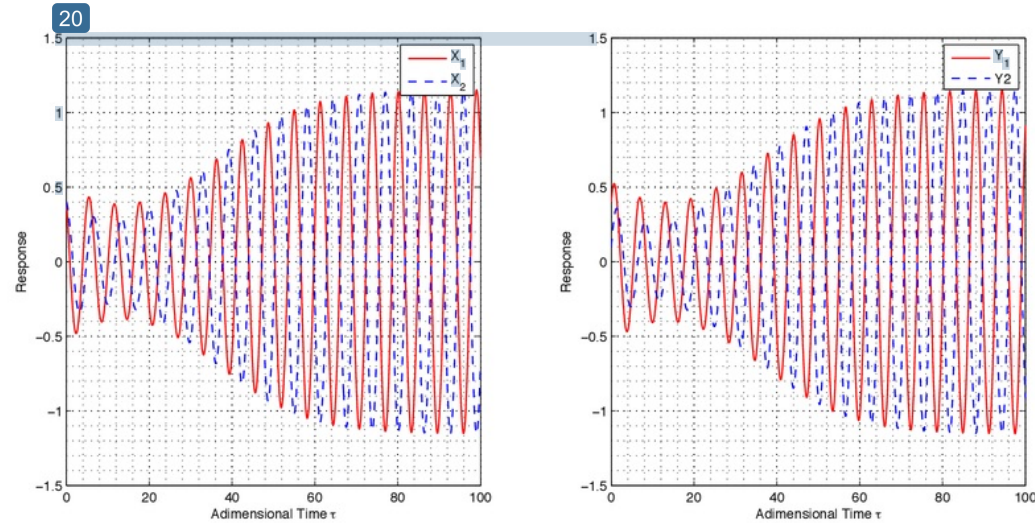
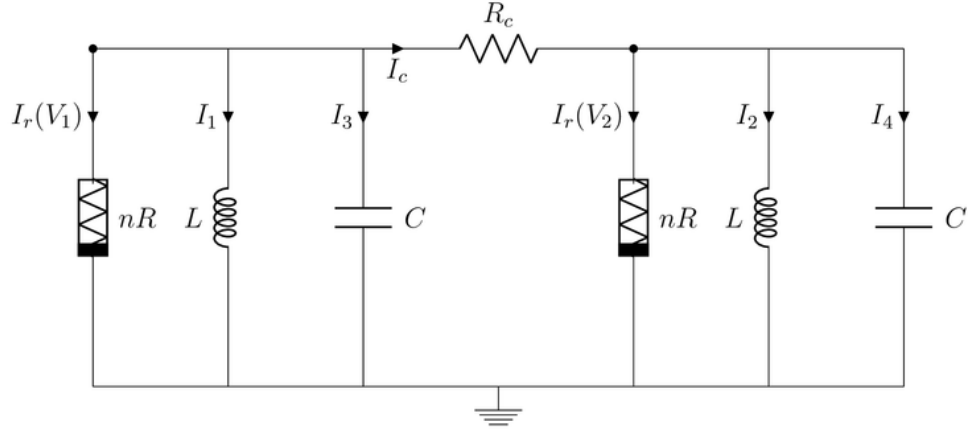


Figure 4.4: Oscillatory responses against dimensionless time. Left: X_1 and X_2 . Right: Y_1 and Y_2

4.1.2 ³³ Van Der Pol Oscillators coupled with Resistance

Diagram of the electronic circuit model



Equations for the electronic circuit model

Again, finding the current voltage equations of the system using the Kirchhoff laws and the capacitance equation, we can obtain:

$$V_1 = \frac{Q_3}{C}$$

$$V_2 = \frac{Q_4}{C}$$

Adding the voltages that cross the same node:

$$V_1 = L\dot{I}_1$$

$$V_2 = L\dot{I}_2$$

Using the fact that the input current in a node should be equal to the output current in the same node:

$$I_1 + I_R(V_1) + I_3 = I_c \quad (4.23)$$

$$I_2 + I_R(V_2) + I_4 = -I_c \quad (4.24)$$

Where the nonlinear resistance is given by the cubic term discussed before:

$$I_R(V) = -g_1 V + g_3 V^3$$

From the relation current to charge:

$$I_4 = \dot{Q}_4 = \dot{V}_2 C \quad (4.25)$$

$$I_3 = \dot{Q}_3 = \dot{V}_1 C \quad (4.26)$$

Rewriting equations 4.25 and 4.26 in terms of equations 4.23 and 4.24:

$$I_1 + I_R(V_1) + \dot{V}_1 C = I_c$$

$$I_2 + I_R(V_2) + \dot{V}_2 C = -I_c$$

The next equation is given by the coupling resistor:

$$-R_c I_c = V_1 - V_2$$

In summary, the system has five equations as follows:

$$\begin{aligned} L\dot{I}_1 &= V_1 \\ L\dot{I}_2 &= V_2 \\ C\dot{V}_1 &= -I_1 - I_c - (-g_1 V_1 + g_3 V_1^3) \\ C\dot{V}_2 &= -I_2 + I_c - (-g_1 V_2 + g_3 V_2^3) \\ R_c \dot{I}_c &= V_2 - V_1 \end{aligned}$$

Then, the set of equations are:

$$\begin{aligned} C\dot{V}_1 &= -I_1 + \frac{(V_1 - V_2)}{R_c} + g_1 V_1 - g_3 V_1^3 \\ C\dot{V}_2 &= -I_2 - \frac{(V_1 - V_2)}{R_c} + g_1 V_2 - g_3 V_2^3 \\ L\dot{I}_1 &= V_1 \\ L\dot{I}_2 &= V_2 \end{aligned}$$

Writing the set of equations in vector form, we have that:

$$\dot{X} = \begin{bmatrix} \dot{V}_1 \\ \dot{V}_2 \\ \dot{I}_1 \\ \dot{I}_2 \end{bmatrix} = \begin{bmatrix} \frac{-I_1}{C} + \frac{(V_1 - V_2)}{CR_c} + \frac{g_1 V_1 - g_3 V_1^3}{C} \\ \frac{-I_2}{C} - \frac{(V_1 - V_2)}{CR_c} + \frac{g_1 V_2 - g_3 V_2^3}{C} \\ \frac{V_1}{L} \\ \frac{V_2}{L} \end{bmatrix} = \vec{f}(x) \quad (4.27)$$

Dimensionless set of equations

Using again the dimensionless method, the variables are declared as follow:

$$\begin{aligned} V_1 &= x_c X_1 \\ t &= t_c \tau \\ I &= i_c \ell_1 \end{aligned}$$

Where $\ell = y$. We already derived x_c , t_c and i_c such that X_1 , τ and ℓ_1 don't have units. Using the results of the last section, we have:

$$\begin{aligned} x_c &= \sqrt{\frac{g_1}{g_3}} \\ t_c &= \sqrt{LC} \\ i_c &= \sqrt{\frac{C}{L}} \sqrt{\frac{g_1}{g_3}} \end{aligned}$$

The voltage and current in terms of the dimensionless variables are:

$$\begin{aligned} V_1 &= \sqrt{\frac{g_1}{g_3}} X_1 \\ t &= \sqrt{LC} \tau \\ I &= \sqrt{\frac{C}{L}} \sqrt{\frac{g_1}{g_3}} y_1 \end{aligned}$$

Replacing the last set of equations in our set of equations, obtaining:

$$\begin{aligned} C \sqrt{\frac{g_1}{g_3}} \frac{dX_1}{\sqrt{LC} d\tau} &= -\sqrt{\frac{C}{L}} \sqrt{\frac{g_1}{g_3}} y_1 + g_1 \sqrt{\frac{g_1}{g_3}} X_1 - g_3 \left(\sqrt{\frac{g_1}{g_3}} \right)^3 X_1^3 - \frac{(V_1 - V_2)}{R_c} \\ C \sqrt{\frac{g_1}{g_3}} \frac{dX_1}{\sqrt{LC} d\tau} &= -\sqrt{\frac{C}{L}} \sqrt{\frac{g_1}{g_3}} y_1 + g_1 \sqrt{\frac{g_1}{g_3}} X_1 - g_3 \left(\sqrt{\frac{g_1}{g_3}} \right)^3 X_1^3 - \frac{\left(\sqrt{\frac{g_1}{g_3}} X_1 - \sqrt{\frac{g_1}{g_3}} X_2 \right)}{R_c} \\ \sqrt{\frac{C}{L}} \frac{dX_1}{d\tau} &= -\sqrt{\frac{C}{L}} y_1 + g_1 X_1 - \frac{g_1}{3} X_1^3 - \frac{(X_1 - X_2)}{R} \\ \frac{dX_1}{d\tau} &= -y_1 + g_1 \sqrt{\frac{L}{C}} X_1 - \frac{g_1}{3} \sqrt{\frac{L}{C}} X_1^3 - \sqrt{\frac{L}{C}} \frac{(X_1 - X_2)}{R} \end{aligned}$$

From the terms that accompany X_1 , we are going to create the following variables:

$$\begin{aligned} \beta &= \frac{1}{R} \sqrt{\frac{L}{C}} \\ \mu &= g_1 \sqrt{\frac{L}{C}} \end{aligned}$$

Rewriting the current equation in terms of the new variable:

$$\boxed{\frac{dX_1}{d\tau} = -y_1 + \mu \left(X_1 - \frac{X_1^3}{3} \right) - \beta(X_1 - X_2)} \quad (4.28)$$

Now solving for the voltage equation:

$$\begin{aligned} V_1 &= L \frac{dI_1}{dt} \\ L \frac{dy_1}{\sqrt{LC} d\tau} \sqrt{\frac{C}{L}} \sqrt{\frac{g_1}{g_3}} &= \sqrt{\frac{g_1}{g_3}} X_1 \\ \boxed{\frac{dy_1}{d\tau} = X_1} & \end{aligned} \quad (4.29)$$

Setting the equations in a matrix form, we have:

$$\dot{X} = \begin{bmatrix} \dot{X}_1 \\ \dot{X}_2 \\ \dot{y}_1 \\ \dot{y}_2 \end{bmatrix} = \begin{bmatrix} -y_1 + \mu(X_1 - X_1^3) - \beta(X_1 - X_2) \\ -y_2 + \mu(X_2 - X_2^3) + \beta(X_1 - X_2) \\ X_1 \\ X_2 \end{bmatrix} = \vec{f}(x) \quad (4.30)$$

Solving the system of equations with Matlab. Coupling with Resistance

Listing 4.3: System of Linear Equations to be solved for Coupling with Resistance

```

function [X_dot] = Rcoupling(beta,mu,t,X)
x1=X(1);
x2=X(2);
y1=X(3);
y2=X(4);
x1_dot= mu*(x1 -x1^3)-y1-beta*(x1-x2);
x2_dot= mu*(x2 -x2^3)-y2+beta*(x1-x2);
y1_dot=x1;
y2_dot=x2;
X_dot=[x1_dot;x2_dot;y1_dot;y2_dot];
end

```

11 Listing 4.4: Solver used to solve the System of Linear Equations of the Coupling with Resistance

```

% Two R coupled oscillators solver
clear
%Current parameter gamma = R sqrt(C/L)
beta=0.1;
tSolution=[0,5000];
tStable=4000;
%Voltage parameter mu=g1 sqrt(L/C)
mu=0.1;

% STABLE SOLUTION
Xo=[1.4;1.4;1.4;1.4];
[t,X] = ode45(@(t,X)Rcoupling(beta,mu,t,X), tSolution, Xo);

% DIFFERENT INITIAL CONDITIONS
Xo=[1.4;1.4;1.4;1.4];
tSolution=[0,5000];
[t1,X1] = ode45(@(t,X)Rcoupling(beta,mu,t,X), tSolution, Xo);
Xo=[1.4;-1.4;1.4;1.4];
[t2,X2] = ode45(@(t,X)Rcoupling(beta,mu,t,X), tSolution, Xo);

```

The values that were chosen for the linear coupling variable of the currents across each oscillator $\beta = \frac{1}{R} \sqrt{\frac{L}{C}}$ and for the magnitude of the non linearity variable $\mu = g_1 \sqrt{\frac{L}{C}}$ were 0.1 for both. This is a weakly coupling, this means that they are coupled relative to the attractiveness of their limit cycles.

Results of Simulation coupling with Resistance

Current-voltage relation for one oscillator and voltage-voltage relation for two oscillators

The appearance of the limit cycle is shown in fig: 4.5 when we take the relation between current Y_1 against voltage X_1 for one oscillator, indicating the nonlinear, self-sustained nature of the oscillator. On the other hand, the relation between voltages X_2 against X_1 for two oscillators is showing the in-phase characteristic of the coupling with R, here they achieve synchronisation under the same initial conditions.

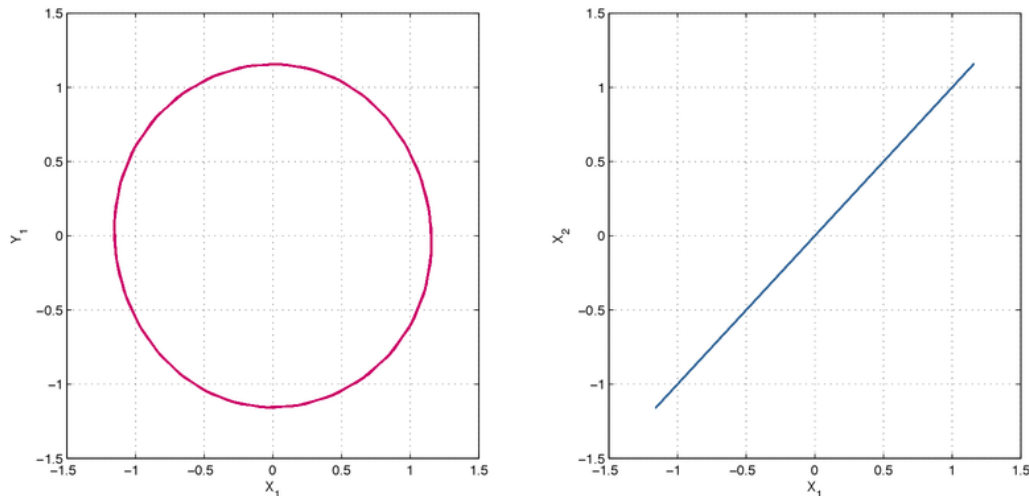


Figure 4.5: Left: Limit cycle appearance in relation Y against X for one oscillator. Right: In-phase synchronisation in relation X_2 and X_1 of two oscillators.

Current-voltage relation for two oscillators

Remembering that the current properties of the system reside in the variable Y and the voltage in X , the current voltage behaviours of the two coupled by R oscillators are shown in fig: 4.6, here we can see that the two oscillators are exactly attracted to

the same limit cycle in the phase state. This means that the coupling is not affecting their amplitude, just their trajectories to the limit cycle.

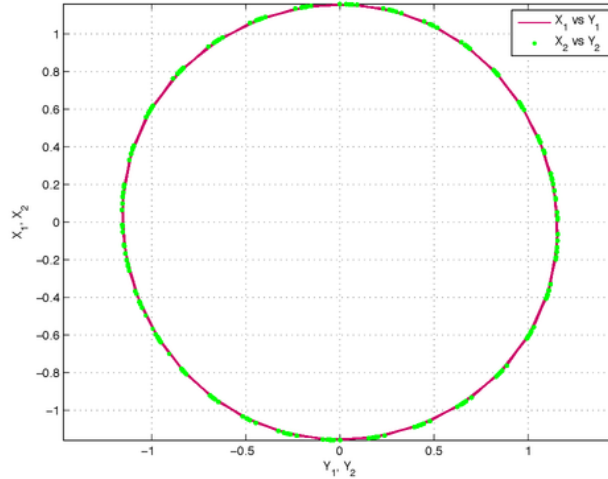


Figure 4.6: Limit cycle appearance in relation X_1 and X_2 against Y_1 and Y_2 for two oscillators.

Current-voltage relation for two oscillators with different initial conditions

In this case, the oscillators have the same absolute value for the initial condition but one of them have a different sign in the voltage variable X_2 . As fig:4.7 shown, the change of sign in the second oscillator doesn't have an effect in the coupling behaviour, both are in-phase with respect to each other, no matter the difference in phase at the beginning of the oscillation.

The intuitive explanation to this in-phase coupling for the R connection between two oscillators is that the resistance is dissipating energy, then it is not changing the oscillations in the voltage of each oscillator, given that it is not introducing any different source of energy. The pair of oscillators can use this resistance to send information with respect to each others voltage oscillation in order to find in phase synchronisation.

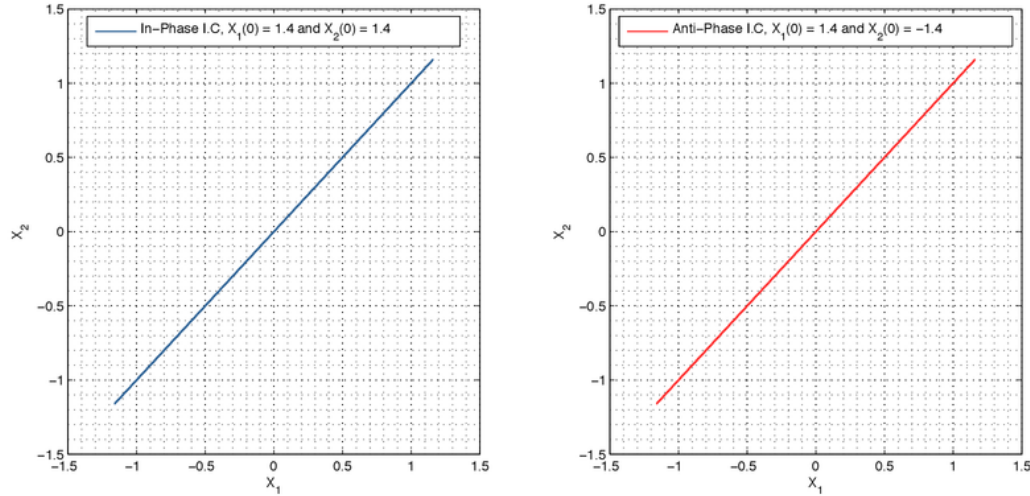


Figure 4.7: Relation X_2 against X_1 . Left: Same initial conditions. Right: Different initial conditions

Oscillatory responses of current and voltage

The oscillatory behavior of the current and voltages for the two oscillators can be seen in 4.8. The in-phase synchronisation achieves stabilisation of their periodic oscillation at $t=20$, however, the simulation goes until 100 to show that the periodicity remains after the steady state. The in-phase characteristics are present in current and in voltage.

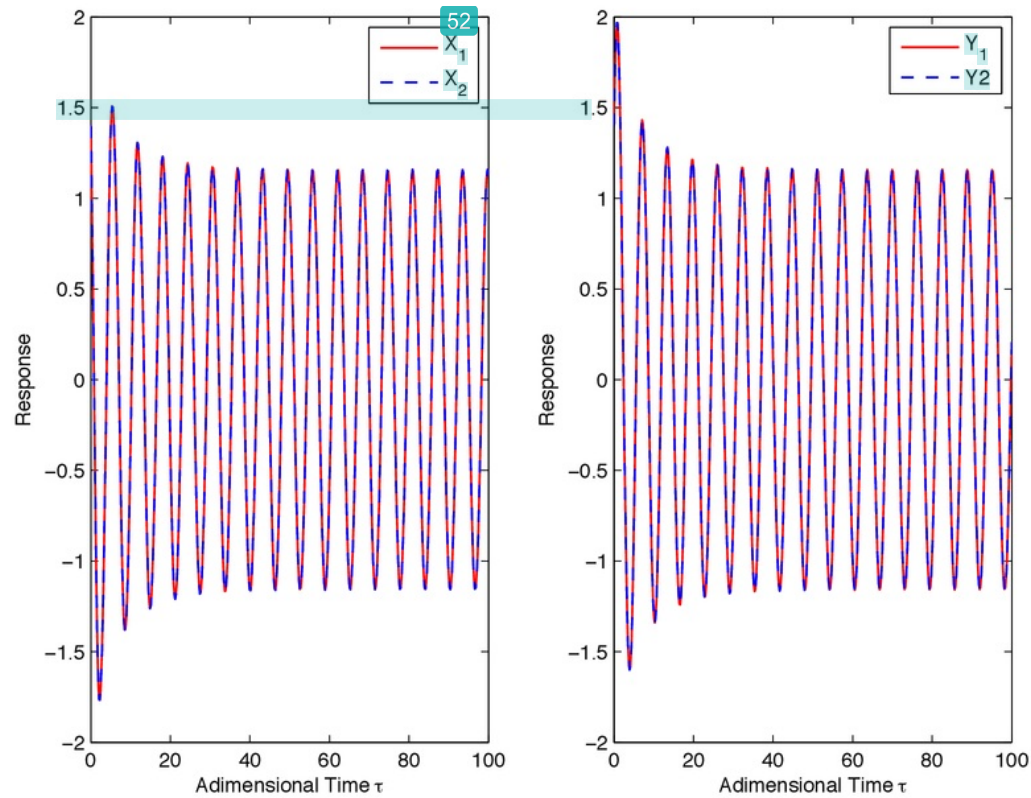
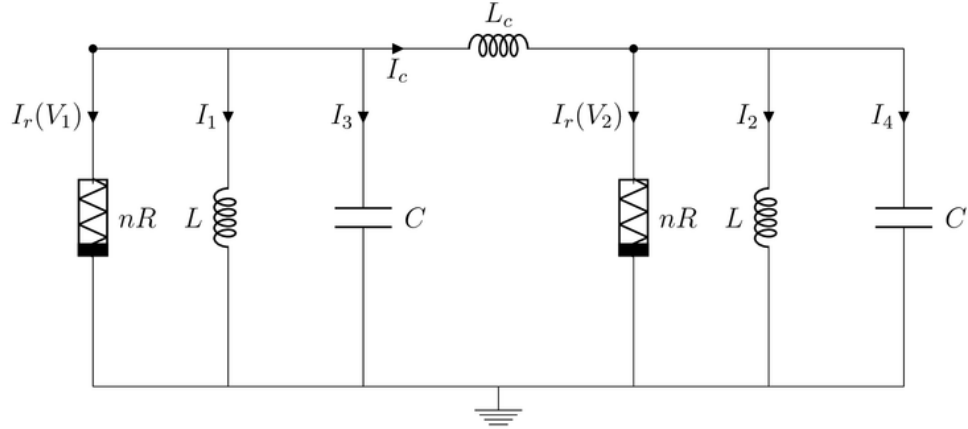


Figure 4.8: Oscillatory responses against dimensionless time. Left: X_1 and X_2 . Right: Y_1 and Y_2

33 4.1.3 Van Der Pol Oscillators coupled with Inductance

Diagram of the electronic circuit model



Equations for the electronic circuit model

Again, finding the current voltage equations of the system using the Kirchhoff laws and the capacitance equation, we can obtain:

$$\begin{aligned} V_1 &= \frac{Q_3}{C} \\ V_2 &= \frac{Q_4}{C} \end{aligned}$$

Adding the voltages that cross the same node:

$$\begin{aligned} V_1 + L\dot{I}_1 &= 0 \\ V_2 + L\dot{I}_2 &= 0 \end{aligned}$$

Using the fact that the input current in a node should be equal to the output current in the same node:

$$I_1 + I_R(V_1) + I_3 = -I_5 \quad (4.31)$$

$$I_2 + I_R(V_2) + I_4 = I_5 \quad (4.32)$$

Where the nonlinear resistance is given by the cubic term discussed before:

$$I_R(V) = -g_1V + g_3V^3$$

From the relation current to charge:

$$I_4 = \dot{Q}_4 = \dot{V}_2 C$$

$$I_3 = \dot{Q}_5 = \dot{V}_3 C$$

Rewriting equations 4.31 and 4.32 in terms of the voltages:

$$\begin{aligned} I_1 + I_R(V_1) + \dot{V}_3 C &= -I_5 \\ I_2 + I_R(V_2) + \dot{V}_2 C &= I_5 \end{aligned}$$

The last equation corresponds to the coupling inductance and is given by:

$$-L_c \dot{I}_5 = V_1 - V_2$$

In summary, the set of equations are:

$$\begin{aligned} L \dot{I}_1 &= -V_1 \\ L \dot{I}_2 &= -V_2 \\ C \dot{V}_3 &= -I_5 - I_1 - (-g_1 V_1 + g_3 V_1^3) \\ C \dot{V}_2 &= I_5 - I_2 - (-g_1 V_2 + g_3 V_2^3) \\ L_c \dot{I}_5 &= V_2 - V_1 \end{aligned}$$

Dimensionless set of equations

Following the same procedure for normalisation as was done in the last two sections:

$$C \frac{dV_1}{dt} = -I_5 - I_1 + g_1 V_1 - g_3 V_1^3$$

Using the change of variables: $V_1 = x_c X_1$, $I_1 = i_c y_1$ and $t = t_c \tau$ with $t_c = \sqrt{LC}$.

$$\begin{aligned} x_c &= \sqrt{\frac{g_1}{g_3}} \\ i_c &= \sqrt{\frac{C}{L}} \sqrt{\frac{g_1}{g_3}} \end{aligned}$$

Replacing the set of equations with the new variables and using $\mu = \sqrt{\frac{C}{L}}g_1$, we get:

$$\begin{aligned}\frac{C}{\sqrt{CL}}\sqrt{\frac{g_1}{g_3}}\dot{X}_1 &= -\sqrt{\frac{C}{L}}\sqrt{\frac{g_1}{g_3}}y_1 - \sqrt{\frac{C}{L}}\sqrt{\frac{g_1}{g_3}}y_c + g_1\sqrt{\frac{g_1}{g_3}}X_1 - g_3\left(\sqrt{\frac{g_1}{g_3}}X_1\right)^3 \\ \frac{C}{\sqrt{CL}}\dot{X}_1 &= -\frac{C}{L}y_1 - \sqrt{\frac{C}{L}}y_c + g_1X_1 - g_3\left(\sqrt{\frac{g_1}{g_3}}\right)^2 X_1^3 \\ \dot{X}_1 &= -y_1 - y_c + \sqrt{\frac{C}{L}}g_1X_1 - \sqrt{\frac{C}{L}}g_1X_1^3 \\ \dot{X}_1 &= -y_1 - y_c + \mu(X_1 - X_1^3)\end{aligned}\quad (4.33)$$

Now, to find the coupling term y_c , we change the equation for the voltage and the current:

$$\begin{aligned}L\frac{dI}{dt} &= -V_1 \\ L\sqrt{\frac{C}{L}}\sqrt{\frac{g_1}{g_3}}\frac{1}{\sqrt{LC}}\dot{y}_1 &= -\sqrt{\frac{g_1}{g_3}}X_1 \\ \dot{y}_1 &= -X_1\end{aligned}\quad (4.34)$$

Replacing in the voltage across the coupling inductance and using the new variable $\alpha = \frac{L}{L_c}$:

$$\begin{aligned}L_c\dot{I}_c &= V_2 - V_1 \\ L_c\sqrt{\frac{C}{L}}\sqrt{\frac{g_1}{g_3}}\frac{1}{\sqrt{LC}}\dot{y}_c &= \sqrt{\frac{g_1}{g_3}}(X_2 - X_1) \\ \dot{y}_c &= \frac{L}{L_c}(X_2 - X_1) \\ \dot{y}_c &= \alpha(X_2 - X_1) \\ \dot{y}_c &= \alpha(-y_2 + \dot{y}_1) \\ y_c &= \alpha(y_1 - y_2)\end{aligned}\quad (4.35)$$

The normalized system of linear equations in a matrix form is:

$$\dot{X} = \begin{bmatrix} \dot{X}_1 \\ \dot{X}_2 \\ \dot{y}_1 \\ \dot{y}_2 \end{bmatrix} = \begin{bmatrix} -y_1 - \alpha(y_1 - y_2) + \mu(X_1 - X_1^3) \\ -y_2 - \alpha(y_1 - y_2) + \mu(X_2 - X_2^3) \\ -X_1 \\ -X_2 \end{bmatrix} = \vec{f}(x) \quad (4.36)$$

Solving the system of equations with Matlab. Coupling with Inductance

¹²
Listing 4.5: System of Linear Equations to be solved for the Inductance Coupling

```
function [X_dot] = IndCoupledOscillators(alpha, mu, t, X)
x1=X(1);
x2=X(2);
y1=X(3);
y2=X(4);

x1_dot = y1;
y1_dot = -x1 + alpha*(x2-x1) + mu*(y1-y1^3);
x2_dot = y2;
y2_dot = -x2 + alpha*(x1-x2) + mu*(y2-y2^3);
X_dot=[x1_dot;x2_dot;y1_dot;y2_dot];
end
```

¹²
Listing 4.6: Solver used to solve the System of Linear Equations of the Inductance Coupling

```
% Two coupled oscillators with inductancesolver
clear
alpha=0.1;
mu=0.1;
tSolution=[0,10000];
MaxStep=0.1*abs(tSolution(1)-tSolution(2)); % This is matlab
% default
tStable=9000;
% This options specify how we want the solver to behave, the solver
% tries different methods to achieve convergence of the system,
% in some cases it even tries implicit solvers.
```

```

options=odeset('Stats','off','MaxStep',MaxStp,'Jacobian'
,...  

@(t,X) JacobianIndCoup(alpha,mu,t,X)); % Max step of  

the  

%iteration, odeset('  

MaxStep',1e-3)  

% STABLE SOLUTION  

% X=[x1;x2;y1;y2];  

Xo=[0.4;0.4;0.4;0.4]; % x2=-1.4  

t,X] = ode23tb(@(t,X) IndCoupled0scillators(alpha,mu,t,X),...  

tSolution, Xo, options);  

% DIFFERENT INITIAL CONDITIONS  

Xo=[0.4;0.4;0.4;0.4];  

tSolution=[0,10000];  

[t1,X1] = ode23tb(@(t,X) IndCoupled0scillators(alpha,mu,t,X),...  

tSolution, Xo, options);  

Xo=[0.4;-0.4;0.4;0.4];  

[t2,X2] = ode23tb(@(t,X) IndCoupled0scillators(alpha,mu,t,X),...  

tSolution, Xo, options);

```

Result of Simulation coupling with Inductance

Current-voltage relation for one oscillator and voltage-voltage relation for two oscillators

The appearance of the limit cycle is shown in fig: 4.9 when we take the relation between current Y_1 against voltage X_1 for one oscillator, indicating the nonlinear, self-sustained nature of the oscillator even after the coupling with the inductance, this oscillatory behavior is still present. On the other hand, the relation between voltages X_2 against X_1 for the coupled oscillators is showing the in-phase characteristic of the coupling with R, here they achieve in-phase synchronisation under the same initial conditions, but they present anti-phase synchronisation under different initial conditions.

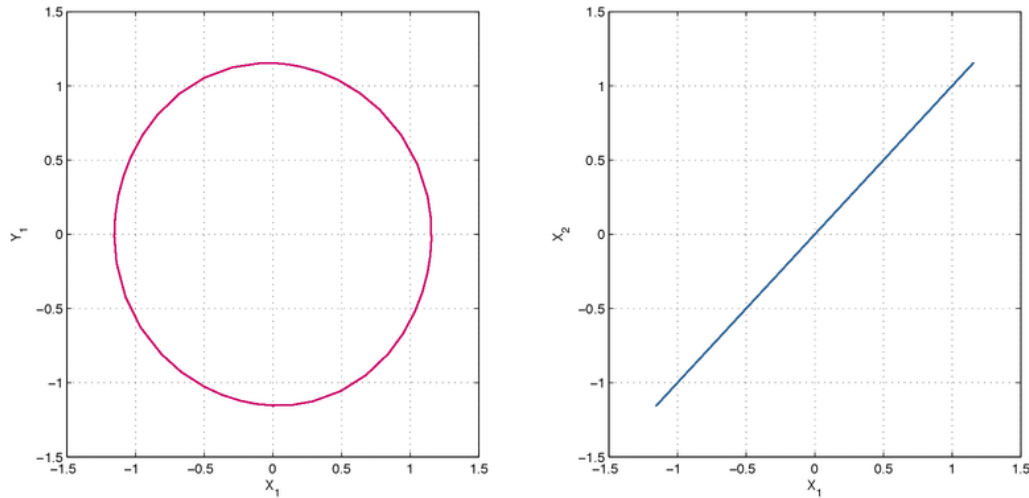


Figure 4.9: Left: Limit cycle appearance in relation Y against X for one oscillator. Right: In-phase synchronisation in relation X_2 and X_1 of two oscillators with the same initial conditions.

Current-voltage relation for two oscillators

The current voltage behaviours of the oscillators coupled by inductance are shown in fig: 4.10, here we can see that the two oscillators are attracted to the same limit cycle in the phase space. This means that the inductance coupling is weakly affecting their trajectory to the limit cycle. On the other hand, the coupling is allowing the in-phase and anti-phase synchronisation of the oscillators as can be seen in fig:4.11.

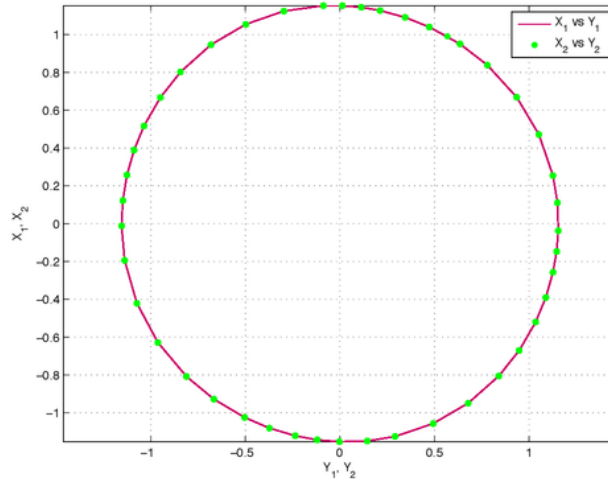


Figure 4.10: Limit cycle appearance in relation X_1 and X_2 against Y_1 and Y_2 for two oscillators.

Current-voltage relation for two oscillators with different initial conditions

In this case, the oscillators have the same absolute value for the initial condition but one of them have a different sign in the voltage variable X_2 . As fig:4.11 shown, the change of sign in the second oscillator generates the anti-phase synchronisation while the same initial conditions generate the in-phase synchronisation.

The intuitive explanation to the presence of in-phase and anti-phase synchronisation when oscillators are coupled for the inductance is the oscillatory nature of the inductance by its own, the second derivative term of this coupling is creating oscillatory dynamics in the shared medium between the two oscillators and it is keeping the information of their initial conditions.

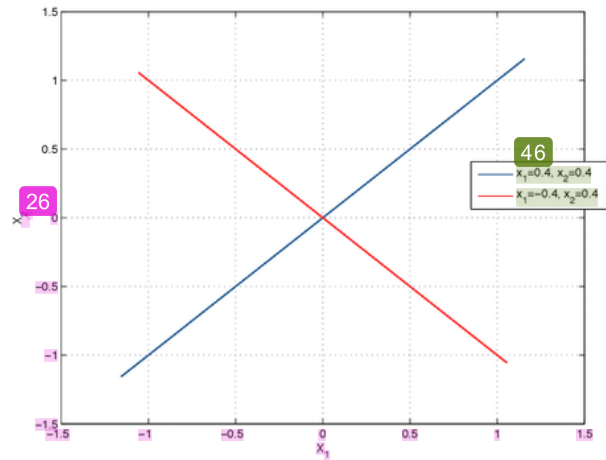


Figure 4.11: Relation X_2 against X_1 . In-phase synchronisation for same initial conditions and anti-phase synchronisation for different initial conditions

Oscillatory responses of current and voltage

The oscillatory behavior of the current and voltages for the two oscillators under same initial conditions can be seen in figure 4.12 and the oscillatory behavior of the current and voltages for the two oscillators under different initial conditions can be seen in figure 4.13. In the two cases we can appreciate the periodicity after the steady state is achieved. For the case of different initial conditions, it is possible to see that the anti-phase is maintained along time.

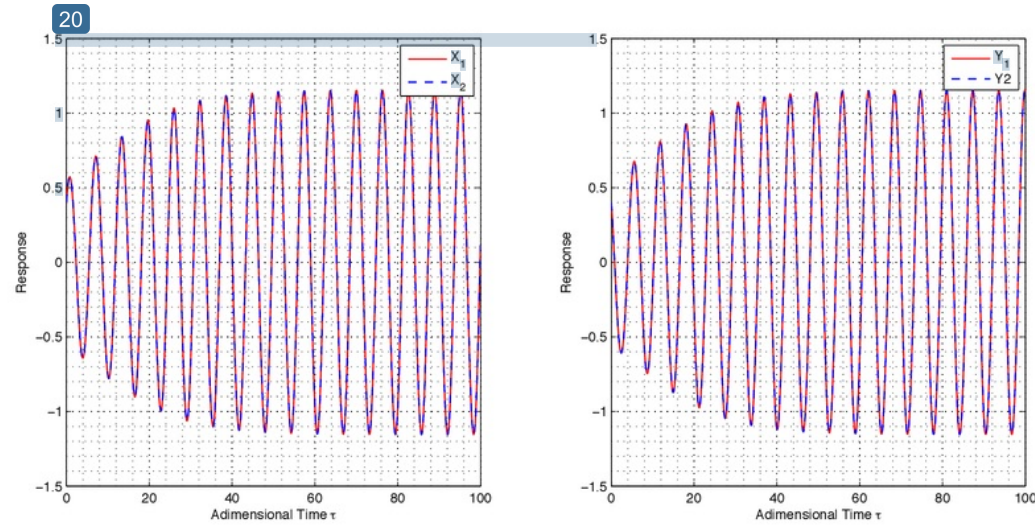


Figure 4.12: Oscillatory responses against dimensionless time under same initial conditions. Left: X_1 and X_2 . Right: Y_1 and Y_2

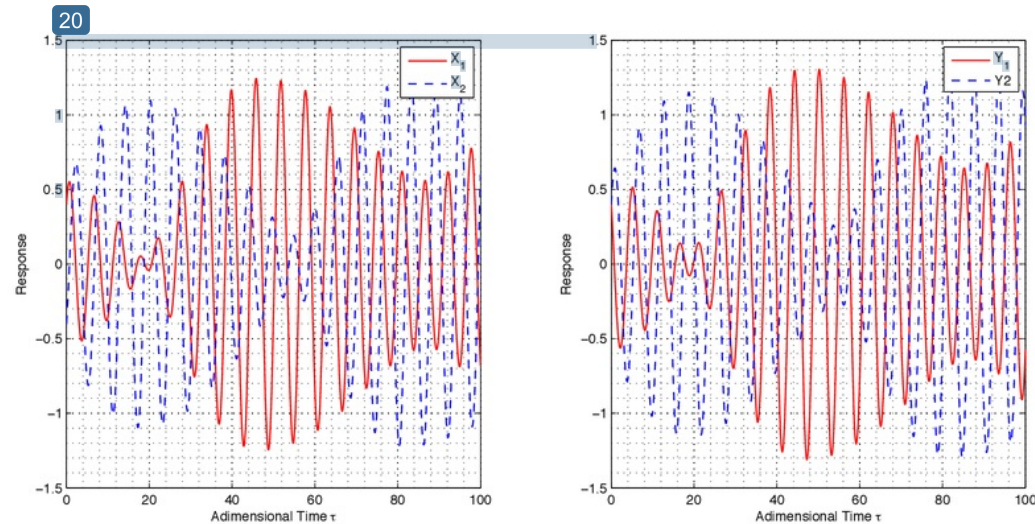


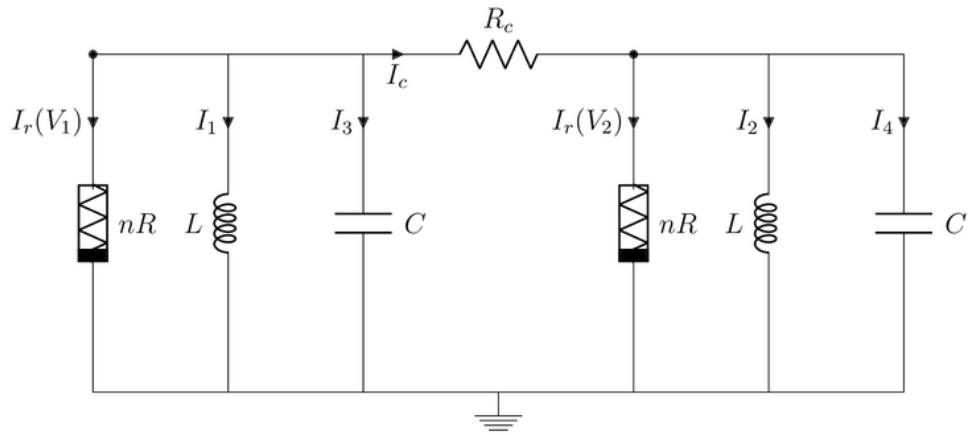
Figure 4.13: Oscillatory responses against dimensionless time under different initial conditions. Left: X_1 and X_2 . Right: Y_1 and Y_2

4.2 Experimental Results

4.2.1 Setup Electronic Circuit

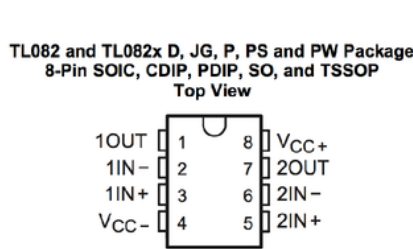
The initial objective of this thesis was to build the circuit for the two oscillators and find the limit cycle representative of their synchronous activity.

Van Der Pol Oscillators coupled with Resistance

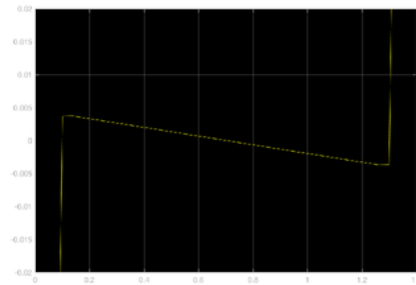


Nonlinear Resistance

The circuit used for the nonlinear resistor is an TL082x JFET-Input Operational Amplifier, the pin configurations are presented in fig: 4.14a. The nonlinear characteristics of this amplifier can be seen in fig:4.14b. In fig:4.15a is shown the setup



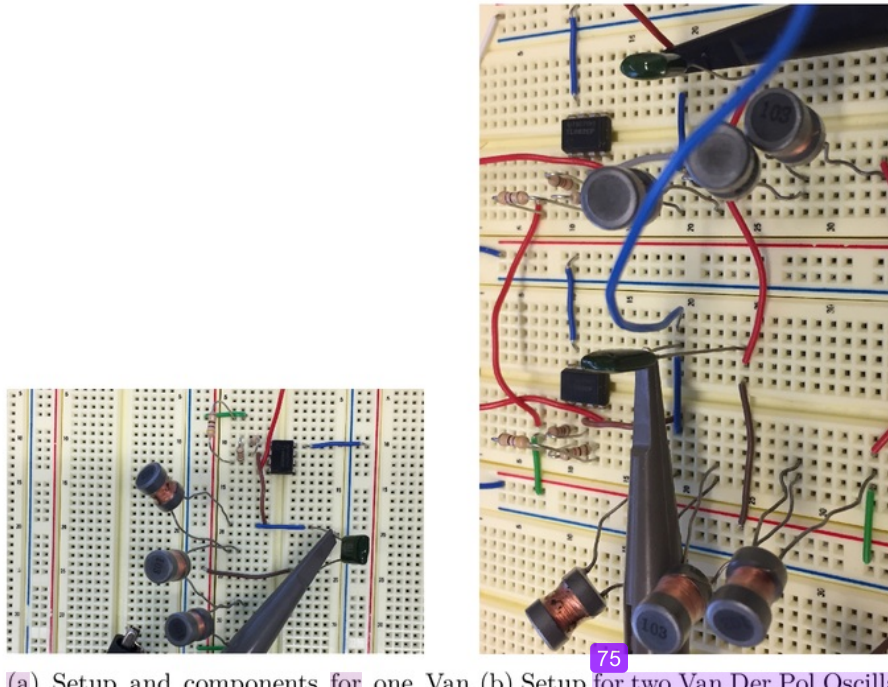
(a) Operational amplifier used as nonlinear resistor



(b) Nonlinear resistor response

for one Van Der Pol oscillator with its respective components. The inductance was

built by three inductance in series and the capacitance is the input to the external resistance. In fig:4.15b can be seen the setup for the two Van der Pol oscillators



(a) Setup and components for one Van Der Pol Oscillator (b) Setup for two Van Der Pol Oscillators connected by Resistance

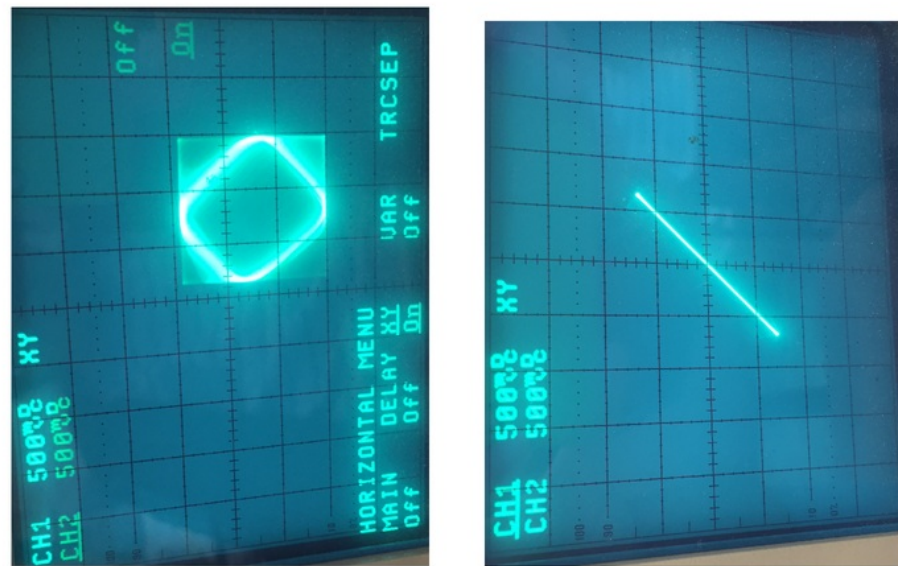
coupled by the external resistance. The value of the coupled resistance was changed until synchronisation was achieved.

4.2.2 Results experimental setup

In the next figures, we can see the oscilloscope results during the data acquisition. In subfigure 4.16a is the limit cycle that the trajectories of each oscillator are following in phase space. In subfigure 4.16b is the relation between the voltages of the two oscillators, they are synchronising in-phase as was expected to this type of coupling. In subfigure 4.16c are the oscillatory responses for the voltages of the two oscillators in time, their periodicity is in phase as was expected [Kuznetsov *et al.* 2009].

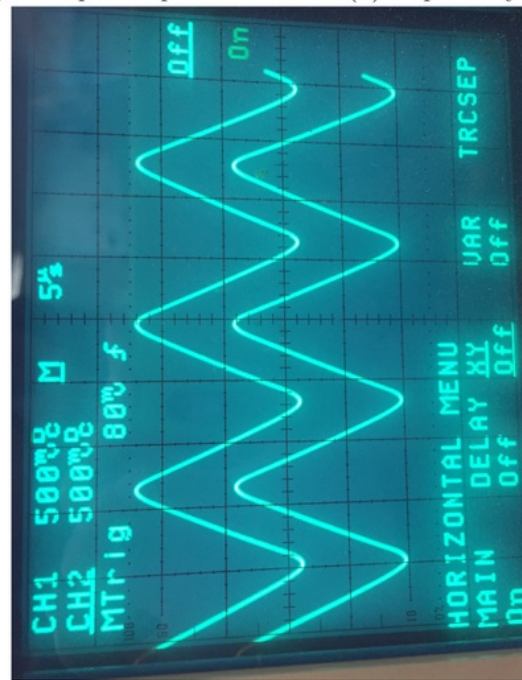
After this extensive analysis ²⁴ of the Van Der Pol oscillator and the different couplings between two Van Der Pol oscillators, it is of interest for the aim of this thesis, the coupling with an inductance given that this will generate periodical oscillations and

in-phase and anti-phase couplings, characteristics that were not presented in the other coupling elements. The central feature of the Van Der Pol oscillator is the nonlinear resistance which creates the pumping instate of damping for small perturbations, this effect is desirable in our model of subthreshold signal behavior at the synapse level.



(a) Limit Cycle in phase space

(b) In-phase synchronisation



(c) Oscillatory response for the two oscillators

4.3 Sub-threshold dynamical analysis

The motivation for the following analysis is the fact that we are interested in the transmission properties of subthreshold signals at the synapses. Here we are going to explore how this subthreshold signals behave in a collective manner where structural connectivity plays a crucial role. This theoretical analysis is performed to elucidate how real synaptic connectomics in neurons plays a different role in the creation of collective behaviour.

4.3.1 Signal-Coupled Sub-threshold Hopf-Type Systems Show a Sharpened Collective Response 18

The following is an analysis of the paper [Gomez *et al.* 2016]. Here they present the behavior of a Hopf-type system when it is coupled. First we start by analysing the equation of the system, and how it behaves:

$$\dot{z} = (\mu + i)\omega z - \omega|z|^2 z \quad (4.37)$$

This equation is better visualised if we separate its real and imaginary parts. Assuming that $z = x + iy$, we get:

$$\dot{z} = \dot{x} + i\dot{y} \quad (4.38)$$

$$\dot{x} = -x^3\omega - xy^2\omega + x\mu\omega - y\omega \quad (4.39)$$

$$\dot{y} = -y^3\omega - yx^2\omega + y\mu\omega + x\omega \quad (4.40)$$

By studying \dot{x} and \dot{y} , see figure 4.17. We can see that we have two possible states for this system, separated by a Hopf bifurcation at $\mu = 0$. The sub-threshold state (fig. 4.17a), in which the system decays regardless on the initial conditions, with $\mu < 0$. And the above-threshold state (fig. 4.17b), in which the real and imaginary part of the system oscillate in a stationary state, and the magnitude of z stays constant. Additionally, for $\mu > 0$ there is an unstable stationary point at $(x, y) = (0, 0)$ and a circular limit cycle at $\sqrt{x^2 + y^2} = r = \sqrt{\mu}$, in polar coordinates.

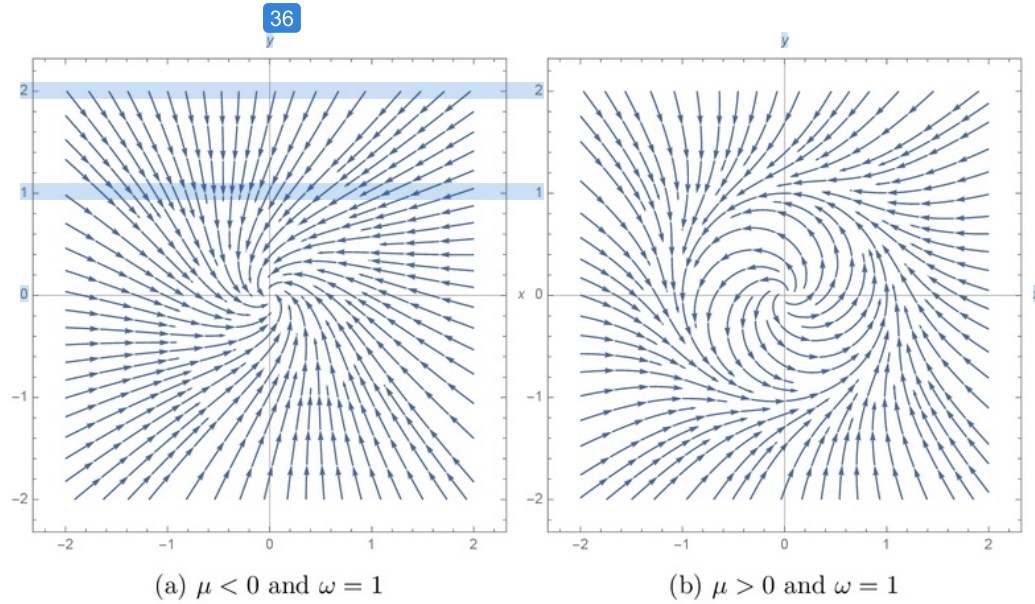


Figure 4.17: behaviorof the Hopf system considering it as a coupled system of two real differential equations.

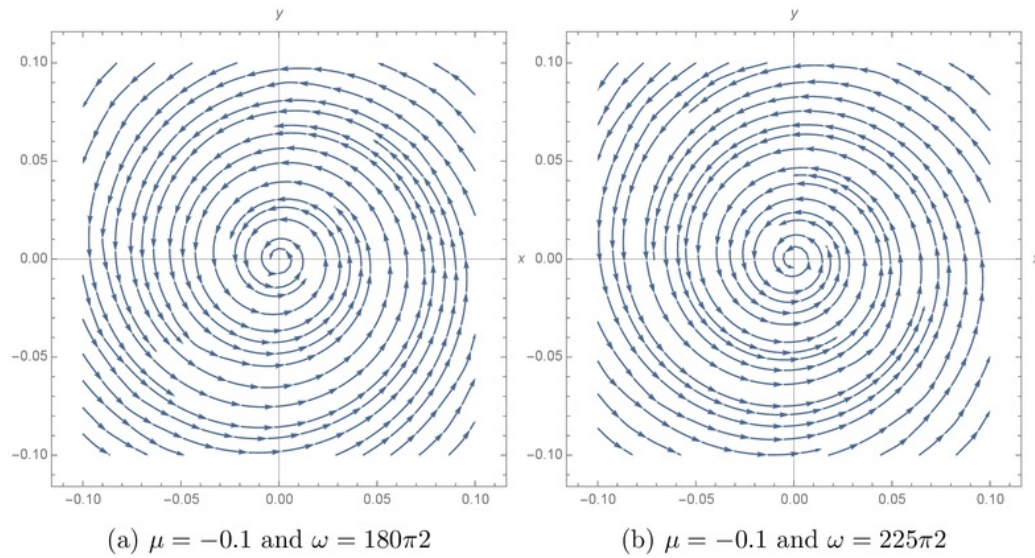


Figure 4.18: Oscillatory decay to fixed point of two Hopf systems with close frequencies

The systems under interest are a sub-threshold Hopf systems, in which the input signal is a weak signal, and it will decay to zero if the input is turned off. The systems will have $\mu < 0$, $\omega_1 = 180 \cdot 2\pi$ and $\omega_2 = 225 \cdot 2\pi$, their behavior can be seen in figures 4.18a and 4.18b, both system are relatively similar given their proximity in frequency, and they decay to zero overtime to their fixed point if there is not an input signal.

What is interesting to study is the coupling of these systems, when a small input signal is fed:

$$\dot{z}_1 = \omega_1 \left[(\mu + i)z_1 - |z_1|^2 z_1 + \frac{g_{21}}{2} z_2 + h_0 e^{i\omega t} \right] \quad (4.41)$$

$$\dot{z}_2 = \omega_2 \left[(\mu + i)z_2 - |z_2|^2 z_2 + \frac{g_{12}}{2} z_1 + h_0 e^{i\omega t} \right] \quad (4.42)$$

Here the coupling g_{21} ²¹ g_{12} , h_0 will have different small magnitudes and there will be a sweep in forcing frequency ω , to see the response of the system. What we are interested in seeing is the response of the system given the coupling.

The system is studied under different input amplitudes h_0 , in this case it will be studied for 20dB, 40dB and 60dB. In figure 4.19, the frequency response for different parameters can be observed. The upper curves in all plots on figure 4.19 are the 20dB response, the middle curves correspond to the 40dB, and the lower curves correspond to 60dB.

In figure 4.19a, we can see the frequency response of the two oscillators with a coupling of zero and a damping term of $\mu = -0.1$, the same for figure 4.19b, where the damping term is smaller.

In figure 4.19c, we can see how the coupling term brings the oscillators closer in the resonant frequency. However the coupling in figure 4.19c is not strong enough to cause a single resonant frequency of the two oscillators.

Figure 4.19d, shows the coupling that occurs when the coupling term is strong enough. Both oscillators have the same resonant frequency, and they resonate in

unison with the input signal. This resonance behavior motivates finding the coupling term $g = g_{21} = g_{12}$, for which the same resonant frequency for both oscillators appears.

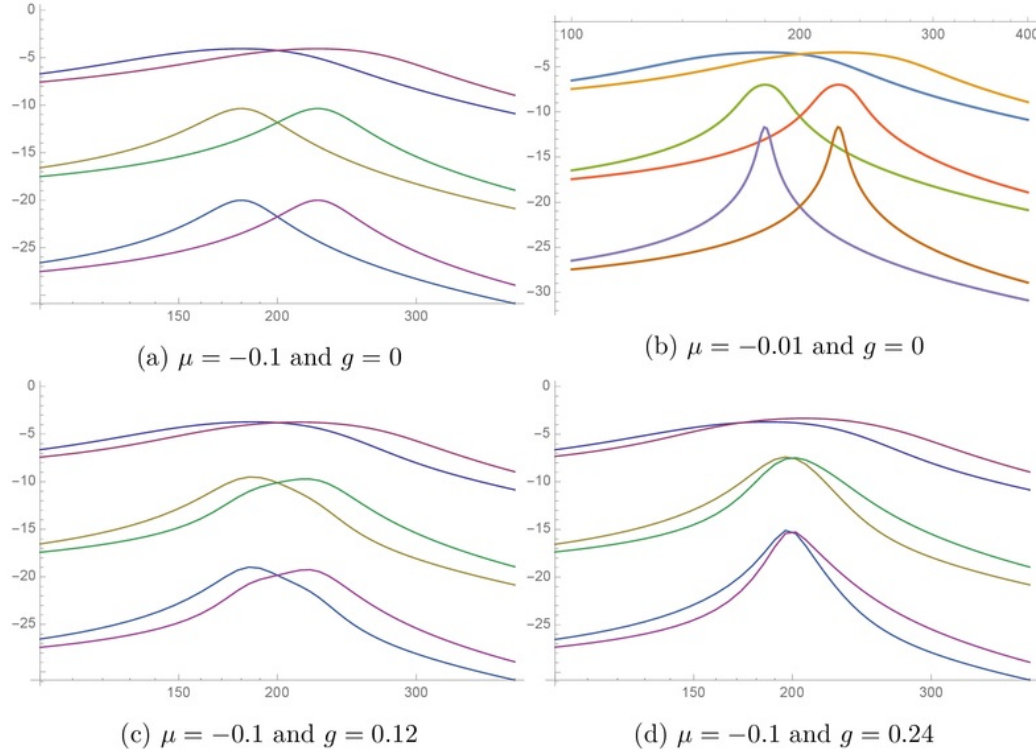


Figure 4.19: Influence of the coupling term.

The previous result motivates finding the critical coupling g_c at which the systems couple. For this we write the system 4.42 as a set of 4 real equations, and calculate the Jacobian for this system:

$$J = \begin{pmatrix} -3\omega_1 x_1^2 - y_1^2 \omega_1 + \mu \omega_1 & -2x_1 y_1 \omega_1 - \omega_1 & \frac{g \omega_1}{2} & 0 \\ \omega_1 - 2x_1 y_1 \omega_1 & -\omega_1 x_1^2 - 3y_1^2 \omega_1 + \mu \omega_1 & 0 & \frac{g \omega_1}{2} \\ \frac{g \omega_2}{2} & 0 & -3\omega_2 x_2^2 - y_2^2 \omega_2 + \mu \omega_2 & -2x_2 y_2 \omega_2 - \omega_2 \\ 0 & \frac{g \omega_2}{2} & \omega_2 - 2x_2 y_2 \omega_2 & -\omega_2 x_2^2 - 3y_2^2 \omega_2 + \mu \omega_2 \end{pmatrix} \quad (4.43)$$

Evaluated at the origin the Jacobian is:

$$J_{00} = \begin{pmatrix} \mu\omega_1 & -\omega_1 & \frac{g\omega_1}{2} & 0 \\ \omega_1 & \mu\omega_1 & 0 & \frac{g\omega_1}{2} \\ \frac{g\omega_2}{2} & 0 & \mu\omega_2 & -\omega_2 \\ 0 & \frac{g\omega_2}{2} & \omega_2 & \mu\omega_2 \end{pmatrix} \quad (4.44)$$

After a long algebraic development by hand and using the software mathematica, we can find when the eigenvalues real part is zero, to see where they cross the imaginary axis, in order to determine the critical coupling g_c for the system. The four eigenvalues for the jacobian J_{00} are:

$$\begin{aligned} \lambda_{1,2} &= \frac{1}{2}\Re\left(\mu(\omega_1 + \omega_2) \pm \sqrt{g^2\omega_1\omega_2 + (\mu + i)^2(\omega_1 - \omega_2)^2}\right) \\ \lambda_{3,4} &= \frac{1}{2}\Re\left(\mu(\omega_1 + \omega_2) \pm \sqrt{g^2\omega_1\omega_2 + (\mu - i)^2(\omega_1 - \omega_2)^2}\right) \end{aligned}$$

Making the first two eigenvalues zero, we get the implicit equation:

$$\mu(\omega_1 + \omega_2) = \Re\left(\sqrt{g_c^2\omega_1\omega_2 + (\mu + i)^2(\omega_1 - \omega_2)^2}\right) \quad (4.45)$$

To obtain the critical value of the coupling g_c . This equation is correct, it is worth highlighting that the original paper has an error in this equation(equation 4 in the paper), and it does not give the desired results, however 4.45 generates the correct answer.

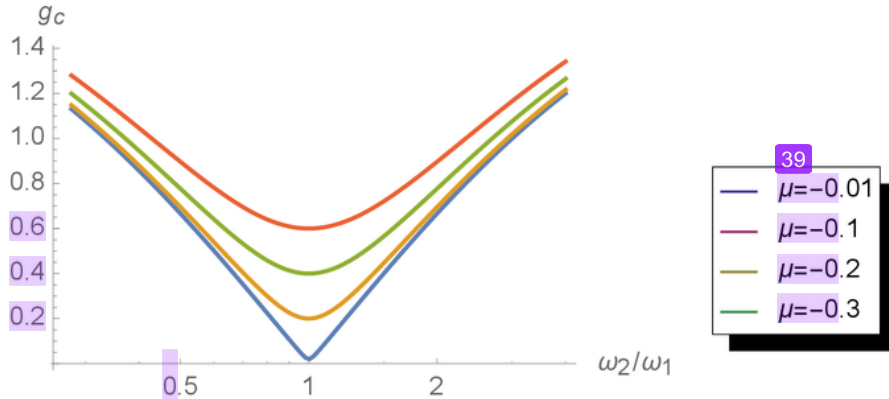


Figure 4.20: g_c as function of μ and the ratio of characteristic frequencies of the oscillators.

In figure 4.20 the critical coupling is evaluated for different characteristic frequencies of the oscillators, and different μ . It is clear, that the closer the characteristic frequencies of the system, the smaller the coupling needs to be for both systems to resonate at the same frequency, this happens for all μ in figure 4.20.

From now on, we want to extend the scope of the paper [Gomez *et al.* 2016] adding more elements and terms to the system of equations. First we can extend this to systems with more elements, and different characteristic frequencies, to see if all systems oscillate at the same frequency when coupled. It can be done for 10 oscillators, in this case for the frequencies 173, 179, 185, 191, 197, 203, 209, 215, 221, and 227 Hz. Figure 4.21 shows the coupling of the 10 oscillators for different μ values. If they were not coupled, each would resonate at their own frequency.

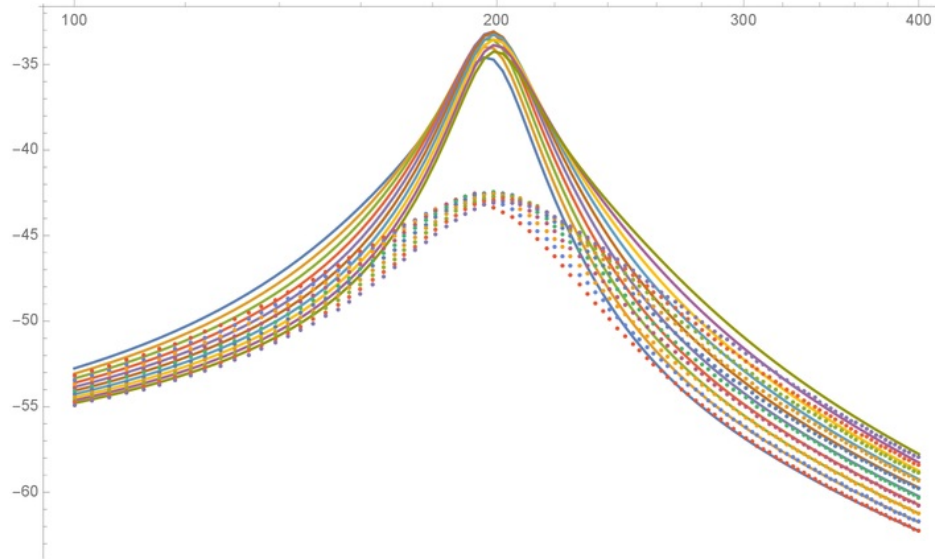


Figure 4.21: 10 oscillators with different characteristic frequency, for $\mu = -0.2$ and $\mu = -0.3$.

Subcritical System, adding a 5th order term

When we add a 5th order term to the equation we get, the following equation:

$$\dot{z} = (\mu + i)\omega z + \omega|z|^2z - \omega|z|^4z \quad (4.46)$$

Which can be separated into its real and imaginary parts getting:

$$\dot{z} = \dot{x} + i\dot{y} \quad (4.47)$$

$$\dot{x} = -\omega x^5 - 2x^3y^2\omega + x^3\omega + x\mu\omega - xy^4\omega + xy^2\omega - y\omega \quad (4.48)$$

$$\dot{y} = -\omega y^5 - 2y^3x^2\omega + y^3\omega + y\mu\omega - yx^4\omega + yx^2\omega + x\omega \quad (4.49)$$

We plot its \dot{x} and \dot{y} derivatives as function of x and y , in figure 4.22.

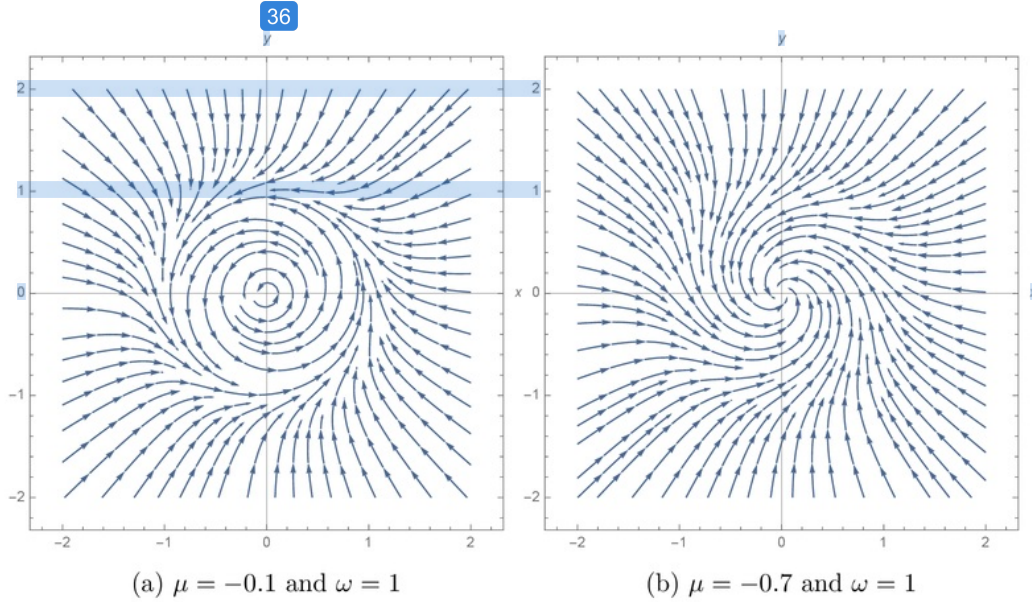


Figure 4.22: behavior of the subcritical system

Because of the 5th order term, this system is more sensitive to the value of μ , in comparison to what we found before. In figure 4.22a we see an stationary state for $\mu = -0.1$, and for $\mu = -0.7$ we see a fixed point at the origin.

If we couple two of such systems with different characteristic frequency we have:

$$\dot{z}_1 = \omega_1 \left[(\mu + i)z_1 + |z_1|^2 z_1 - |z_1|^4 z_1 + \frac{g_{21}}{2} z_2 \right] \quad (4.50)$$

$$\dot{z}_2 = \omega_2 \left[(\mu + i)z_2 + |z_2|^2 z_2 - |z_2|^4 z_2 + \frac{g_{12}}{2} z_1 \right] \quad (4.51)$$

In this case because our system oscillates spontaneously, we don't need a forcing term, but rather a very small initial condition, that should move the systems from the unstable origin. In figure 4.23, we see the behavior of the real parts of both systems, for $\mu_1 = \mu_2 = -0.1$, $\omega_1 = 180 \cdot 2\pi$ and $\omega_2 = 225 \cdot 2\pi$. This spontaneous oscillation is desirable for the purpose of this thesis, given that we are analysing the state of our neurons in the absence of action potential stimulation, we want to consider the case in which there is a latent constant transmission of information in the form of small amplitude waves that reside in the subthreshold regime and which spontaneously

emerge as a consequence of constructive interference. In this case the resonant state is found for slightly perturbations of the initial condition for our proposal.

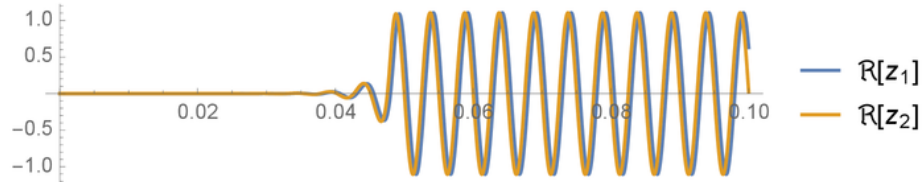


Figure 4.23: Two coupled subcritical systems with the same small value for μ but different frequencies.

4.3.2 Four Subcritical coupled systems in a Network

Given that the purpose of this thesis is the analysis of the real synaptic connectivity from experimental data, if we want to propose the subcritical system as a candidate for modelling the synaptic behaviour, we can observe its effects in a network with different topologies in order to address the importance in the neuronal distribution of synapses. We now explore the behavior of four subcritical systems coupled on a network, each with the following equation:

$$\dot{z}_j = (\mu + i)\omega_j z_j + \omega_j |z_j|^2 z_j - \omega_j |z_j|^4 z_j + \sum_{k \neq j}^N \frac{g_{j,k}}{N} z_k \quad (4.52)$$

Where the term $g_{j,k}$ is the graph matrix that defines the connection of the systems, ω_j is the characteristic frequency of each system and $\mu = -0.1$ is the same for all systems. We chose different frequencies for the systems, $\omega_1 = 180 \cdot 2\pi$, $\omega_2 = 220 \cdot 2\pi$, $\omega_3 = 260 \cdot 2\pi$ and $\omega_4 = 300 \cdot 2\pi$.

The selected network topology is bidirectional, meaning that the systems see each other with the same magnitude and is given by 4.24. For our purposes, we can imagine that this configuration is the three dimensional state of the brain where the effect of neighbouring synapses should be considered in a volumetric way. We can imagine that each node is a synapse from different neurons or that they are in the same neuron but they are under the effect of feed-forward transmission of information.

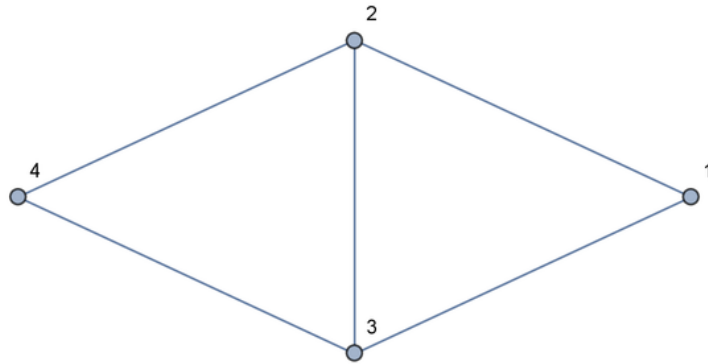


Figure 4.24: Network topology to couple the 4 systems.

The compared response of the systems can be seen in figure 4.25. All systems oscillate at the same frequency, however they exhibit a phase difference, for example the phase difference between 1 and 2 is moderate, between 1 and 3 is higher, and between 1 and 4 they oscillate in opposite directions. This selected phase representation is done with the intention of presenting the consequences of a possible interferometry effect.

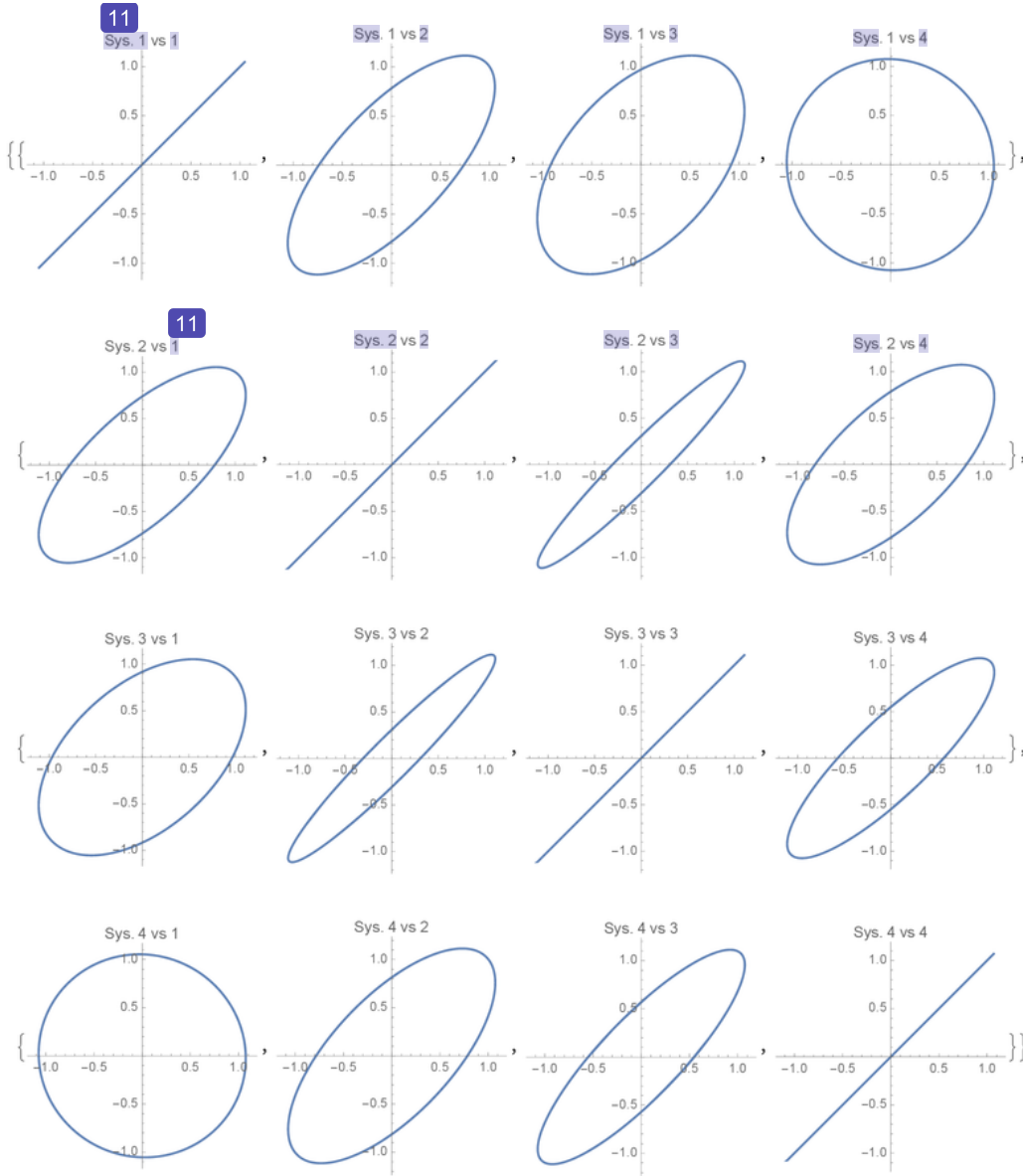


Figure 4.25: Response of the real part of each system compared with the others. This is the long term response of the systems, once transient effects have dissipated.

We now study the same systems but with a different network topology that can be seen in figure 4.26.

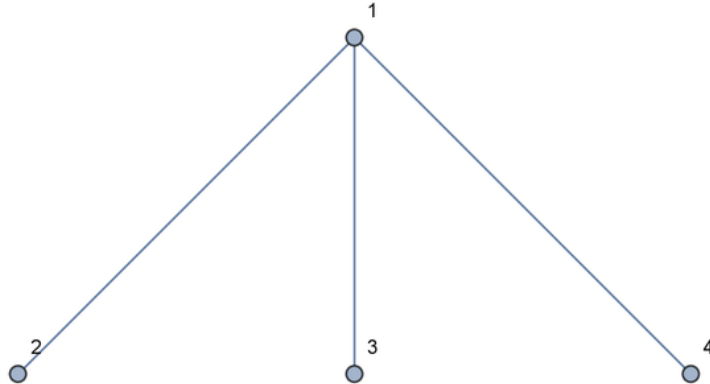


Figure 4.26: Another network topology to couple the 4 systems.

In this network topology, the only coupling that occurs happens through the first system. Therefore it is expected that the systems won't couple as easily as in the first case. In fact, this is the case the numerical solution had to evolve for 200 times more time than in the first case. The solution to this network coupling can be seen in figure 4.27. The coupling in this case is not as strong as before, the first three systems somehow couple, however the fourth oscillates at a different frequency producing a Lissajous like behavior with the other three systems.

This results suggest that network topology have a strong effect on how its constituent systems couple and how coupling in different synaptic structural configuration will have a totally different effect in the postsynaptic neuron.

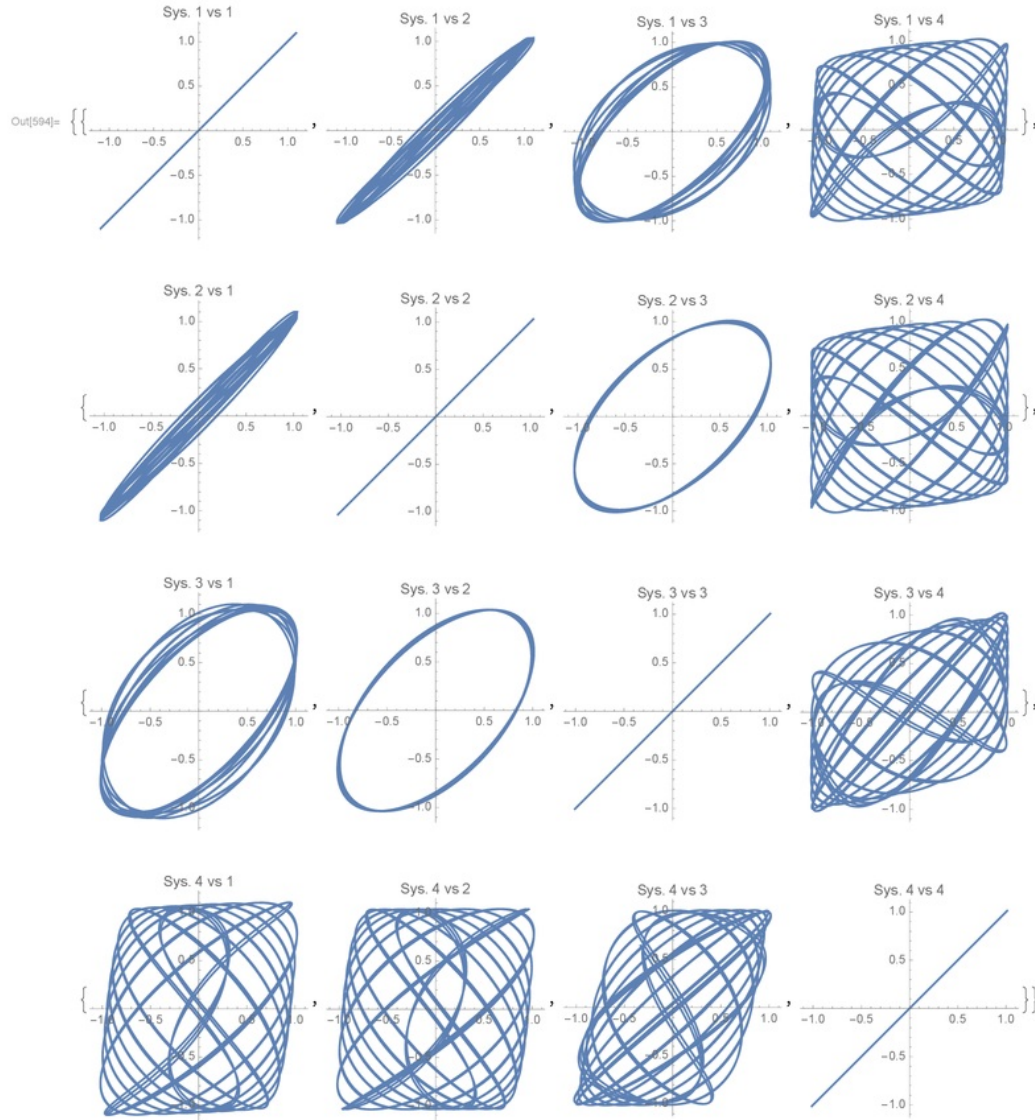


Figure 4.27: Response of the real part of each system compared with the others. This is the long term response of the systems, once transient effects have dissipated.

4.4 Analysis of a Biophysical synaptic model

Creating a simplified model of the dynamics of a synapse is absolutely valuable given the importance of the synapse as the mechanism for information storage and consequently memory formation and because current models of a synapse are composed of around 22 coupled equations it is necessary to simplify it if we want to analyse the behavior of a collection of synapses. In order to propose a simplified model of a synapse, it is good to start by analysing the state of the art of the most detailed biophysical model of a synapse, we will finish this section considering their main physical characteristics, their advantages and disadvantages.

The purpose of this section is to analyse the current components of an already existing model of a synapse. The following model was chosen given that is one of the most complete biophysical models that can be easily access thanks to the open provision done by the authors. It is called, A Mathematical Model of Tripartite Synapse: Astrocyte Induced Synaptic Plasticity[Tewari & Majumdar 2012]. Tripartite in the sense that the model consists of three parts: a pre-synaptic bouton, a post-synaptic dendritic spine-head and an astrocyte responsible for the control of the Ca^{2+} dynamics. Parameters for this model are based on experimental data and the graphs of this section were done with their matlab implementation of the model.

General aspects of the model are: Pre-synaptic action potential train was generated using the Hodgkin-Huxley (HH) model. The model considers two time scales in Ca^{2+} concentration dynamics fast and slow Ca^{2+} influx in the pre-synaptic bouton and Glutamate dynamics at all stages of the synapse.

4.4.1 General aspects

Pre-synaptic potentials

The pre-synaptic action potentials are simulated with the Hodgkin-Huxley (HH) model.

$$C \frac{dV_{pre}}{dt} = I_{app} - g_k n^4 (V_{pre} - V_K) - g_{Na} m^3 h (V_{pre} - V_{Na}) - g_L (V_{pre} - V_L) \quad (4.53)$$

$$\frac{dm}{dt} = \alpha_m(1-m) - \beta_m m, \quad \frac{dh}{dt} = \alpha_h(1-h) - \beta_h h, \quad \frac{dn}{dt} = \alpha_n(1-n) - \beta_n n \quad (4.54)$$

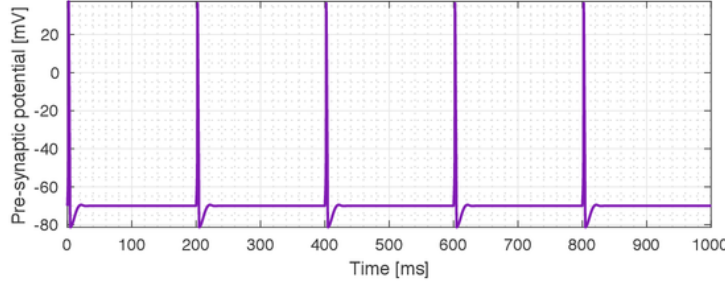


Figure 4.28: HH model variable for study. v : V_{pre} , pre-synaptic potential. Plotted using the model provided by [Tewari & Majumdar 2012]

Here V_{pre} (see figure 4.28) is the pre-synaptic potential in mV, I_{app} is the applied current density, g_k , g_{Na} and g_L conductances, and V_K , V_{Na} and V_L are the reversal potentials, both conductances and potentials are parameters given in the HH model. m is Na^+ activation h is Na^+ inactivation, and n is K^+ activation (see figure 4.29), the following are experimental parameters given by:

$$\alpha_n = \frac{-0.01(-V_{pre} - 60)}{e^{-(V_{pre} + 60)/10} - 1} \quad \alpha_m = \frac{0.1(-V_{pre} - 45)}{e^{-(V_{pre} + 45)/10} - 1} \quad \alpha_h = 0.07e^{-(V_{pre} + 70)/20} \quad (4.55)$$

$$\beta_n = 0.125e^{-(V_{pre} + 70)/80} \quad \beta_m = 4e^{-(V_{pre} + 70)/18} \quad \beta_h = \frac{1}{e^{-(V_{pre} + 40)/10} + 1} \quad (4.56)$$

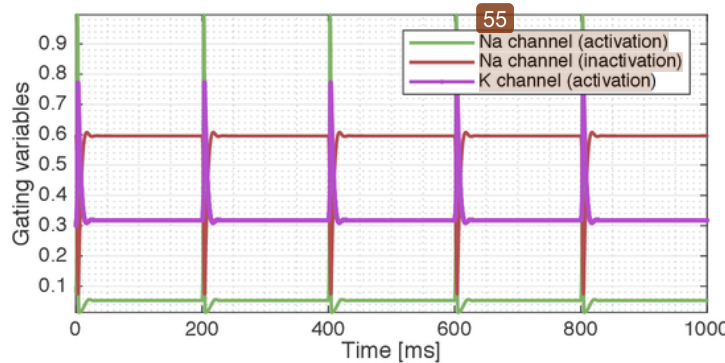


Figure 4.29: HH model variables for study. m : Gating variable for Na channel (activation), h : Gating variable for Na channel (inactivation), n : Gating variable for K channel (activation). Plotted using the model provided by [Tewari & Majumdar 2012]

4.4.2 Ca²⁺ Dynamics

The Action potential generates a increase in Ca²⁺ concentration, this is attributed to the action potential c_{fast} and the intracellular reserves c_{slow} , this two calcium concentration variables have different time scales, that is why their names vary:

$$c_i = c_{fast} + c_{slow} \quad (4.57)$$

they quantify the c_{fast} contribution with:

$$\frac{dc_{fast}}{dt} = -\frac{I_{Ca}A_{btn}}{z_{Ca}FV_{btn}} + J_{PMleak} - \frac{I_{PMCa}A_{btn}}{z_{Ca}FV_{btn}} \quad (4.58)$$

Where each of its terms is explained by the following equations, where I_{Ca} is the current through the N-type Ca²⁺ channel. And V_{Ca} is the reversal potential.

$$I_{Ca} = \rho_{Ca}m_{Ca}^2g_{Ca}(V_{pre} - V_{Ca}) \quad V_{Ca} = \frac{RT}{z_{Ca}F} \ln \left[\frac{c_{ext}}{c_i^{rest}} \right] \quad (4.59)$$

This equations have other time varying terms, and their dynamics are important, such as the single channel opening probability:

$$\frac{dm_{Ca}}{dt} = \frac{(m_{Ca}^\infty - m_{Ca})}{\tau_{m_{Ca}}} \quad (4.60)$$

In this equations m_{Ca}^∞ is a fitted Boltzmann-function for the whole cell current. The other currents and terms are given by:

$$I_{PMCa} = \nu_{PMCa} \frac{c_i^2}{c_i^2 + K_{PMCa}^2}, J_{PMleak} = \nu_{leak}(c_{ext} - c_i), m_{Ca}^\infty = \frac{1}{1 + \exp(V_{m_{Ca}} - V_m)/k_{m_{Ca}}} \quad (4.61)$$

they now model the intracellular reserves c_{slow} , it is important to take into account that it is not enough to have the right concentration of calcium but it also needs to occur in specific microdomains, in this sense the model requires to make an adjustment in the parameters in order to take into account the spatial dimensions constraints, intracellular calcium concentration is given by:

$$\frac{dc_{slow}}{dt} = -J_{chan} - J_{ERpump} - J_{ERleak} \quad (4.62)$$

$$\frac{dc_{ER}}{dt} = -\frac{1}{c_1} \frac{dc_{slow}}{dt} \quad (4.63)$$

$$\frac{dp}{dt} = \nu_g \frac{g_a^{0.7}}{k_g^{0.7} + g_a^{0.7} - \frac{1}{\tau_p}(p - p_0)} \quad (4.64)$$

$$\frac{dq}{dt} = \alpha_q(1 - q) - \beta_q q \quad (4.65)$$

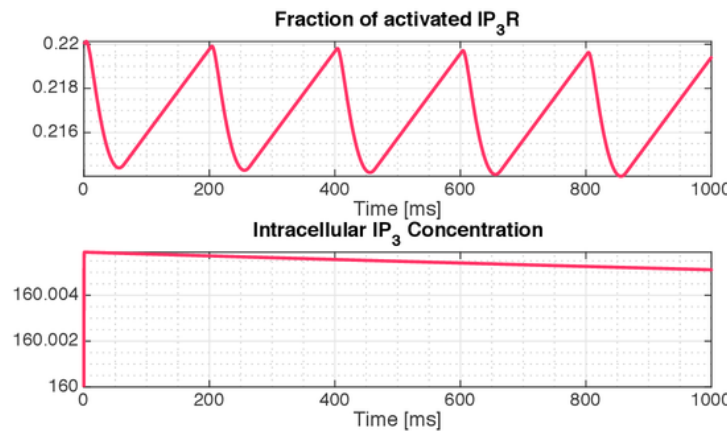


Figure 4.30: Bouton Ca Dynamics. The corresponding 2 variables of the model are p: intracellular IP_3 concentration, q: fraction of activated IP_3R , gating variable. Plotted using the model provided by [Tewari & Majumdar 2012]

Where c_{ER} correspond to concentration in the Endoplasmatic Reticulum (ER), J_{chan} is the flux of Ca from the ER into the intracellular space through IP_3R , J_{ERpump} is the Ca pumped back into the ER, and J_{ERleak} are the ions filtered through simple diffusion.

Other terms are experimental constants. Further experimental details can be found in [Tewari & Majumdar 2012]

$$m_\infty = \frac{p}{p + d_i} \quad n_\infty = \frac{c_i}{c_i + d_5} \quad \alpha_q = a_2 d_2 \frac{p + d_1}{p + d_3} \quad \beta_q = a_2 c_i \quad (4.66)$$

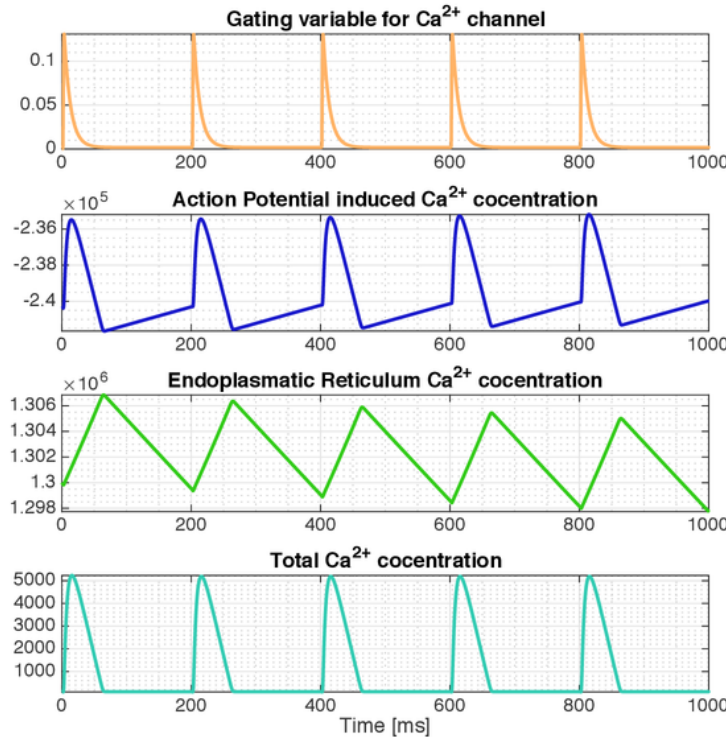


Figure 4.31: Bouton Ca Dynamics. The corresponding 4 graphs are as follows: m_c : Gating variable for Ca channel, c_{fast} : Ca due to AP, c_{er} : ER Calcium concentration also c_{slow} scaled, c : c_i total Ca concentration, Plotted using the model provided by [Tewari & Majumdar 2012]

Coupling

This part of the model connects to the previous one through the $V_{pre} = V_m$ in the current through the N-type channel, and in the Boltzmann function for the single channel opening probability through the $V_{pre} = V_m$.

¹³ 4.4.3 Glutamate release dynamics in bouton

Here they model the Glutamate release as a vesicle process, where R is the fraction of releasable vesicles, I the fraction of inactive vesicles and E the fraction of effective vesicles released in the cleft. P_r corresponds to the vesicles ready to be released, modelled by a concentration dependent Poisson process.

$$\frac{dR}{dt} = \frac{1}{\tau_{rec} - P_r R} \quad (4.67)$$

$$\frac{dE}{dt} = -\frac{E}{\tau_{inact} + P_r R} \quad (4.68)$$

$$I = 1 - R - E \quad (4.69)$$

Coupling

This process is coupled with the previous one, through a Poisson process dependent on the internal concentration of calcium c_i , this internal concentration is dependent on the slow and large scale calcium variables.

$$\lambda(c_i) = a_3 \left(1 + \exp \left(\frac{a_1 - c_1}{a_2} \right) \right)^{-1} \quad (4.70)$$

Where $\lambda(c_i) = P_r$.

13 4.4.4 Glutamate dynamics in synaptic cleft

Here they explain the glutamate concentration in the synaptic cleft, where g is the glutamate concentration and g_c the rate of glutamate clearance:

$$\frac{dg}{dt} = n_v \cdot g_v \cdot E - g_c \cdot g \quad (4.71)$$

Coupling

This process depends on the effective fraction of vesicles released in the cleft E calculated before.

4.4.5 Astrocyte Ca^{2+} dynamics

Here they model the astrocytic Ca^{2+} concentration c_a taking into account, the IP_3 concentration p_a :

$$\frac{dc_a}{dt} = (r_{c_a} m_\infty^3 n_\infty^3 h^3 + r_L)(c_0 - (1 + c_{1,a})c_a) - \nu_{ER} \frac{c_a^2}{c_a^2 + K_{ER}^2} \quad (4.72)$$

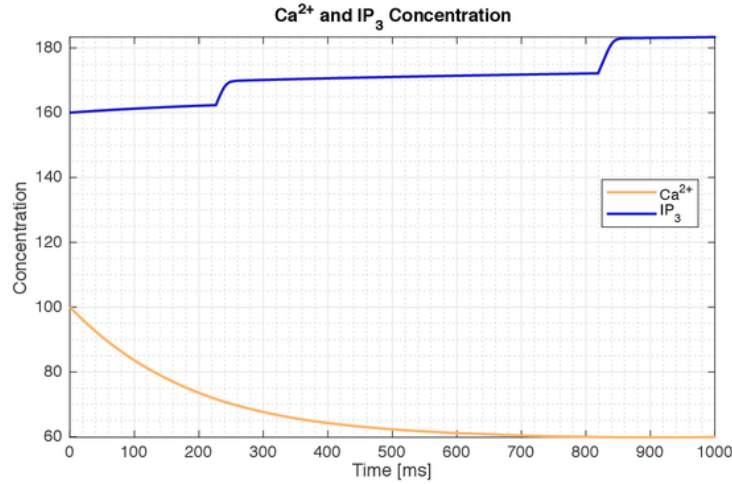


Figure 4.32: Astrocyte Ca dynamics. ca: Calcium concentration and IP_3 concentration. Plotted using the model provided by [Tewari & Majumdar 2012]

$$\frac{dh}{dt} = \frac{h_\infty - h}{\tau_h} + G_h(t) \quad (4.73)$$

In the following system of equations it is presented the Hill function, Hill which is used for reactions with dependencies but whose intermediate steps in the dynamical coupling are unknown.

$$m_{\infty,a} = \text{Hill}(p_a, d1) \quad (4.74)$$

$$n_{\infty,a} = \text{Hill}(c_a, d5) \quad (4.75)$$

$$\text{Hill}(x^n, K) = \frac{x^n}{x^n + K^n} \quad (4.76)$$

$$h_\infty = \frac{Q_2}{Q_2 + c_a} \quad (4.77)$$

$$\tau_h = \frac{1}{a_2(Q_2 + c_a)} \quad (4.78)$$

$$Q_2 = d_2 \frac{p_a + d_1}{p_a + d_3} \quad (4.79)$$

Coupling

Here glutamate concentration g calculated earlier, modulates the behavior of the astrocytic Ca^{2+} .

4.4.6 Glio-transmitter release dynamics in astrocyte

Ca^{2+} stimulates the release of glio-transmitter, it is modelled It is assumed that release site contains three independent gates ¹³ with different opening and closing constants. Modelled by the following equation with $j = 1, 2, 3$.

$$\frac{dO_j}{dt} = k_j^+ \cdot c_a - (k_j^+ \cdot c_a + k_j^-) \cdot O_j \quad (4.80)$$

Now the probability that the release site is activated is expressed as:

$$P_{ra} = O_1 \cdot O_2 \cdot O_3 \quad (4.81)$$

And because it is a vesicle-like process it is modelled similar to the glutamate vesicle release.

$$\frac{dR_a}{dt} = \frac{I_a}{\tau_{rec}^a} - \Theta(c_a - c_a^{thresh}) \cdot P_{ra} \cdot R_a \quad (4.82)$$

$$\frac{dE_a}{dt} = -\frac{E_a}{\tau_{inact}^a} + \Theta(c_a - c_a^{thresh}) \cdot P_{ra} \cdot R_a \quad (4.83)$$

$$I_a = 1 - R_a - E_a \quad (4.84)$$

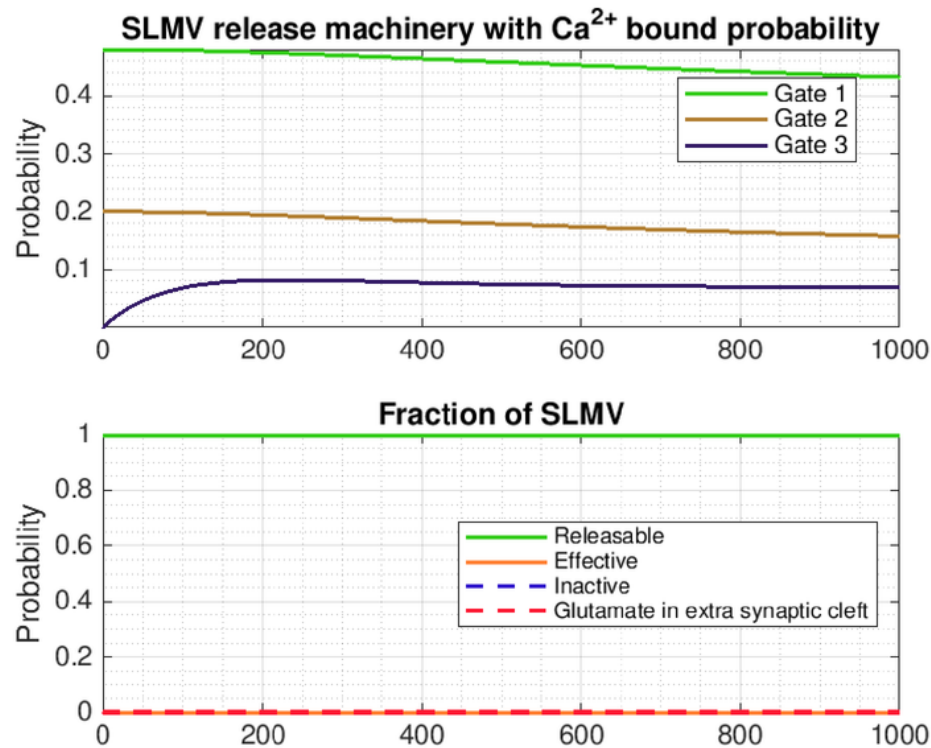


Figure 4.33: Astrocyte Ca dynamics. Top Site 1,2,3 of Synaptic- Like Micro-vesicle (SLMV) release machinery with calcium bound. Bottom: Fraction of releasable SLMVs, Fraction of effective SLMVs, Fraction of inactivated SLMVs. Plotted using the model provided by [Tewari & Majumdar 2012]

Where R_a is the fraction of releasable synaptic-like micro vesicles, E_a is the effective fraction and I_a is the inactive fraction.

Coupling

This process is coupled with the astrocytic Ca^{2+} , through the Ca concentration c_a .

6
4.4.7 Glutamate dynamics in extra-synaptic cleft

35
The previous process causes the release of glutamate in the extra-synaptic cleft, modelled in the same fashion as the usual glutamate release:

$$\frac{dg_a}{dt} = n_a^v \cdot g_a^v \cdot E_a - g_a^c \cdot g_a \quad (4.85)$$

4
Where n_a^v represents the number of vesicles ready to be released, g_a^v is the glutamate concentration in one of the vesicles, g_a^c is the clearance rate and g_a is the glutamate concentration.

Coupling

This process depends on the vesicle fraction E_a caused by the Ca^{2+} concentration.

4.4.8 Dendrite Spine-head dynamics

In this part of the model, the shape and volume of the spine-head complex. The same for the specific resistance and capacitance modelled by equation 4.86. Given that we are interested in the spine-head connectivity, it is necessary an equation for the post-synaptic potential change in passive membrane as in equation 4.87. The AMPAR current is also presented and depends on the gating AMPAR variable given by the same HH description 4.89, AMPAR conductance and AMPAR reversal potential.

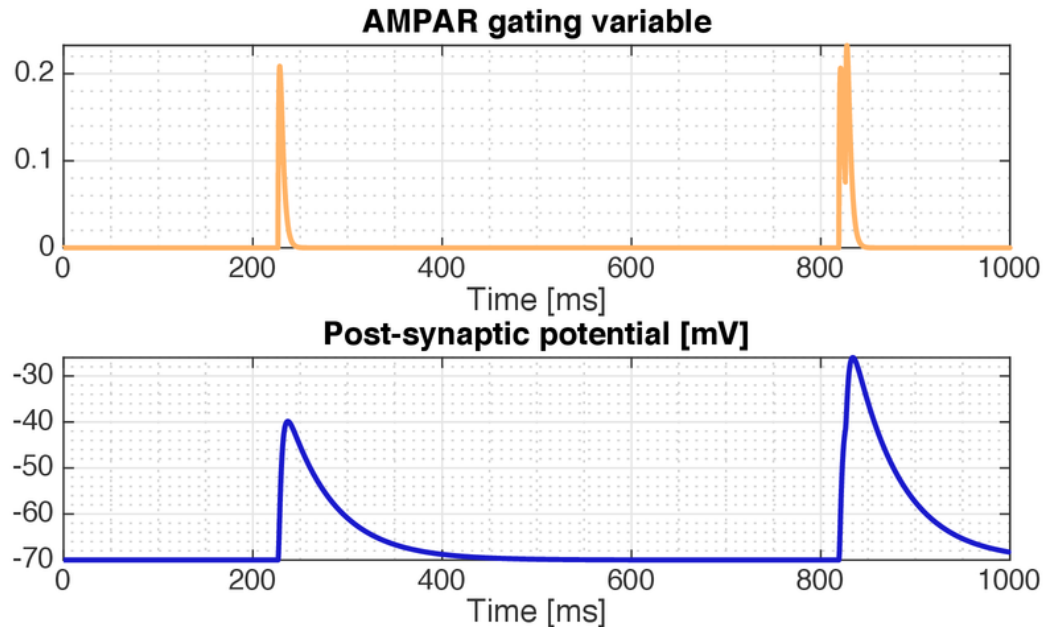


Figure 4.34: Dendrite Spine-head dynamics. m_{amp} : AMPAR gating variable, V_{post} : Post-Synaptic Membrane potential. Plotted using the model provided by [Tewari & Majumdar 2012]

$$R_m = \frac{R_M}{A_{spine}} \quad (4.86)$$

$$\tau_{post} \frac{dV_{post}}{dt} = -(V_{post} - V_{post}^{rest}) - R_m \cdot I_{AMPA} \quad (4.87)$$

$$I_{AMPA} = g_{AMPA} m_{AMPA} (V_{post} - V_{AMPA}) \quad (4.88)$$

$$\frac{dm_{AMPA}}{dt} = \alpha_{AMPA} g (1 - m_{AMPA}) - \beta_{AMPA} m_{AMPA} \quad (4.89)$$

As in the other gating variables, α and β are the opening and closing rates of the receptor.

12

4.4.9 Oscillatory behaviorin the Model

The purpose of this section of the thesis is the exploration of oscillatory activity at the synapse leveL it is of interest the exploration of the dynamical variables that show an oscillatory behaviour, this periodicities allow for simplifications in the model and describe the plausibility of the synapse as an oscillator. For example the calcium concentration in the Endoplasmatic Reticulum inside the pre-synaptic neuron, has an oscillatory pattern in response to an oscillatory input: Plotted using the model provided by [Tewari & Majumdar 2012]

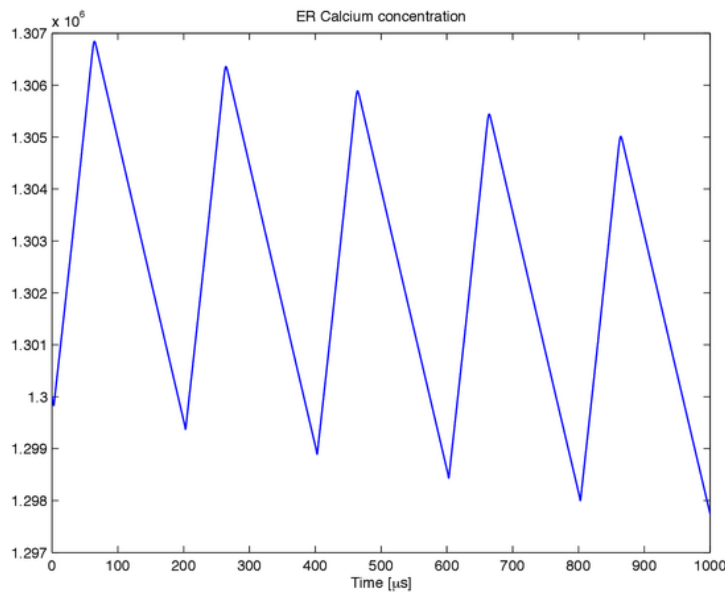


Figure 4.35: Calcium concentration in the Endoplasmatic Reticulum inside the presynaptic neuron. Plotted using the model provided by [Tewari & Majumdar 2012]

This response is the calcium concentration as a result of inside concentration and not, calcium coming inside the cell. Another oscillatory behaviorrelated to Calcium, is the Ca channel opening probability, for a single channel, its results can be observed below:

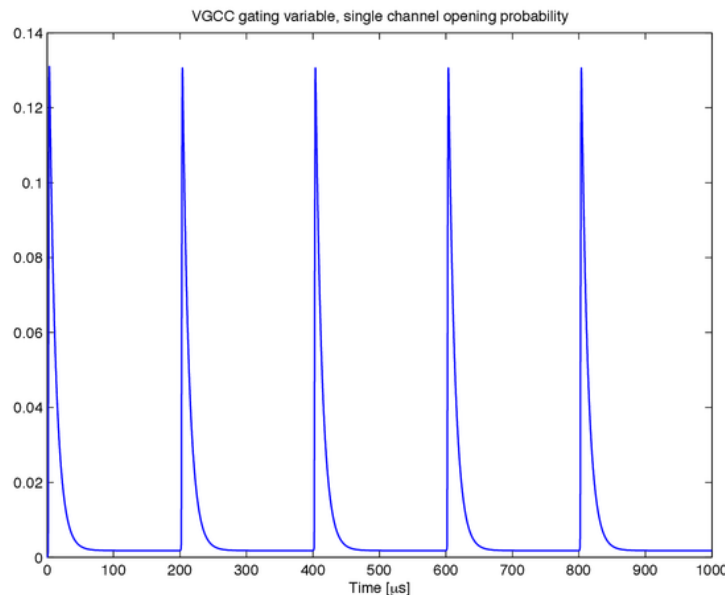


Figure 4.36: Calcium channel opening probability. Plotted using the model provided by [Tewari & Majumdar 2012]

It is interesting to see, how for the total calcium concentration, two variables have oscillatory behavior with the same frequency, but a different system response, this is a good indicator of a frequency modulator between this two complexes. Another variable related to calcium concentration is the secondary messenger molecule IP_3 , which mediates the citoplasmatic Ca concentration, this molecule is known for causing the IP_3R channels to open and initiates astrocytic Ca^{2+} oscillations, the behavior of this molecule is:

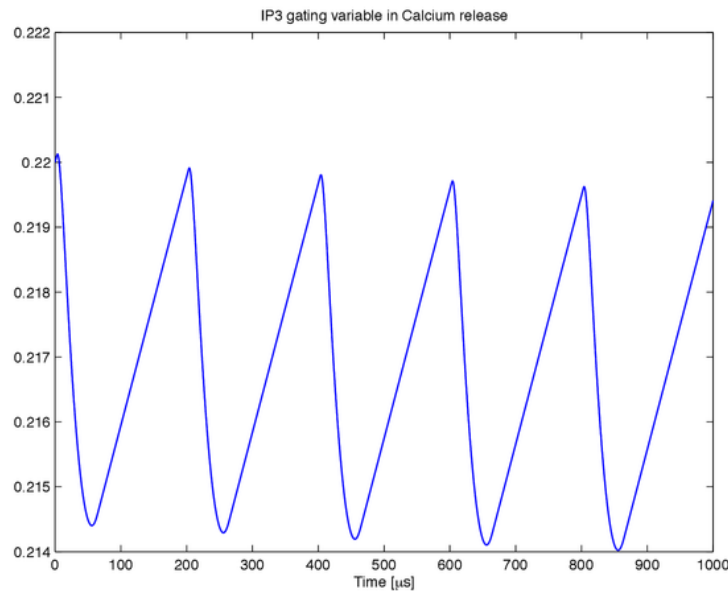


Figure 4.37: m_{IP_3} is the gating variable responsible of initiating astrocytic Ca^{2+} oscillations. Plotted using the model provided by [Tewari & Majumdar 2012]

Calcium concentration causes the release of vesicles into the synaptic cleft, carrying glutamate, one of the most abundant neurotransmitters, the synaptic vesicle release is explained by two variables, both of which can be seen next:

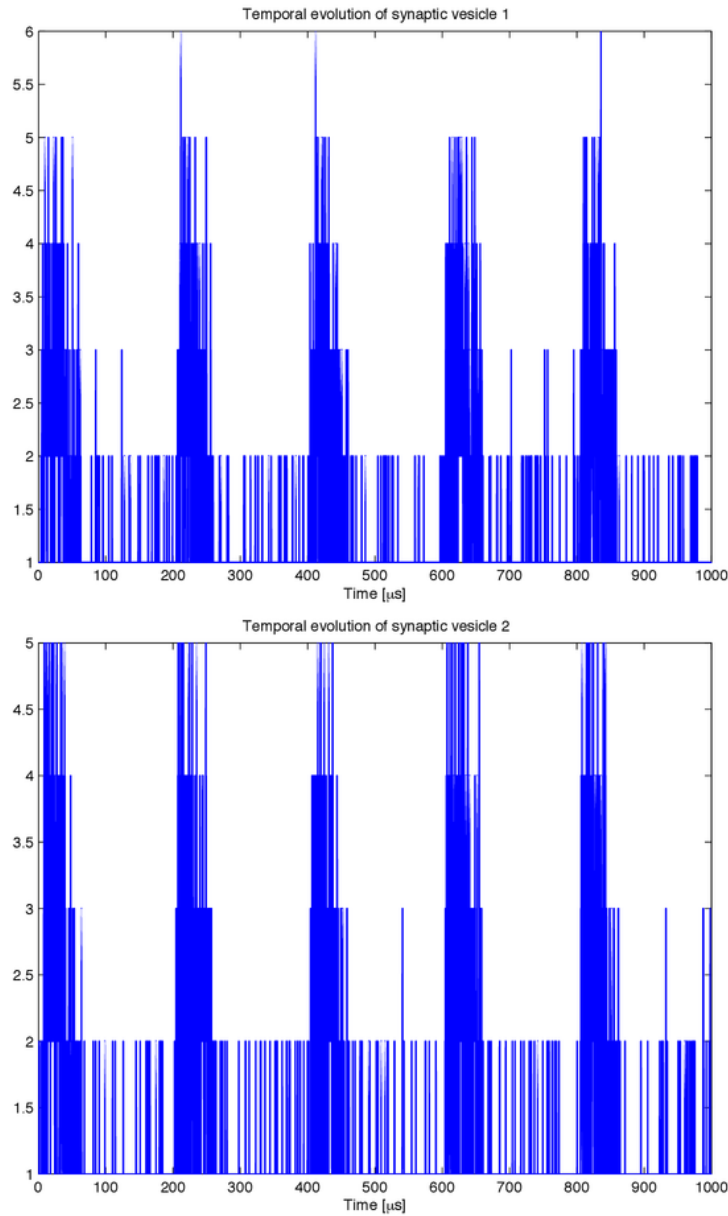
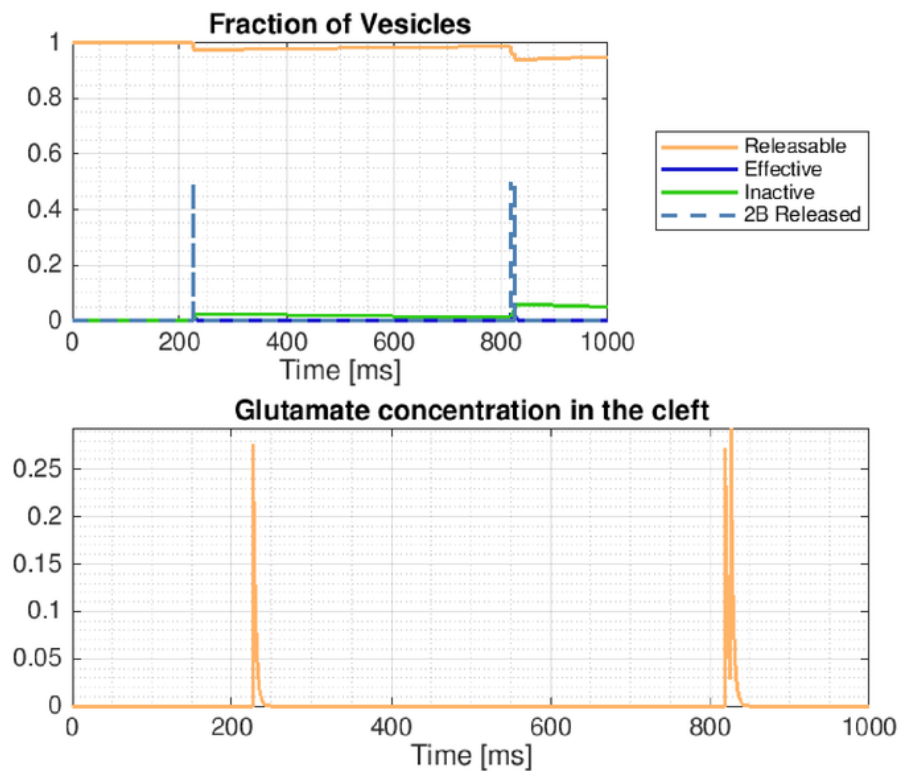


Figure 4.38: Two variables involved in synaptic vesicle release. Plotted using the model provided by [Tewari & Majumdar 2012]

The vesicle release into the synaptic cleft, also exhibits an oscillatory behaviour, highlighting the oscillatory nature of the pre-synaptic neuron. And although oscilla-

tory signals are arriving at the post-synaptic neuron, periodic behavior is absent in the post-synaptic variables which shows the non-linear behavior of this system. In conclusion, pre-synaptic neurons are bombarding the post-synaptic neuron with oscillatory signals at the synapse and this waves have a change in nature, a transformation that is going to be presented in 5 as the wave-particle dual nature of synaptic activity together with its interferometry consequences for constructive and destructive interference that is modulating the transmission of information in the postsynaptic neuron.



13
Figure 4.39: Glutamate release dynamics in bouton. Top: Releasable fraction of vesicles, Effective fraction of vesicles in synaptic cleft, Inactivated fraction of vesicles, Fraction of Vesicles to be released. Bottom: Glutamate concentration in cleft. Plotted using the model provided by [Tewari & Majumdar 2012]

Chapter 5

Results: Theoretical Proposal

Here I analyse the case in which a train of action potentials in the pre-synaptic neuron does not cause the post-synaptic to fire, which is about 99% of the neuron's life [KATCHALSKY 1976]. When a train of action potentials arrives at the synapse in the pre-synaptic neuron, it is converted into a chemical signal, this chemical signal is converted into an small electrical signal that preserves the original frequency, see figure 5.1.

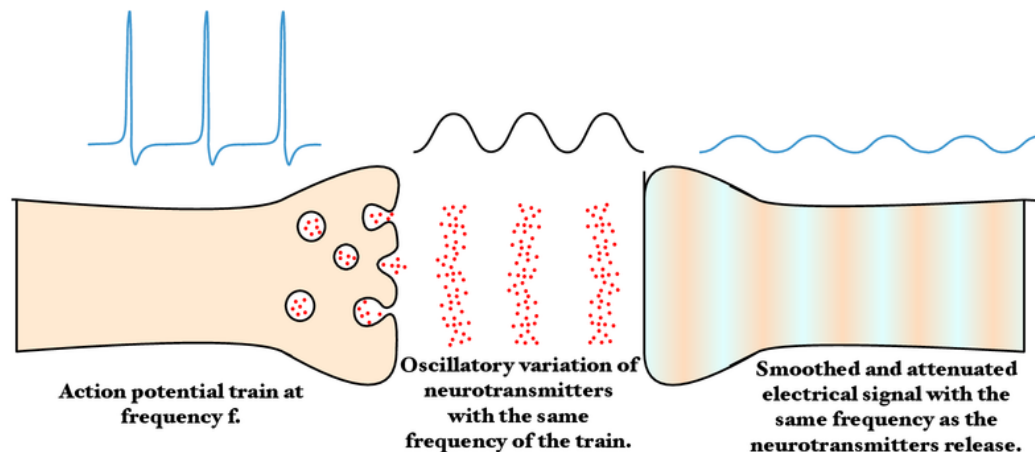


Figure 5.1: A train of action potentials in the pre-synaptic neuron, is smoothed out by being converted into an oscillation of neurotransmitters concentrations in the synaptic cleft. This neurotransmitters concentration is then turned into low amplitude electrical signal in the post-synaptic neuron. The original frequency of the train of action potentials is preserved.

5.1 The synapse as a system

Analyzing this process in more detail, when the action potential reaches the tip of the axon of the pre-synaptic neuron, it triggers the movement of vesicles that release neurotransmitters, that travel through the synaptic cleft via a diffusive process towards the post-synaptic neuron. Afterwards an electrical signal is converted into a diffusive process modulated by the frequency of the pulse. Once the neurotransmitters reach the post-synaptic neuron, this oscillatory chemical signal is converted back into an oscillatory electrical signal.

This process can be modeled interpreting the train of action potentials as the input signal, and what happens with the vesicles, the synaptic cleft and the receptors can be interpreted as a system that transforms the input signal into a smoothed signal with lower amplitude. This idea can be seen in figure 5.2.



Figure 5.2: Vesicles, neurotransmitters and synaptic cleft as a system that transforms the train of spikes into a smoothed out version with the same primary frequency.

The following assumptions will apply for the model in figure 5.2:

- The post-synaptic neuron will not emit an action potential, but will transmit small subthreshold signals.
- The synaptic cleft dimensions stays the same, plasticity or changes in the configuration of the synapse are not happening.

If the above conditions are met the system in figure 5.2 behaves as a time invariant system, which means that its output can be written as the input convolved with the impulse response of the system. In short words we can apply Fourier analysis to it. Thus, we can write:

$$\boxed{\text{Output}} = \boxed{\text{Input}} * \boxed{\text{Impulse Response of the System}} \quad (5.1)$$

To obtain the impulse response of the system we need to analyze what happens at the synaptic cleft in more detail. When vesicles release neurotransmitters into the synaptic cleft, they release the concentration with approximately the same velocity at which the vesicles fused with the cellular membrane. As this blob of concentration travels through the synaptic cleft, it spreads by diffusion as seen in figure 5.3.

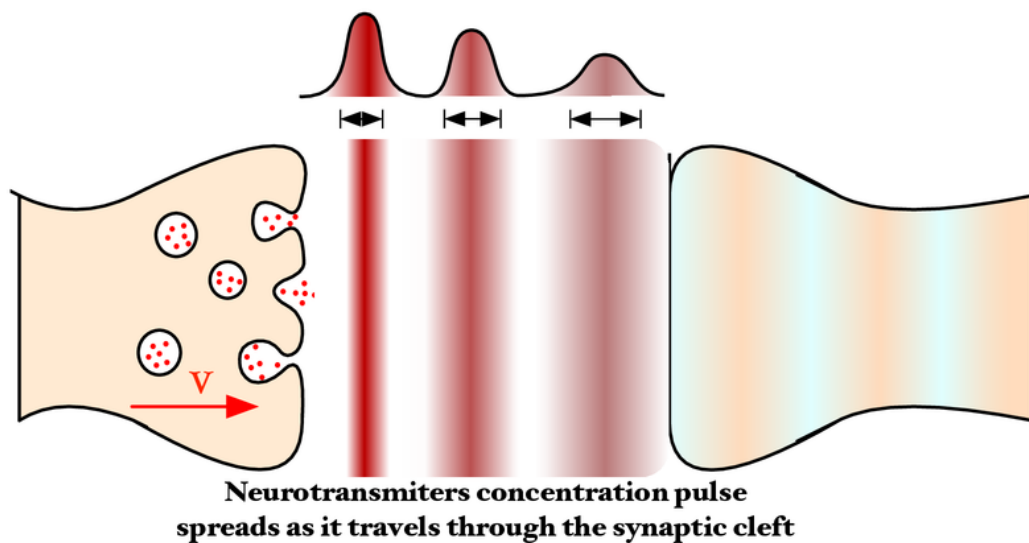


Figure 5.3: A neurotransmitter concentration leaves the pre-synaptic neuron with a certain velocity, as it travels through the synaptic cleft, it spreads by diffusion of its concentration.

Therefore, the post-synaptic neuron receives a smoothed concentration wave, which is then converted into a small periodic electrical signal, proportional to the original concentration.

5.1.1 Vesicles and Diffusion at the synaptic cleft

The concentration gradient moves through the synaptic cleft, and as it moves it also diffuses, remembering that the medium is 80% water at the interior of the cell. Thus, the post-synaptic neuron receives a diffused concentration potential. Assuming that the concentration pulse is on a fluid moving at constant velocity for simplicity, the dominant effect on the spread of the signal is diffusion.

Diffusion in the direction along the synaptic cleft can be quantified, in the frame of the moving concentration pulse, by the 1D diffusion equation:

$$\frac{\partial c(x, t)}{\partial t} = D \frac{\partial^2 c(x, t)}{\partial x^2} \quad (5.2)$$

This equation is solved applying the Fourier transform in space using:

$$\mathcal{F}\{g^{(n)}(x)\} = (2\pi i s)^n \mathcal{F}g(s)$$

for the derivative. Thus equation 5.2 becomes:

$$\frac{\partial \mathcal{F}c(s, t)}{\partial t} = -2\pi^2 s^2 D \mathcal{F}c(s, t) \quad (5.3)$$

Where $\mathcal{F}c(s, t)$, is the Fourier transform of the concentration. Equation 5.3 is a first order differential equation in time, therefore:

$$\mathcal{F}c(s, t) = \mathcal{F}c(s, 0) e^{-2\pi^2 s^2 D t} \quad (5.4)$$

To solve this equation we use the following Fourier identities:

$$\frac{1}{\sqrt{2\pi t}} e^{-x^2/2t} \xleftrightarrow{\mathcal{F}} e^{-2\pi^2 s^2 t}, \quad g(ax) \xleftrightarrow{\mathcal{F}} \frac{1}{|a|} \mathcal{F}g\left(\frac{s}{a}\right), \quad f * g \xleftrightarrow{\mathcal{F}} (\mathcal{F}f)(\mathcal{F}g)$$

Applying the inverse Fourier Transform to equation 5.4 we get:

$$\begin{aligned} \mathcal{F}^{-1}\mathcal{F}c(s, t) &= \mathcal{F}^{-1}\mathcal{F}c(s, 0) * \mathcal{F}^{-1}\{e^{-2\pi^2 s^2 D t}\} \\ c(x, t) &= c(x, 0) * \left[\frac{1}{\sqrt{2\pi D t}} e^{\frac{-x^2}{2Dt}} \right] \end{aligned} \quad (5.5)$$

Where equation 5.5 explains how the concentration pulse spreads as it travels to the synaptic cleft. For now we assume that the synaptic cleft has a defined size, that is the concentration pulse travels a predefined distance, which we will call d_c . Additionally the vesicles release the neurotransmitters at a velocity v_n that in average is a constant. Therefore, the concentration pulse spreads over a time t that we can predict:

$$t = \frac{d_c}{v_n}, \quad d_c = \text{Synaptic cleft width}, \quad v_d = \text{Velocity of neurotransmitters wave}$$

The equations before are a simplification of the main idea, that concentration pulses travel the synaptic cleft at a more or less standard time, as most synaptic clefts exhibit the same dimensions. Thus we can write the total spread, that the concentration pulse suffers while traveling through the synaptic cleft as:

$$c(x, d_c/v_n) = c(x, 0) * \left[\frac{1}{\sqrt{2\pi D(d_c/v_n)}} e^{\frac{-x^2}{2D(d_c/v_n)}} \right] \quad (5.6)$$

Additionally, we can now absorb the diffusion constant D , d_c and v_n in one single constant that quantifies the spread of the signal as it travels through the synaptic cleft, this will be ζ :

$$c(x, d_c/v_n) = c(x, 0) * \left[\frac{1}{\sqrt{2\pi\zeta}} e^{\frac{-x^2}{2\zeta}} \right] \quad (5.7)$$

We have to remember that this solution is in the coordinate system of the pulse, the concentration pulse is emitted by the pre-synaptic neuron and is absorbed by the post-synaptic neuron. Furthermore, the concentration of neurotransmitters will be a function of the voltage in the neuron $c(t) = Ap(t)$. With this in mind we can rewrite the concentration pulse at neuron as a voltage function of time:

$$c(x, 0) = A_{in}p_{in}(t), \text{ Voltage converted to concentration pulse. Pre-synaptic.} \quad (5.8)$$

$$c(x, d_c/v_n) = A_{out}p_{out}(t), \text{ Concentration converted to voltage. Post-synaptic.} \quad (5.9)$$

$$e^{\frac{-x^2}{2\zeta}} = e^{\frac{-(A_{in}t)^2}{2\zeta}}, \text{ Spatial convolution converted to time convolution at the synapse.} \quad (5.10)$$

The neuron converts voltage signals to concentration signals at the pre-synaptic neuron, and concentration signals to voltage at the post-synaptic neuron. In the same way as a video camera in our phone, converts a visual signal into a digital signal, and then screen converts a digital signal into a visual signal. Therefore, the spatial convolution in equation 5.7 can be converted to a time convolution:

$$A_{out}p_{out}(t) = A_{in}p_{in}(t) * \left[\frac{1}{\sqrt{2\pi\zeta}} e^{\frac{-(A_{in}t)^2}{2\zeta}} \right] \quad (5.11)$$

We have differentiated the voltage-concentration conversion at the pre and post-synaptic neuron, because these two conversion have a different underlying process.

Rearranging equation 5.11, we have:

$$p_{out}(t) = \frac{1}{A_{out}} p_{in}(t) * \left[\frac{1}{\sqrt{2\pi\zeta/A_{in}^2}} e^{\frac{-t^2}{2\zeta/A_{in}^2}} \right] \quad (5.12)$$

7

Equation 5.12 explains what happens to the action potential as it reaches the end of the pre-synaptic neuron, is converted to a chemical signal and then back into an electrical signal. $1/A_{out}$ is a scaling constant that quantifies how much the amplitude of the signal is reduced. Additionally, the Gaussian present in equation 5.12 is normalized, thus the convolution smooths the signal. We now have a mathematical representation of the system in figure 5.2. To understand better what happens in equation 5.2, we can see figure 5.4, where the input signal of spikes pulses is smoothed and becomes small, the system block in figure 5.4 embodies the behavior of the synapse.

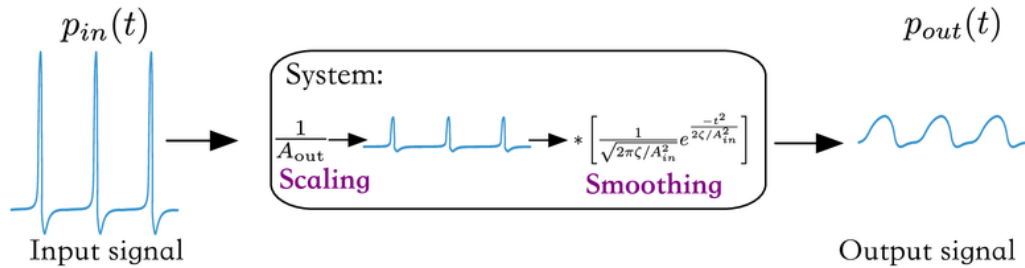


Figure 5.4: The synapse as a system.

We now have a mathematical explanation for the system in figure 5.2 and the conceptual equation 5.1, where we have explained the vesicles, neurotransmitters synaptic cleft, and receptors as a system quantified in our final result in equation 5.12.

5.1.2 A train of action potentials crossing the synapse

We have just derived what happens at the synapse (see sec 5.1.1). Now we apply the result of equation 5.12, to predict what will happen to a train of action potentials.

First we need to write a train of action potentials in mathematical terms, for now I propose to model them as a train of Dirac's deltas, as this captures the main characteristics, especially the fact that they arrive at a certain frequency at the end of the synaptic neuron. This idea is illustrated in figure 5.5.⁵⁴

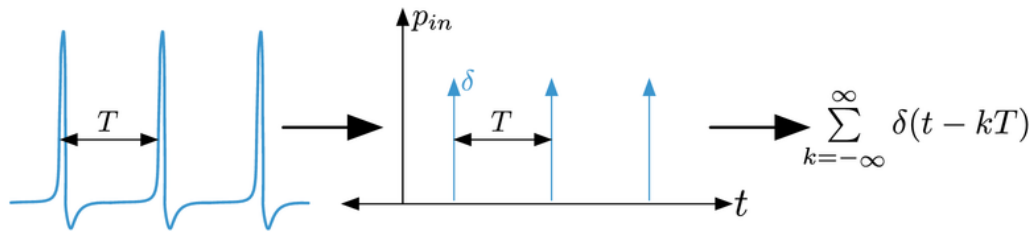


Figure 5.5: A train of action potentials written as Dirac's deltas. The time interval between one action potentials is T .

We can express the train of action potentials as a train of Dirac's deltas, in reality we will have a bounded train of action potentials. However, for now and without loss of generality I will write it as an infinite train of deltas as it is a well known function in Fourier analysis:

$$\text{Action potentials spaced } T = \sum_{k=-\infty}^{\infty} \delta(t - kT) = \Pi_T(t) \quad (5.13)$$

With this way of writing the action potentials, $\Pi_T(t)$, we can now see what will happen to the electric signal as it travels to the synapse, using our result in equation 5.12 and equation 5.13, we have:

$$p_{in}(t) = \Pi_T(t) \quad (5.14)$$

Thus:

$$p_{out}(t) = \frac{1}{A_{out}} \text{III}_T(t) * \left[\frac{1}{\sqrt{2\pi\zeta/A_{in}^2}} e^{\frac{-t^2}{2\zeta/A_{in}^2}} \right] \quad (5.15)$$

$$= \frac{1}{A_{out}} \left[\sum_{k=-\infty}^{\infty} \delta(t - kT) \right] * \left[\frac{1}{\sqrt{2\pi\zeta/A_{in}^2}} e^{\frac{-t^2}{2\zeta/A_{in}^2}} \right] \quad (5.16)$$

$$= \frac{1}{A_{out}} \sum_{k=-\infty}^{\infty} \delta(t - kT) * \frac{1}{\sqrt{2\pi\zeta/A_{in}^2}} e^{\frac{-(t-kT)^2}{2\zeta/A_{in}^2}} \quad (5.17)$$

58

And using the fact that $\delta(t - a) * f(t) = f(t - a)$, we obtain:

$$p_{out}(t) = \frac{1}{A_{out}} \frac{1}{\sqrt{2\pi\zeta/A_{in}^2}} e^{\frac{-(t-kT)^2}{2\zeta/A_{in}^2}}$$

(5.18)

This is a surprising result, a train of action potentials has become a train of smooth Gaussian functions, which perfectly resembles a wave. Now, what we quantitatively saw in figure 5.4 is expressed in equation 5.18. The synapse converts a train of action potentials in a small oscillatory signal. The behavior of a sub-threshold signal going in a post-synaptic neuron can be easily modeled by an oscillator that outputs a Gaussian like wave. Furthermore, this behavior has been studied by expressing a train of action potentials as deltas, however, if we write the action potential in more detail, the signal will be even closer to a wave, because a delta is sharpest signal that can exists, and it became a smooth gaussian. Therefore, an action potential which is a continuous signal, will be more smoothed by the synapse, and the output will become closer to a sinusoidal wave.

With this, I have demonstrated that for the purpose of studying the signals going into a single neuron, we can substitute the input synapse by an oscillator that outputs waves of a predefined frequency.

Chapter 6

Conclusion and Future directions

6.1 Summary of contributions

The model that is proposed in this thesis for a synapse, is an oscillatory constructive and destructive interference pattern of wave activity, that smooths the train of action potential and keeps its frequency through scaling, convolution and Fourier transform of its information content. The system is composed of an input wave that is transformed through interferometry, as slits in analogy to Young's experiment but with the real synaptic distribution or ionic structural distribution depending on the level of analysis that wants to be achieved.

Analysing synapses with the wave-particle viewpoint is computational efficient for studies of memory and learning where it is crucial to detect the appearance and disappearance of synaptic contacts and plasticity. With this framework, synapses are amplitudes of wave activity that vanish or emanate depending on the collective oscillatory behavior.

This study is a potential tool for data analysis where it is required a transformation from the postsynaptic signal to the presynaptic wave input or viceversa. This approach can also be useful in computational tasks both in software and hardware that can make use of real biological network architectures as templates of interference generators that are able to solve different computations. The main observations from the analysed Hopf systems is that it is of interested for the aim of this thesis, the coupling of oscillators with an inductance given that this will generate periodical oscillations and in-phase and anti-phase couplings, char-

acteristics that were not presented in the other coupling elements like resistors or capacitance. The central feature of the Van Der Pol oscillator is the nonlinear resistance which creates pumping instead of damping for small perturbations, this effect is desirable for the analysis of sub-threshold signal behavior at the synapse level.²⁴

Given that spontaneous oscillations are an important assumption, considering the most common scenario in the lifespan of a neuron where it is 99% of the time in a sub-threshold regime and many of them die without ever making a spike, we do not need a forcing term in the oscillator modelling, but rather a very small initial condition, that should move the systems from the unstable origin. Neurons in the absence of action potential stimulation, are in a latent constant transmission of information in the form of small amplitude waves that reside in the sub-threshold regime and which spontaneously emerge as a consequence of constructive interference. In this case the resonant state is found for slightly perturbations of the initial condition for our proposal.

The analysis of different topologies suggest that the structure of the network have a strong effect on how its constituent systems couple and how coupling in different synaptic structural configuration will have a totally different effect in the postsynaptic neuron.

From the biophysical analysis it was observed that although oscillatory signals are arriving at the post-synaptic neuron, periodic behavior is absent in the post-synaptic variables which shows the non-linear behavior of this system. Instead, pre-synaptic neurons are bombarding the post-synaptic neuron with oscillatory signals at the synapse and this waves have a change in nature, a transformation that is presented in ⁵ as the wave-particle dual nature of synaptic activity together with its interferometry consequences for constructive and destructive interference that is modulating the transmission of information in the postsynaptic neuron.

6.2 Vision for the future

I would like to mention that given the abrupt stop that this work had to suffer one year ago, I was not able to show in this document many findings from this theoretical

proposal. Nonetheless, given that this findings are beyond the scope of the initial objectives for a master thesis and since the size of this document is already very large, the development of this results would be presented in future work and they are slightly presented in the following section.

6.2.1 Medium term goals

- Analysis of ion channels as wave perturbations
- Analysis of energy constraints considering oscillations in Glutamate cycle
- Analysis of interaction with astrocytes for as new carriers of long range correlations, allowing the generation of long distant pattern waves.
- Analysis of mesoscopic oscillations and connection with macroscopic oscillations

6.2.2 Long term goals

- Improvement of the model considering perturbation details of the arriving wave function
- Applying quantum field theory in the analysis of long range correlation

Bibliography

- [~ ouweling " et al. 2001] Arthur R ~ ouweling ", Rashmi H Mod, Paul Gantera, Jean-Marc Fellousa and Terrence J Sejnowski. *Models of frequency preferences of prefrontal cortical neurons.* Neurocomputing, vol. 3840, pages 231–238, 2001.
- [Bullock 1993] Theodore Holmes. Bullock. How do brains work? : papers of a comparative neurophysiologist. Birkhäuser, Boston :, 1993.
- [Desmaisons et al. 1999] D Desmaisons, J D Vincent and P M Lledo. *Control of action potential timing by intrinsic subthreshold oscillations in olfactory bulb output neurons.* The Journal of neuroscience : the official journal of the Society for Neuroscience, vol. 19, no. 24, pages 10727–37, dec 1999.
- [Eccles 1964] John C. Eccles. The Physiology of synapses. Springer,, Berlin :, 1964.
- [Gerstner et al. 2014] Wulfram Gerstner, Werner M. Kistler, Richard Naud and Liam Paninski. *Neuronal Dynamics.* Cambridge University Press, Cambridge, 2014.
- [Gomez et al. 2016] Florian Gomez, Tom Lorimer and Ruedi Stoop. *Signal-Coupled Subthreshold Hopf-Type Systems Show a Sharpened Collective Response.* Physical Review Letters, vol. 116, no. 10, page 108101, mar 2016.
- [Hebb 1949] D. O. Hebb. *The organization of behavior; a neuropsychological theory.* New York, Wiley,, 1949.
- [Hodgkin & Huxley 1990] A.L. Hodgkin and A.F. Huxley. *A quantitative description of membrane current and its application to conduction and excitation in nerve.* Bulletin of Mathematical Biology, vol. 52, no. 1, pages 25 – 71, 1990.
- [Jiang et al. 2016] Haibo Jiang, Yang Liu, Liping Zhang and Jianjiang Yu. *Anti-phase synchronization and symmetry-breaking bifurcation of impulsively coupled oscillators.* Communications in Nonlinear Science and Numerical Simulation, vol. 39, pages 199 – 208, 2016.
- [KATCHALSKY 1976] A. KATCHALSKY. *Membrane Thermodynamics.* In Aharon Katzir-Katchalsky, éditeur, Biophysics and Other Topics, pages 269 – 286. Academic Press, 1976.

- ¹⁵ [Kawato *et al.* 1982] Mitsuo Kawato, Koji Fujita, Ryoji Suzuki and Arthur T. Winfree. *A three-oscillator model of the human circadian system controlling the core temperature rhythm and the sleep-wake cycle.* Journal of Theoretical Biology, vol. 98, no. 3, pages 369 – 392, 1982.
- ⁴¹ [Koch 1999] Christof Koch. *Biophysics of computation : information processing in single neurons.* Oxford University Press, 1999.
- ²⁹ [Kuznetsov *et al.* 2009] A.P. Kuznetsov, N.V. Stankevich and L.V. Turukina. *Coupled van der PolDuffing oscillators: Phase dynamics and structure of synchronization tongues.* Physica D: Nonlinear Phenomena, vol. 238, no. 14, pages 1203 – 1215, 2009.
- ⁴³ [Llinás 1999] Rodolfo R. (Rodolfo Riascos) Llinás. *The squid giant synapse : a model for chemical transmission.* Oxford University Press, 1999.
- ²⁸ [Matthews *et al.* 1991] Paul C. Matthews, Renato E. Mirollo and Steven H. Strogatz. *Dynamics of a large system of coupled nonlinear oscillators.* Physica D: Nonlinear Phenomena, vol. 52, no. 23, pages 293 – 331, 1991.
- [Pur 2008] Neuroscience /. Sinauer Associates,, Sunderland, Mass. :, 4th ed. édition, 2008.
- ¹⁹ [Strogatz 2001] Steven H. (Steven Henry) Strogatz. *Nonlinear dynamics and chaos : with applications to physics, biology, chemistry, and engineering.* 2001.
- ²² [Tewari & Majumdar 2012] Shivendra G Tewari and Kaushik Kumar Majumdar. *A mathematical model of the tripartite synapse: astrocyte-induced synaptic plasticity.* Journal of biological physics, vol. 38, no. 3, pages 465–496, 2012.

Wave-Particle uncertainty principle in neurons. From oscillatory synapses to action potential

ORIGINALITY REPORT

10%

SIMILARITY INDEX

PRIMARY SOURCES

- | | | |
|----|---|------------------|
| 1 | sulcus.berkeley.edu
Internet | 254 words — 1% |
| 2 | dissertations.port.ac.uk
Internet | 202 words — 1% |
| 3 | www.jneurosci.org
Internet | 176 words — 1% |
| 4 | www.isibang.ac.in
Internet | 102 words — < 1% |
| 5 | quotes.schollz.com
Internet | 97 words — < 1% |
| 6 | Shivendra G. Tewari. "A mathematical model of the tripartite synapse: astrocyte-induced synaptic plasticity", Journal of Biological Physics, 05/27/2012
Crossref | 85 words — < 1% |
| 7 | "Encyclopedia of Computational Neuroscience", Springer Nature, 2015
Crossref | 59 words — < 1% |
| 8 | metro.inter.edu
Internet | 53 words — < 1% |
| 9 | complex.ffn.ub.es
Internet | 51 words — < 1% |
| 10 | loveacceptforgive.com
Internet | |

50 words — < 1%

-
- 11 www.slideshare.net Internet 45 words — < 1%
- 12 researchspace.auckland.ac.nz Internet 43 words — < 1%
- 13 Shivendra Tewari. "A mathematical model for astrocytes mediated LTP at single hippocampal synapses", Journal of Computational Neuroscience, 03/28/2012 Crossref 39 words — < 1%
- 14 www.naun.org Internet 32 words — < 1%
- 15 Partonen, T.. "Medication Effects", Encyclopedia of Sleep, 2013. Crossref 31 words — < 1%
- 16 Eugene M Izhikevich. "Resonance and selective communication via bursts in neurons having subthreshold oscillations", Biosystems, 2002 Crossref 29 words — < 1%
- 17 static1.squarespace.com Internet 29 words — < 1%
- 18 www.ini.ethz.ch Internet 29 words — < 1%
- 19 www.db-thueringen.de Internet 27 words — < 1%
- 20 polis.unipmn.it Internet 27 words — < 1%
- 21 Karl A. Seeler. "System Dynamics", Springer Nature, 2014 Crossref 27 words — < 1%

- 22 Ali Mahdavi, Fariba Bahrami, Mahyar Janahmadi. "Studying the effect of dysregulation of NMDA receptors function in schizophrenia", 2014 22nd Iranian Conference on Electrical Engineering (ICEE), 2014
Crossref
- 23 www.scribd.com Internet 25 words — < 1%
- 24 B. Z. Kaplan. "An 'improved' van-der-Pol equation and some of its possible applications", International Journal of Electronics, 8/1/1976
Crossref
- 25 Alden, John A., Francis Hutchinson, and Richard G. Compton. "Can Cyclic Voltammetry at Microdisc Electrodes Be Approximately Described by One-Dimensional Diffusion?", The Journal of Physical Chemistry B, 1997.
Crossref
- 26 hal.univ-lorraine.fr Internet 23 words — < 1%
- 27 papers.cnl.salk.edu Internet 23 words — < 1%
- 28 www.hal.inserm.fr Internet 21 words — < 1%
- 29 International Journal of Bifurcation and Chaos, 1991.
Crossref
- 30 openair.rgu.ac.uk Internet 20 words — < 1%
- 31 open.library.ubc.ca Internet 20 words — < 1%
- 32 www dblp.org Internet 19 words — < 1%

- 33 W. O. Criminale. "Limit Cycle-Strange Attractor Competition", Studies in Applied Mathematics, 2/2004 18 words — < 1%
Crossref
- 34 B. Connors. "Intrinsic oscillations of neocortex generated by layer 5 pyramidal neurons", Science, 01/25/1991 18 words — < 1%
Crossref
- 35 tel.archives-ouvertes.fr 17 words — < 1%
Internet
- 36 tesis.pucp.edu.pe 16 words — < 1%
Internet
- 37 Taro Tezuka, Christophe Claramunt. "Connectivity estimation of neural networks using a spike train kernel", 2015 International Joint Conference on Neural Networks (IJCNN), 2015 15 words — < 1%
Crossref
- 38 D. Chawla. "The Relationship Between Synchronization Among Neuronal Populations and Their Mean Activity Levels", Neural Computation, 08/1999 15 words — < 1%
Crossref
- 39 A. A. Tsiatis. "On the inefficiency of the adaptive design for monitoring clinical trials", Biometrika, 06/01/2003 15 words — < 1%
Crossref
- 40 tolstoy.newcastle.edu.au 15 words — < 1%
Internet
- 41 www.tbi.univie.ac.at 14 words — < 1%
Internet
- 42 en.wikipedia.org 14 words — < 1%
Internet
- 43 www.scirp.org 13 words — < 1%
Internet

44	dimacs.rutgers.edu Internet	13 words — < 1%
45	uthscsa.influent.utsystem.edu Internet	12 words — < 1%
46	magnum.ime.uerj.br Internet	12 words — < 1%
47	Sophie Pinchinat. "Taxonomy and Expressiveness of Preemption: A Syntactic Approach", Lecture Notes in Computer Science, 1998 Crossref	12 words — < 1%
48	www.archive.org Internet	12 words — < 1%
49	arxiv.org Internet	11 words — < 1%
50	Haibo Jiang, Yang Liu, Liping Zhang, Jianjiang Yu. "Anti-phase synchronization and symmetry-breaking bifurcation of impulsively coupled oscillators", Communications in Nonlinear Science and Numerical Simulation, 2016 Crossref	11 words — < 1%
51	augusta.otago.ac.nz Internet	10 words — < 1%
52	www2.swccd.edu Internet	10 words — < 1%
53	www.cs.bham.ac.uk Internet	10 words — < 1%
54	www.copsmodels.com Internet	9 words — < 1%
55	Park, E.H.. "Role of potassium lateral diffusion in non-synaptic epilepsy: A computational study",	9 words — < 1%

-
- 56 I. Pastor. "Ordered and chaotic behavior of two coupled van der Pol oscillators", Physical Review E, 07/1993 9 words — < 1%
Crossref
-
- 57 dspace.c3sl.ufpr.br 9 words — < 1%
Internet
-
- 58 Lecture Notes in Electrical Engineering, 2012. 8 words — < 1%
Crossref
-
- 59 repository.ntu.edu.sg 8 words — < 1%
Internet
-
- 60 Keener. "Excitability", Interdisciplinary Applied Mathematics, 2009 8 words — < 1%
Crossref
-
- 61 Mehdi Borjkhan, Fariba Bahrami, Mahyar Janahmadi. "Computational modeling of opioid-induced synaptic plasticity in hippocampus", PLOS ONE, 2018 8 words — < 1%
Crossref
-
- 62 www.ling.ed.ac.uk 8 words — < 1%
Internet
-
- 63 www.docstoc.com 8 words — < 1%
Internet
-
- 64 R.Y. Beregov, A.V. Melkikh. "De-synchronization and chaos in two inductively coupled Van der Pol auto-generators", Chaos, Solitons & Fractals, 2015 8 words — < 1%
Crossref
-
- 65 www.cond-mat.de 8 words — < 1%
Internet
-
- 66 www.mtome.com 8 words — < 1%
Internet

- 67 Pardalopoulou, Maria(Erni, Daniel and Solbach, Klaus). "On the coupling between ridged and rectangular waveguide via a non-offset longitudinal slot", DuEPublico: University of Duisburg-Essen Publications Online, 2011.
Publications 8 words — < 1 %
- 68 www.csun.edu Internet 8 words — < 1 %
- 69 A. Serfaty de Markus. "Reduction of computational errors using nonstandard finite difference models", The Journal of Difference Equations and Applications, 1/1/2005
Crossref 8 words — < 1 %
- 70 Anders Rehfeld, Malin Nylander, Kirstine Karnov. "Chapter 14 Nerve Tissue", Springer Nature, 2017
Crossref 8 words — < 1 %
- 71 www.doria.fi Internet 8 words — < 1 %
- 72 Florian Gomez, Tom Lorimer, Ruedi Stoop. "Signal-Coupled Subthreshold Hopf-Type Systems Show a Sharpened Collective Response", Physical Review Letters, 2016
Crossref 7 words — < 1 %
- 73 R. Houweling, A.. "Models of frequency preferences of prefrontal cortical neurons", Neurocomputing, 200106
Crossref 7 words — < 1 %
- 74 Maurizio Pittà. "Glutamate regulation of calcium and IP3 oscillating and pulsating dynamics in astrocytes", Journal of Biological Physics, 06/12/2009
Crossref 6 words — < 1 %
- 75 Z. E. MUSIELAK. "HIGH-DIMENSIONAL CHAOS IN DISSIPATIVE AND DRIVEN DYNAMICAL SYSTEMS", International Journal of Bifurcation and Chaos, 2009
Crossref 6 words — < 1 %

David Desmaisons, Jean-Didier Vincent, Pierre-Marie Lledo.

76

"Control of Action Potential Timing by Intrinsic
Subthreshold Oscillations in Olfactory Bulb Output
Neurons", The Journal of Neuroscience, 1999

6 words — < 1%

Crossref

EXCLUDE QUOTES OFF
EXCLUDE BIBLIOGRAPHY OFF

EXCLUDE MATCHES OFF